

An Investigation Towards Developing Capability Profiles of Rapid Prototyping Technologies With a Focus on 3D-Printing



by

Neal de Beer

Thesis presented in partial fulfilment
of the requirements for the degree of
Master of Science in Engineering
(Industrial) at the University of
Stellenbosch.

Study leader: Prof. D. Dimitrov

March 2004



Declaration

I, the undersigned, hereby declare that the work contained in this thesis is my own original work and has not previously in its entirety or in part been submitted at any university for a degree.

Ek, die ondergetekende verklaar hiermee dat die werk gedoen in hierdie tesis my eie oorspronklike werk is wat nog nie voorheen gedeeltelik of volledig by enige universiteit vir 'n graad aangebied is nie.

Signature:

Date:



Synopsis

Rapid prototyping (RP) technologies have expanded vastly over recent years. With the advent of new materials along with new processes, each technology has been contributing to the diversities in different fields of application for the growing technologies. In the course of improvement, it is however critical to understand exactly what the capability of each individual technology is in order to compare future improvements, or even to compare current processes and technologies.

The objective of this research has been to develop capability profiles of prominent RP technologies: 3D-Printing (3DP), Selective Laser Sintering (SLS), and Laminated Object Manufacturing (LOM) – in which different characteristics of each technology are measured and quantified.

A capability profile may be regarded as a set of building blocks that give a representation of the RP technology's ability and is defined by quantifying the following characteristics:

Accuracy (both dimensional- and geometrical accuracy)

Surface finish measures

Strength and elongation

Build time, and

Cost

The significance behind developing capability profiles lies in the need to more accurately describe and compare each of the different processes – especially Z Corporation's 3DP, since although this process is regarded as very capable in many areas, little has been published to substantiate this opinion.

When users of these technologies are pushing the limits of their machines, it becomes critical to know exactly what these boundaries are in order to know with some measure of certainty that they will be able to fulfil a certain customer demand or expectation. For South Africa in particular, the industry's growing interest in rapid prototyping is triggering inevitable questions as to whether a certain RP technology can produce the desired solutions to their



problems. The South African industry's growing awareness about rapid prototyping is opening new doors for better solutions to new and existing problems – but ultimately, *before* investing money, customers want to know if RP is going to meet the standards needed to solve their solutions.

On a more general level, this study can also be seen to bear significance in contributing to research in what has become known as rapid manufacturing (RM). This term is defined as the manufacture of end-use products using additive manufacturing techniques. RM must guarantee long-term consistent component use for the entire product life cycle or for a defined minimal period for wearing parts [1].

However, before it is possible to guarantee long-term consistency of components, one must first ensure consistency of the process. Once a process is consistent, the next question becomes: What is it capable of doing consistently?

This study aims to answer this question for the three processes (3DP, SLS and LOM) mentioned earlier. In doing so, this study and its development of capability profiles, seeks to contribute and be of value in both academic circles as well as for industry partners and system manufacturers.



Opsomming

Snelle Prototipering (SP) tegnologieë het die afgelope jare ongelooflike groei ondervind. Met die ontwikkeling van nuwe materiale tesame met nuwe prosesse, het elke tegnologie bygedra tot 'n diversiteit in moontlike toepassings vir 'n verskeidenheid van velde. Met 'n mikpunt van aaneenlopende verbetering, is dit egter krities om te verstaan presies wat elke individuele tegnologie se vermoëns is. Dit maak dit dan moontlik om toekomstige verbeteringe te vergelyk, of om selfs huidige prosesse met mekaar te vergelyk.

Die doel van hierdie navorsing was om vermoënsprofile van prominente SP tegnologieë te ontwikkel: 3D-Printing (3DP), Selective Laser Sintering (SLS) en Laminated Object Manufacturing (LOM) – waarin verskillende karaktereienskappe van elke tegnologie gemeet en gekwantifiseer word.

'n Vermoënsprofiel mag beskou word as 'n stel boustene wat 'n weerspieëling gee van die SP tegnologie se vermoë en word gedefinieer deur die kwantifisering van die volgende karaktereienskappe:

Akkuraatheid (beide dimensionele- en geometriese akkuraatheid)

Oppervlakgehalte metings

Treksterktes en verlengings

Bou- of vervaardigingstye, en

Kostes

Die rede waarom dit belangrik is om vermoënsprofile te ontwikkel berus by die behoefte om die verskillende prosesse met meer akkuraatheid te beskryf en te vergelyk – veral Z Corporation se 3DP. Alhoewel hierdie proses algemeen beskou word as baie bevoeg in vele areas, is min informasie al gepubliseer om hierdie opinie te ondersteun.

Wanneer gebruikers van hierdie tegnologieë hul masjiene tot die limiete druk, begin dit krities raak om presies te weet wat daardie grense is, sodat hulle met 'n sekere mate van sekerheid sal kan sê of hulle sal kan voldoen aan kliënte se behoeftes of verwagtinge. Die Suid-Afrikaanse industrie se



belangstelling in SP tegnologieë begin al hoe meer groei, en daarmee saam, begin vrae ontstaan tot watter mate snelle prototipering wel werkbare oplossings kan produseer vir hul probleme. Hierdie groeiende bewustheid van die Suid-Afrikaanse industrie begin dus ook nou nuwe paaie openbaar vir beide nuwe en ou probleme – maar uiteindelik, *voordat* kliënte egter bereid sal wees om geld te belê, sal hulle wil weet of snelle prototipering die standaarde gaan behaal wat nodig sal wees om juis hierdie oplossings te verwesenlik.

Op 'n meer breë vlak, beoog hierdie studie om ook 'n bydrae te maak in die groeiende navorsingsveld van snelle vervaardiging (SV). Hierdie is 'n term wat gedefinieer word as die vervaardiging van endgebruiker produkte, met die benutting van byvoegings-vervaardigings tegnieke. SV moet versekering bied vir komponente se werkverrigting op die lange duur vir die hele produk se lewenssiklus, of ten minste vir 'n gedefinieerde minimale tydperk in die geval van slytasie-parte [1].

Maar voordat dit moontlik sal wees om hierdie versekering te bied, moet mens eers die versekering kan bied van 'n proses se werkverrigting. Wanneer die prosesse betroubaar en deurlopende resultate lewer, word die volgende logiese vraag gestel: Wat presies, is hierdie proses in staat om betroubaar te lewer?

Hierdie studie beoog om juis hierdie vraag te beantwoord vir die drie prosesse (3DP, SLS en LOM) wat vroeër genoem is. Dienooreenkomstig, met die ontwikkeling van vermoënsprofile van hierdie prosesse, behoort hierdie studie van waarde te wees vir beide akademici, sowel as industrie-lede en vervaardigers van SP tegnologieë.



Acknowledgements

I will praise the Lord with my whole heart,

In the assembly of the upright and in the congregation.

The works of the Lord are great, studied by all who have pleasure in them.

His work is honourable and glorious,

And His righteousness endures forever.

Psalms 111:1-3

The author also wishes to extend his deepest gratitude to the following persons and organisations for contributing to the success of this study and the writing of this thesis report:

To my parents, Kennith and Marie de Beer for their unselfish, unfailing support and encouragement to the degree that only parents are able to give.

To my study leader, Prof Dimitri Dimitrov – thank you for your guidance, patience and giving me opportunities and opening doors for me that I would never be able to have opened on my own without your input and influence.

Thank you Prof Willie van Wijck, for helping to keep rigorous statistical standards in this report, and also for always being there for me with your encouragements and friendly advice.

Thank you Karin Lerm, and Maxwell Smith for your support, encouragement, and all the late nights you spent with me in the measuring lab. You inspired me to do my best.

To Dr. Kristiaan Schreve, for training and helping me with operations on the CMM to obtain the critical measurements that make up this study.

Thank you to Mr. Peter Humphreys for your advice and guidance in developing and producing the benchmark models used in this study. Your



years of experience have proven to be an invaluable resource in fine tuning our research.

To Ockert Strydom, for your help with conducting the tensile strength tests.

To Eugene Erfort and Morne Riddles from Peninsula Technikon, for producing the LOM benchmark parts.

And finally, thanks also to Dr Deon de Beer and Ludrick Barnard from the Free State Technikon for your role in producing the SLS benchmark parts. We look forward to continue this research in collaboration with you.



Table of Contents

DECLARATION	II
SYNOPSIS.....	III
OPSOMMING	V
ACKNOWLEDGEMENTS.....	VII
LIST OF FIGURES	XIII
LIST OF TABLES.....	XVI
GLOSSARY	XVII
1. INTRODUCTION	1
1.1 PROBLEM STATEMENT	1
1.1.1 <i>Lack of Detailed Specifications for Existing Technologies</i>	1
1.1.2 <i>Lack of Standardisation in Defining RP Process Capabilities</i>	3
1.2 RESEARCH OBJECTIVES	4
2. BACKGROUND.....	8
2.1 ESTABLISHED RPM TECHNOLOGIES RELEVANT TO THIS STUDY	8
2.1.1 <i>Stereolithography (SL)</i>	8
2.1.2 <i>Fused Deposition Modelling (FDM)</i>	10
2.1.3 <i>Laminated Object Manufacturing (LOM)</i>	11
2.1.4 <i>Selective Laser Sintering (SLS)</i>	12
2.1.5 <i>3D Printing (3DP)</i>	13
2.2 RPM APPLICATIONS	17
3. INDUSTRY GROWTH.....	20
3.1 ROLE PLAYERS	20
3.2 MARKET SHARES AND UNIT SALES	23
3.3 RPM IN SOUTH AFRICA	27
4. RESEARCH APPROACH AND EXPERIMENTAL BASE.....	30



4.1	TERMINOLOGY USEFUL FOR INTERPRETING PRECISION AND BIAS	30
4.1.1	<i>Test Method</i>	31
4.1.2	<i>Observation</i>	31
4.1.3	<i>Test Determination</i>	31
4.1.4	<i>Test Result</i>	32
4.1.5	<i>Accuracy</i>	32
4.1.6	<i>Bias</i>	33
4.1.7	<i>Precision</i>	33
4.1.8	<i>Repeatability and Reproducibility</i>	34
4.1.9	<i>Repeatability Limit</i>	35
4.1.10	<i>Reproducibility Limit</i>	36
4.1.11	<i>Analysis of Variance (ANOVA)</i>	36
4.1.12	<i>Confidence Interval</i>	36
4.2	VARIABILITY IN TEST RESULTS	37
4.2.1	<i>Sources of Variability</i>	37
4.2.2	<i>Error Model</i>	38
4.3	FACTORS INFLUENCING BIAS AND PRECISION IN 3DP	40
4.4	BENCHMARK APPROACH AND PROCEDURE	43
4.4.1	<i>Benchmarking Objectives</i>	43
4.4.2	<i>Analysis of Existing Benchmarking Parts</i>	43
4.4.3	<i>Benchmark Development</i>	44
4.4.4	<i>Benchmark Evaluation and Suggestions for Future Designs</i>	52
4.5	TEST METHODS FOR DATA GATHERING	59
4.5.1	<i>Dimensional Accuracy</i>	59
4.5.2	<i>Geometric Accuracy</i>	60
4.5.3	<i>Strength and Elongation</i>	67
4.5.4	<i>Surface Roughness</i>	70
5.	DISCUSSION OF RESULTS.....	71
5.1	DIMENSIONAL ACCURACY	71
5.2	GEOMETRIC ACCURACY	74
5.2.1	<i>Profile of a Surface</i>	74
5.2.2	<i>Circularity</i>	77



5.2.3	<i>Concentricity</i>	80
5.2.4	<i>Angular Tolerance</i>	82
5.3	STRENGTH AND ELONGATION	83
5.4	SURFACE ROUGHNESS.....	86
5.5	BUILD TIME AND COST.....	86
5.6	PART DESIGN INFLUENCE ON ACCURACY	87
6.	CONCLUSIONS AND RECOMMENDATIONS	93
	REFERENCES	97
APPENDIX A	DIMENSIONAL ACCURACY DATA SHEETS AND GRAPHS FOR 3DP PROCESS – USING PLASTER POWDER	A1
APPENDIX B	DIMENSIONAL ACCURACY DATA SHEETS AND GRAPHS FOR 3DP PROCESS – USING STARCH POWDER	B1
APPENDIX C	DIMENSIONAL ACCURACY DATA SHEETS AND GRAPHS FOR SLS PROCESS	C1
APPENDIX D	DIMENSIONAL ACCURACY DATA SHEETS AND GRAPHS FOR LOM PROCESS	D1
APPENDIX E	GEOMETRIC ACCURACY DATA SHEETS AND GRAPHS FOR 3DP PROCESS – USING PLASTER POWDER	E1
APPENDIX F	GEOMETRIC ACCURACY DATA SHEETS AND GRAPHS FOR 3DP PROCESS – USING STARCH POWDER	F1
APPENDIX G	GEOMETRIC ACCURACY DATA SHEETS AND GRAPHS FOR SLS PROCESS	G1
APPENDIX H	GEOMETRIC ACCURACY DATA SHEETS AND GRAPHS FOR LOM PROCESS	H1
APPENDIX I	STRENGTH AND ELONGATION DATA SHEETS AND GRAPHS FOR 3DP PROCESS – USING PLASTER POWDER	I1



**APPENDIX J STRENGTH AND ELONGATION DATA SHEETS AND GRAPHS FOR 3DP
PROCESS – USING STARCH POWDERJ1**



List of Figures

FIGURE 1.1: RESEARCH FRAMEWORK FROM GCC	5
FIGURE 2.1: REPRESENTATION OF THE STEREOLITHOGRAPHY PROCESS [4]	9
FIGURE 2.2: REPRESENTATION OF A FUSED DEPOSITION MODELLING PROCESS [4]	10
FIGURE 2.3: REPRESENTATION OF THE LOM PROCESS [4]	11
FIGURE 2.4: REPRESENTATION OF THE SLS PROCESS [6]	12
FIGURE 2.5: THE Z402 3D PRINTER [8]	13
FIGURE 2.6: STEPS IN BUILD PROCESS OF 3DP [8]	14
FIGURE 2.7: THE Z406 COLOUR PRINTER FROM Z CORPORATION [8]	15
FIGURE 2.8: THE Z810 PRINTER FROM Z CORPORATION [8]	15
FIGURE 2.9: THE ZPRINTER 310 FROM Z CORPORATION [8]	16
FIGURE 2.10: AUTOWAXER OVEN FROM Z CORPORATION [8]	17
FIGURE 2.11: MAJOR INDUSTRIAL SECTORS USING RP TECHNOLOGY [2]	18
FIGURE 2.12: DISTRIBUTION OF RP APPLICATIONS IN THE MARKET [2]	19
FIGURE 3.1: MODEL TO DESCRIBE CRITICAL ROLE PLAYERS FOR CONTINUED RP&M INDUSTRY GROWTH [9]	20
FIGURE 3.2: ANNUAL REVENUES FROM PRODUCTS AND SERVICES [2]	24
FIGURE 3.3: RP UNIT SALES WORLDWIDE PER YEAR [2]	24
FIGURE 3.4: CUMULATIVE MARKET SHARES BY MANUFACTURER [2]	26
FIGURE 3.5: PRODUCT DEVELOPMENT COLLABORATION NETWORK OF SA	28
FIGURE 4.1: FACTORS AND THEIR INTERRELATIONSHIPS THAT INFLUENCE ACCURACY [24]	41
FIGURE 4.2: PROCESS FLOW CHART INDICATING SOURCES OF VARIATION [24]	42
FIGURE 4.3: BENCHMARK CUBE USED FOR DETERMINING DIMENSIONAL ACCURACY ...	45
FIGURE 4.4: BENCHMARK PART USED FOR GEOMETRIC ACCURACY	49
FIGURE 4.5: DIFFERENT BUILD SECTIONS TO CREATE FULL-SCALE PARTS [31]	50
FIGURE 4.6: ILLUSTRATION OF JIG USED FOR ASSEMBLY OF SECTIONS [31]	50
FIGURE 4.7: DEFORMATION BEFORE AND AFTER USE OF WEB-SUPPORTS [31]	51
FIGURE 4.8: DIFFERENTIAL HOUSING BEFORE INVESTMENT CASTING AND AFTER ASSEMBLY [31]	51
FIGURE 4.9: POWDER DEFICIENT LAYERS OF TOP FACE OF BENCHMARK CUBE	54
FIGURE 4.10: FEATURES WHERE PAPER REMOVAL WAS PROBLEMATIC	56



FIGURE 4.11: PAPER REMOVAL DIFFICULTIES WITH 6 MM SLOTS.....	57
FIGURE 4.12: PAPER NOT CUT PROPERLY COMPARED TO A PROPER CUT	57
FIGURE 4.13: TWO HALVES OF DIFFERENTIAL HOUSING MADE WITH LOM (A) HELD SEPARATELY, AND (B) HELD TOGETHER	59
FIGURE 4.14: LOM BENCHMARK PART SHOWING FIXTURES OF TWO HALVES.....	61
FIGURE 4.15: DISTRIBUTION OF MEASURE POINTS FOR FREEFORM GEOMETRY	61
FIGURE 4.16: CIRCULAR FEATURES AND THEIR NOMINAL DIAMETERS	64
FIGURE 4.17: EXAMPLE OF CIRCULARITY MEASURES TAKEN	65
FIGURE 4.18: DIAGRAM DEPICTING THE DEFINITION OF CONCENTRICITY	66
FIGURE 4.19: ILLUSTRATION OF ANGULAR TOLERANCE	66
FIGURE 4.20: DIMENSIONS OF TYPE I TEST PIECE FOR TENSILE TESTING	67
FIGURE 4.21: POINTS WHERE DIMENSIONS OF TEST PARTS WERE MEASURED	69
FIGURE 4.22: ILLUSTRATION OF INFILTRATIONS WITH EPOXY RESIN	69
FIGURE 4.23: REPRESENTATION OF ROUGHNESS AVERAGE (R_A).....	70
FIGURE 5.1: AVERAGE ERRORS FOR DIFFERENT PROCESSES.....	73
FIGURE 5.2: STANDARD DEVIATIONS FOR DIFFERENT PROCESSES.....	73
FIGURE 5.3: ERROR DISTRIBUTION OF 3D GEOMETRIC FEATURES USING ZP100 POWDER.	74
FIGURE 5.4: ERROR DISTRIBUTION OF 3D GEOMETRIC FEATURES USING ZP14 POWDER.	75
FIGURE 5.5: ERROR DISTRIBUTION OF SLS PROCESS.....	75
FIGURE 5.6: ERROR DISTRIBUTION OF THE LOM PROCESS.....	76
FIGURE 5.7: CIRCULARITY OF 3DP WITH ZP100 POWDER.	78
FIGURE 5.8: CIRCULARITY OF 3DP WITH ZP14 POWDER.	78
FIGURE 5.9: CIRCULARITY OF THE SLS PROCESS.....	78
FIGURE 5.10: CIRCULARITY OF THE LOM PROCESS.....	79
FIGURE 5.11: CONCENTRICITY OF THE DIFFERENT PROCESSES CONSIDERED	81
FIGURE 5.12: ANGULAR DEVIATIONS MEASURED PER PROCESS.....	83
FIGURE 5.13: MAXIMUM TENSILE STRENGTHS OF ZP100.....	84
FIGURE 5.14: MAXIMUM TENSILE STRENGTHS OF ZP15E	84
FIGURE 5.15: XY FACE OF ZP14 CUBE WITH 4MM WALL THICKNESS.....	89
FIGURE 5.16: : XY FACE OF ZP100 CUBE WITH 4MM WALL THICKNESS	89
FIGURE 5.17: XY FACE OF ZP14 CUBE WITH 10MM WALL THICKNESS.....	90



FIGURE 5.18: XY FACE OF ZP100 CUBE WITH 10MM WALL THICKNESS	90
FIGURE 5.19: XY FACE OF ZP14 CUBE AS SOLID PART	91
FIGURE 5.20: XY FACE OF ZP100 CUBE AS SOLID PART	91
FIGURE 5.21: MAXIMUM DEVIATIONS FOR DIFFERENT WALL THICKNESSES AND MATERIALS	92



List of Tables

TABLE 3.1: 3D PRINTER SALES BY MANUFACTURER AND YEAR [2]	25
TABLE 4.1: SAMPLE AMOUNTS FOR VARYING K -VALUES	48
TABLE 4.2: PRINTING PARAMETERS FOR TEST PART USED IN TENSILE TESTING	68
TABLE 5.1: MEASURED BIAS AND PRECISION OF DIFFERENT PROCESSES.	72
TABLE 5.2: IMPORTANT VALUES OF ERROR DISTRIBUTION OF DIFFERENT PROCESSES	76
TABLE 5.3: CATEGORIES DEFINING REFERENCE AND ACTUAL ELEMENTS FOR CONCENTRICITY	80
TABLE 5.4: TENSILE STRENGTHS REPORTED BY WOHLERS [2]	85
TABLE 5.5: COST AND TIME INVOLVED PER PROCESS.....	87



Glossary

3DP Three-Dimensional Printing

A low-cost variation of RP (see below) that makes use of powder materials and a binder liquid to create three-dimensional geometries. 3DP is usually faster, less expensive, easier to use, and office friendly.

CAD **Computer-Aided Design or Drafting**

CAD is a necessary requirement to most rapid prototyping systems.

CMM **Computer Measuring Machine**

A computer-controlled measuring instrument that is used to measure accuracy and surface profiles of objects to a very high degree of accuracy.

CT Scan **Computed Tomography Scan**

Also known as a CAT scan. A computerized x-ray procedure that produces cross-sectional images of the body. The images are far more detailed than x-ray films.

FDM **Fused Deposition Modelling**

An RP (see below) process that makes use of extruded filaments of polymer materials or wax to produce 3D objects layer by layer.

FFF **Freeform Fabrication**

Another (perhaps more descriptive) name for methods of rapid prototyping

**IT Grade****International Tolerance Grade**

A series of tolerance grades that ranges from IT01 to IT16 and is used to control the size of objects. Each tolerance grade defines a certain maximum deviation for within a specific length range. IT01 – IT7 is used for measuring tools; IT5 – IT11 is applicable to controlling fitting parts; IT8 – IT14 is used for materials; and IT12 – IT16 is a range used for large manufacturing tolerances.

LOM**Laminated Object Manufacturing**

A rapid prototyping process that makes use of pre-treated layers of paper that are laminated together to build 3D objects. The two-dimensional profile of each layer is cut with a laser beam.

MRI Scan**Magnetic Resonance Imaging**

A scanning device that uses a magnetic field, radio waves, and a computer. Signals emitted by normal and diseased tissue during the scan are assembled into an image.

 R_a **Roughness Average**

R_a is used to give an indication of the roughness quality of a surface, and is calculated by an algorithm that measures the average length between the peaks and valleys and the deviation from the mean line on the entire surface within the sampling length. R_a averages all peaks and valleys of the roughness profile and then neutralizes the few outlying points so that the extreme points have no significant impact on the final results. It's a simple and effective method for monitoring surface texture and ensuring consistency in measurement of multiple surfaces

**RM Rapid Manufacturing**

This term is defined as the manufacture of end-use products using additive manufacturing techniques. RM must guarantee long-term consistent component use for the entire product life cycle or for a defined minimal period for wearing parts.

RP Rapid Prototyping

RP is a term used to denote a class of additive fabrication processes by which almost any geometry of three-dimensional objects are created automatically from computer-generated data. Parts can be manufactured either within a few hours or days. In conjunction with several downstream post-processing, lot sizes that range from fifty units to several thousands units can be produced.

SL Stereolithography

An RP technology that makes use of UV-curable photopolymer liquids to produce three-dimensional objects. Each layer of the liquid is hardened by exposing it to beams from a UV-laser.

SLS Selective Laser Sintering

An RP technology that binds together a wide variety of powdered materials such as polymers, foundry sand, and metal. The binding process is facilitated by the heat of a laser beam that brings the material to near-melting point in order to fuse its individual particles together.

STL Standard Triangular Language

A file format used to convert 3D CAD model data to physical parts using RP systems. The STL format uses triangular facets to approximate the shape of an object.



1. Introduction

Rapid prototyping (RP) refers to the physical modelling of a design using digitally-driven, additive processes. RP systems quickly produce models and prototype parts from 3D computer-aided design (CAD) data, CT and MRI scans, and data from 3D digitizing systems. Using an additive approach, RP systems join liquid, powder, or sheet materials to form physical objects. Layer by layer, RP machines process polymers, paper, ceramic, metal, and composites from thin, horizontal cross sections of a computer model [2].

Organizations make use of RP to optimize the process of product development, improve quality and reduce costs. The many applications that already exist include patterns for prototype tooling and for cast metal, visual aids for engineering and for toolmakers, functional models and proposals to name only a few.

RP is having a great impact on the manufacturing industry. Research and a continual drive to improve RP systems and related materials have led to the ability for the technology to produce finished goods in limited lot sizes. Some believe this practice, termed rapid manufacturing (RM), will rapidly grow and ultimately overshadow the rapid prototyping and rapid tooling markets [2].

With RM only beginning to show positive initial growth, rapid prototyping and tooling is however still very relevant today, and is constantly expanding its fields of applications as the market is steadily becoming more aware of the technologies and their capabilities.

1.1 Problem Statement

As RP technologies are expanding, two issues that are being identified in this study need to be addressed:

1.1.1 Lack of Detailed Specifications for Existing Technologies

The well-established RP technologies, such as Stereolithography (SL) and Selective Laser Sintering (SLS) have over their years of existence become well defined by numerous researchers. Subsequently the



capabilities of these technologies are well documented and reliable for use. With other existing and emerging technologies, this is unfortunately not always the case. Many RP technologies still lack critical information that is reliable concerning their respective capabilities in areas such as accuracy, strength, surface finish, and other characteristics such as build time and cost. Many questions relating to the different factors that influence these characteristics also need to be answered so that users will be able to control their processes better.

The Three Dimensional Printing (3DP) technology based on MIT's (Massachusetts Institute of Technology) ink jet technology is one such technology that is in need of research to determine its various capabilities. When Z Corporation began commercialising this technology in 1996 into a variety of printers, the technology was first classified as a typical "concept modeller", since it is able to create 3D models very quickly and cheaply in comparison to other processes. Its popularity has since grown, and Z Corporation now holds the fourth position in cumulative annual machine sales [2].

With the resourceful use of different materials in combination with suitable post-treatment techniques, the technology's classification as a concept modeller has expanded to include a wide variety of additional applications far beyond the original expectations of only generating design iterations. The 3DP technology has successfully been used in applications such as pattern making for investment and vacuum casting as well as for bridge tooling, design aids for tooling equipment, and several medical applications like creating reconstructive surgery aids and prototyping of human organs and implants. With the colour capabilities of the new range 3DP machines, this process is able to satisfy further scientific and engineering needs such as molecular modelling, finite element analysis, thermal analysis and mould flow analysis.



With the advent of these new applications, many promising avenues for further development are opening up. But for these endeavours to be successful and fully exploited, it now becomes imperative to understand better what the capabilities of this technology are. Once the capability of the 3DP process has been defined, a foundation will have been laid from which all role players can make informed decisions.

1.1.2 Lack of Standardisation in Defining RP Process Capabilities

As mentioned above, in many cases the characteristics of many RP systems have not yet been evaluated to its full extents. In the other cases where systems' capabilities have been investigated and reported, the **format** and **level of detail** in which this was done has not always been the same.

Take for instance the characteristic of accuracy, which is a common capability that each RP system should report on. In some cases, the format for accuracy is reported only as a percentage, implying that the deviations of error submit to some linear equation (for all nominal dimensions). In other cases, accuracy is reported as some deviation related to a set distance; for example, 0.1mm per 100mm.

The level of detail used to report the capabilities for each of these characteristics is also a significant consideration. Take again the example of accuracy. The current level of detail that is mostly reported in literature is limited to only reporting on linear dimensional accuracy like the two formats mentioned in the previous paragraph. But what about geometric accuracy? And what about dispersion and other measures of repeatability? Is the accuracy the same for each of the three build axes? These are only some of the questions that begin to open up deeper levels of detail – the answers of which must be communicated to different groups of interested people, depending on who the user is and what the application will be. And the levels of detail that should be reported, should always be included up to the point where the factors that influence the measured value(s) can still



be controlled – e.g. accuracy for different build axes is still a relevant level of detail, because separate scaling factors can still be applied to control the accuracy in each individual axis. The question of relevancy and applicability is then up to readers to selectively determine, not the researchers.

The responsibility of researchers should be to create a standardized structure by which the results of their research can be communicated on a more consistent level.

The author proposes that the solution is to develop so-called capability profiles – i.e. standard structures that relate measured results of a prescribed set of characteristics – of the different RP technologies.

1.2 Research Objectives

The objectives of this study form part of a larger framework of research objectives that are being pursued at the Global Competitiveness Centre in Engineering (GCC) at Stellenbosch University, and are depicted in Figure 1.1.

The two outer columns, Research and Development, form the two legs and pillars for continuous improvement of technologies. The inner column contains the elements that Jacobs has constructed in his “Wheel of progress” [3]. He describes these components to represent the different areas of where research is required for increasing performances in the RP&M industry. He continues to note however, that during the process of improvement, one of these elements soon becomes a limiting factor, impeding the progress until breakthroughs are made. This study aims to contribute to research being done on the component area of Processes.

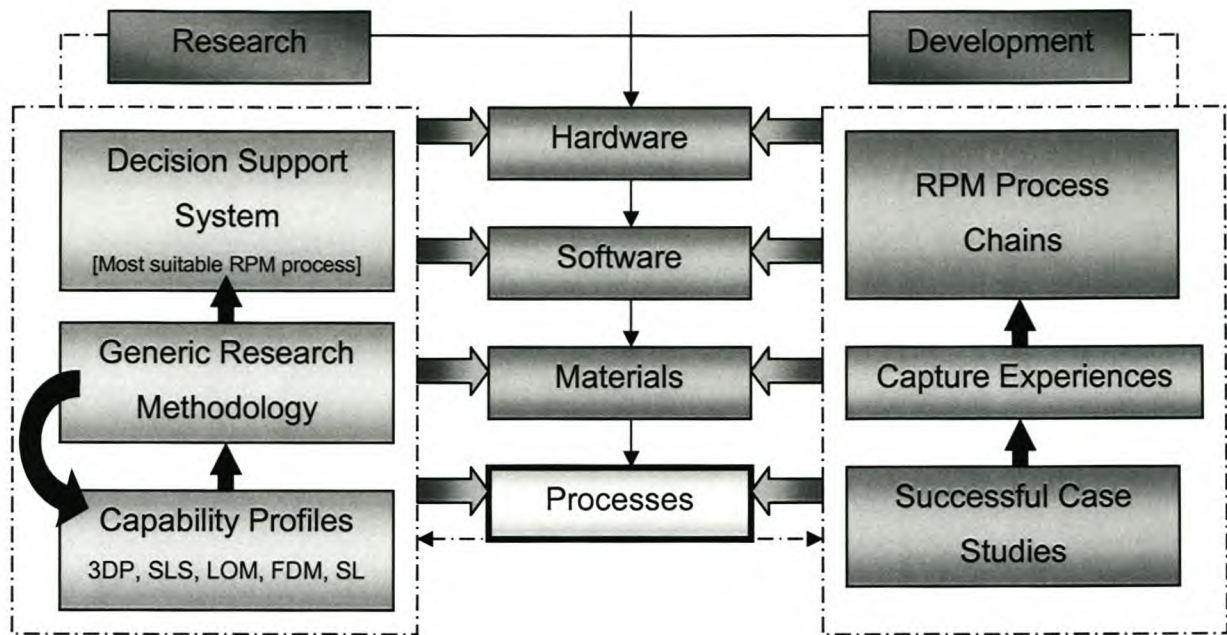


Figure 1.1: Research framework from GCC

Each of the outer columns shown in Figure 1.1 over time gives feedback to these components of the wheel of progress. The Development column on the right contains a progressive aim to create appropriate (and creative) RPM process chains that include best practices for each process. These process chains are captured from experiences gained in completing successful case studies.

The progressive aim on the side of research (Research column on the left) is to develop decision support systems that will aid users in selecting the most suitable RPM process for their need or application. The sources for developing such decision support systems will be the prior development of capability profiles of each of the processes being considered. Once experience is gained in developing capability profiles of some existing RPM processes, the next step is to develop a set of guidelines or instructions that would standardise future research attempts that characterise other existing RPM processes.

The circular arrow that loops back to the lowest block in the Research column of Figure 1.1 implies that this process of developing capability profiles through following a generic research methodology would be an iterative process, because current systems are continually being



improved along with new systems that are emerging. But as the output of RPM processes systematically become more stable and predictable, the knowledge obtained from studying each RPM process will become the structure on which decision support systems will be based.

Two specific research objectives were set for this study, namely; (i) to investigate the capability profiles of Three Dimensional Printing (3DP), Selective Laser Sintering (SLS) and Laminated Object Manufacturing (LOM) and (ii) during this process, investigate the different formats and levels of detail by which their characteristics can be expressed. The steps that were followed to obtain these objectives can be summarized by the following:

1. Identify the different factors that influence accuracy of the 3DP process
2. Identify the factors that create variability in the process chain of the 3DP process.
3. Investigate and develop suitable experimental procedures that will capture measured results necessary to describe each capability profile.
4. Investigate and develop suitable benchmark parts for the different characteristics that make up a capability profile.
5. Create the benchmark parts using the applicable processes and materials considered within the scope of this research.
6. Apply the experimental procedures and obtain measurement results, continuously ensuring integrity and availability of the data.
7. Investigate, compare and interpret the data obtained from measurements.
8. From these conclusions, make recommendations for further research.

With the completion of these objectives, this study will not only be a benefit in terms of pure research, but more importantly, system users



and the public will now have a standard by which to compare these technologies with other competing technologies in its class.



2. Background

2.1 *Established RPM technologies relevant to this study*

An historical overview of the principal and emerging RP technologies will shortly be discussed and is largely extracted from research done by Wohlers Associates, Inc. [2].

2.1.1 *Stereolithography (SL)*

The first commercially available RP technology was developed in 1987 by 3D Systems. The technology was named SL and involves a process that solidifies layers of ultraviolet (UV) light-sensitive liquid polymer using light from a laser. 3D Systems' first commercially available system was the SLA-1, and became the forerunner of today's popular SLA-250 machine.

As with all other RP systems, the necessary first step to creating parts with SL begins with the generation of a CAD model of the designed object. Solid CAD models are more reliable to use, but surface models that have closed and well-defined surfaces that may be considered to be "watertight" have also been used successfully.

From this CAD model, a Standard Triangulation Language (STL) file is created. Since its inception, the STL format has become the industry standard for RPM. It is supported by every major CAD vendor and has also been adopted by all the various RPM system suppliers as the primary interface with their system software.

Creation of the STL file involves the transformation of all boundary surfaces of the CAD model such that each surface is covered by a series of interlocking triangles. In doing so, the part becomes represented by a set of X, Y and Z coordinates at each of the three vertices of these triangles. Along with the coordinates, a fourth piece of information is included which is an index that describes the orientation of the surface normal. This feature is necessary to ensure



that a clear distinction is made between inner and outer surfaces. The triangles may be as large or as small as desired, but smaller triangles result in finer resolution of curved surfaces and improved part accuracy through reduced chordal deviations. Smaller triangles however, increase the amount of data used to describe the part, and may subsequently dramatically increase file sizes. Therefore, depending on the user's needs and preference, a trade-off is ensued between storage space and part accuracy.

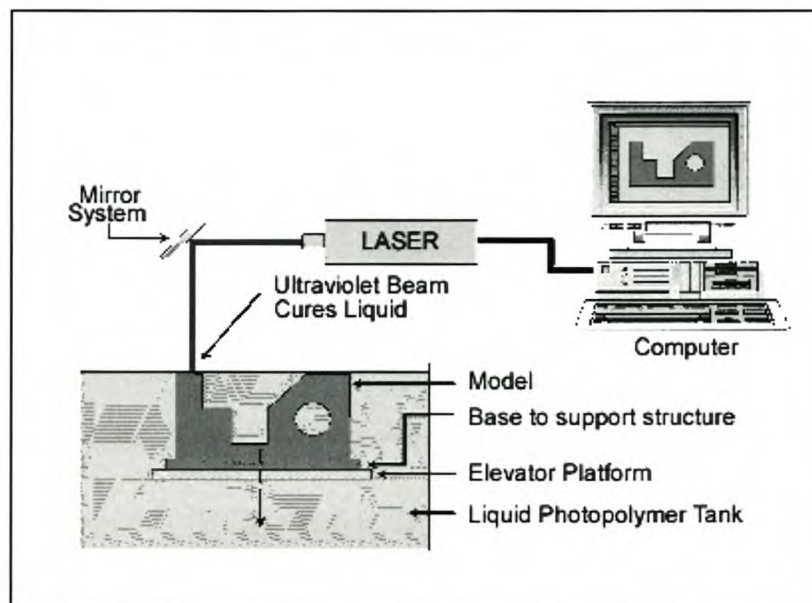


Figure 2.1: Representation of the Stereolithography process [4]

Once the STL file has been generated from the CAD file, the next step involves creating a **SLice** (SLI) file by dividing the part into hundreds of layers (depending on the part height). After the STL and SLI files have been created, multiple SLI files are merged to form a final build file, which can now be used to generate a physical part. The build process starts by creating a series of supports, which are necessary for a number of reasons. Supports act like fixtures in conventional machining. Simply stated, they hold the object in place during the build process. They also act as a means of securing certain adjacent parts of geometry that would otherwise float away from the rest of the geometry. When the part has been built to completion, post-curing is done to ensure that any uncured photopolymer material is solidified.



The built part is then removed and the final product is revealed once the supports have been removed.

2.1.2 Fused Deposition Modelling (FDM)

Fused Deposition Modelling is a process that constructs objects directly from CAD data by using a temperature-controlled head that extrudes thermoplastic material layer by layer. The FDM process starts with importing an STL file of a model into a pre-processing software. This model is oriented and mathematically sliced into horizontal layers varying from $\pm 0.13 - 0.35$ mm thickness. A support structure is created where needed, based on the part's position and geometry. After reviewing the path data and generating the tool paths, the data is downloaded to the FDM machine. A representation of this process is shown in Figure 2.2.

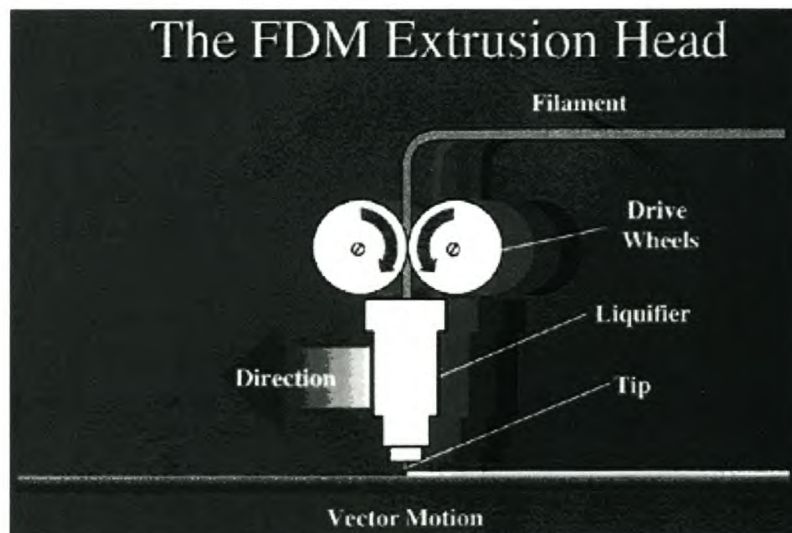


Figure 2.2: Representation of a Fused Deposition Modelling process [4]

FDM offers two types of support structure; break away support structure (SLA) and water-soluble support structure (WaterWorks). WaterWorks uses a soluble material that is dissolved in a water/solvent solution, enabling to simply wash away the model supports. This means that supports can be located in far hidden regions of the part since the manual labour that is required for the



other technologies is eliminated. WaterWorks however, is only compatible with ABS material.

2.1.3 *Laminated Object Manufacturing (LOM)*

Helisys (formerly Hydronetics, Inc.) in Torrance, California, brought their first RP system out in 1991, called Laminated Object Manufacturing. This process produces parts from thin, laminated materials. Through a combination of heat and pressure, a pre-applied adhesive is activated, and consecutive layers of the material (typically adhesive coated paper) are bonded together. The individual cross-sections are cut using a 25- or 50-watt carbon dioxide (CO₂) laser, emitting in the infrared spectrum, at a wavelength of 10.6 microns, Jacobs [3]. The surrounding area of the part sections automatically forms a support around the part being created. In order to facilitate its removal the laser then crosshatches this area. Figure 2.3 illustrates this LOM process. As with stereolithography, the process begins with the creation of CAD, STL and build files. As shown in the figure, the material is applied in a continuous manner and fed onto a take-up roller at the other end of the sheet.

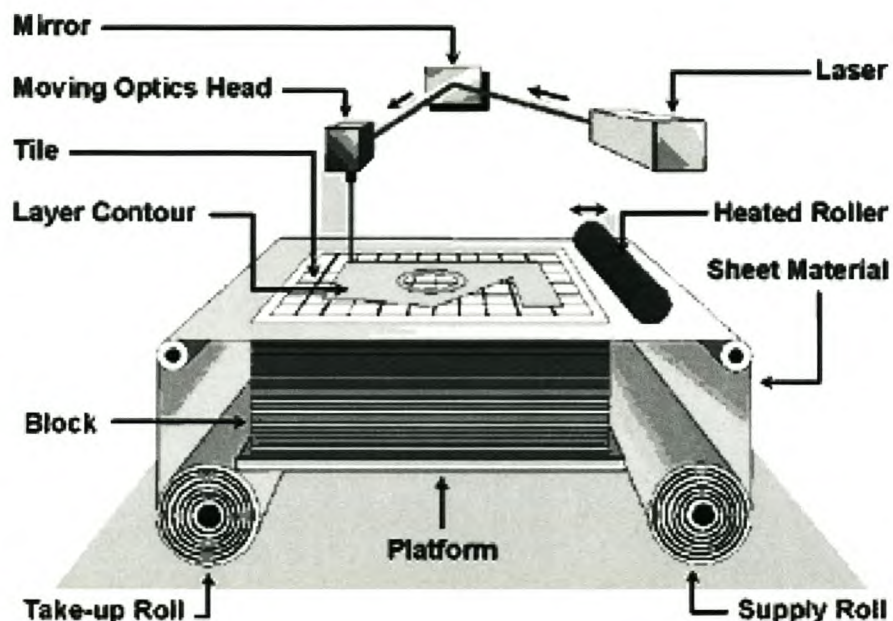


Figure 2.3: Representation of the LOM process [4]



2.1.4 Selective Laser Sintering (SLS)

Selective laser sintering was originally developed at the University of Texas in Austin and first became available from DTM (now a part of 3D Systems) in 1992, [2]. It is a layer manufacturing process that allows one to generate complex 3D parts by consolidating successive layers of powder material on top of each other [5]. It uses thermal energy from a laser to fuse the particles of powdered materials together. The SLS process employs three pistons (as shown in Figure 2.4), of which two are feed pistons. The other holds an elevated build platform that is lowered while subsequent layers of powder are applied and selectively fused to solidify a cross-section. To minimize the required laser output, the powder is maintained at an elevated temperature, just below its fusing point. Due to the explosive potential of small powder particles with large surface-to-volume ratios at elevated temperatures, the process chamber of the machine is operated in an inert gas environment. Commercial machines differ by using either Argon or Nitrogen gas.

In 1994, the German company EOS commercialised a machine called EOSINT, based on laser sintering technology. This range of machines allows the creation of parts in polystyrene, polyamide, glass-filled polyamide, foundry sand, and metal.

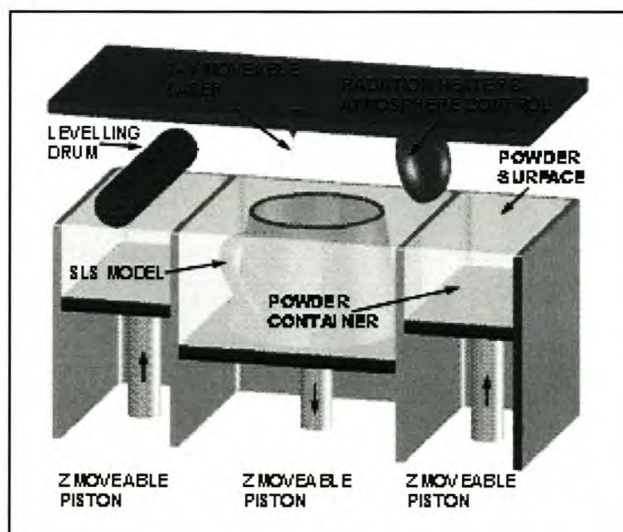


Figure 2.4: Representation of the SLS process [6]



The EOSINT P machine is designed for building parts in thermoplastics powders, while the EOSINT S is designed specifically for foundry sand. The EOSINT M machine can accommodate metal powders. EOS also refers to this metal sintering process as Direct Metal Laser Sintering (DMLS).

2.1.5 3D Printing (3DP)

The Three-Dimensional Printing (3DP) process was invented and patented by Sachs et al. [7] from the Massachusetts Institute of Technology (MIT) in December 1989, and licensed to Z Corporation in 1994. The first system, the Z402, was commercialised in 1996. The Z402 system is the fastest RP machine on the market with a building speed of 25 to 50 mm per hour in the z-axis direction. It produces models using starch- and plaster-based powder materials and a water-based liquid binder.

As with the SLS process, 3DP also makes use of pistons to facilitate the building process. Z Corp.'s 3D printers however, have two pistons and not three. One controls the powder feed tray, while the other controls the build platform. Figure 2.5 shows the Z402 3D printer from



Figure 2.5: The Z402 3D printer [8]



Z Corporation, while Figure 2.6 displays the cycle of steps that are repeated in order to produce a model on this machine. Due to availability, the Z402 printer was used in this study to represent the 3DP process during development of capability profiles.

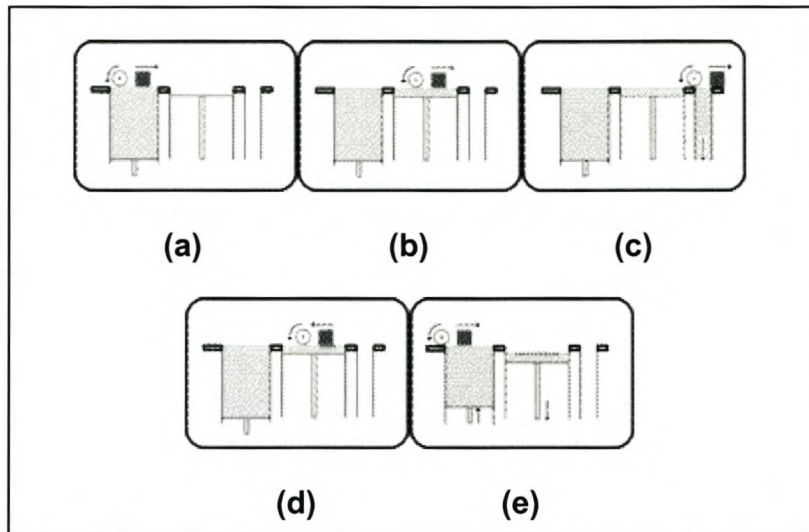


Figure 2.6: Steps in build process of 3DP [8]

Figure 2.6 (a): Collect powder

Figure 2.6 (b): Spread powder

Figure 2.6 (c): Discharge excess powder

Figure 2.6 (d): Print a single layer

Figure 2.6 (e): Feed piston up one layer; build piston down one layer.

In May 2001, Z Corporation replaced the Z402C printer with their Z406 colour printer (Figure 2.7). Later in 2001, it introduced its large format Z810 machine (Figure 2.8).



Figure 2.7: The Z406 Colour printer from Z Corporation [8]

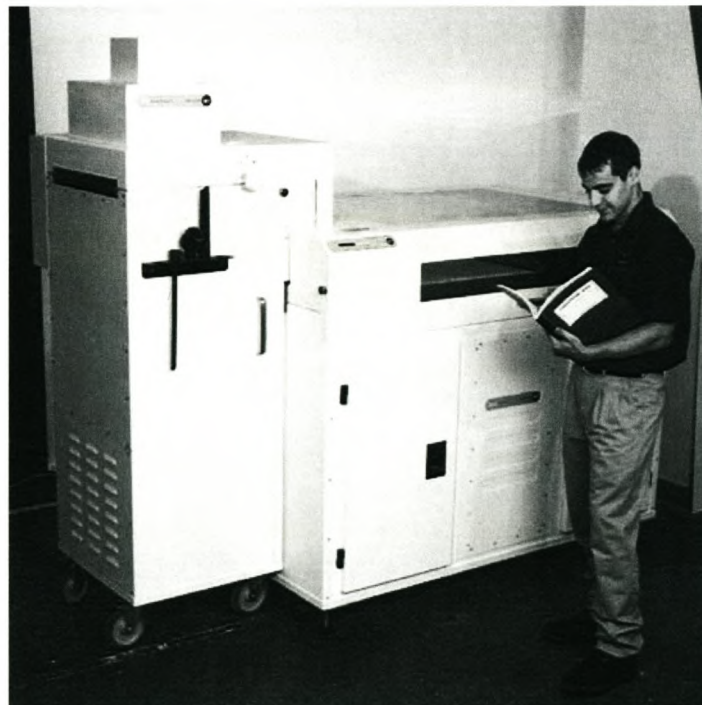


Figure 2.8: The Z810 printer from Z Corporation [8]



The newest printer that Z Corporation introduced to the market last year (2003), is the ZPrinter 310, shown here in Figure 2.9.

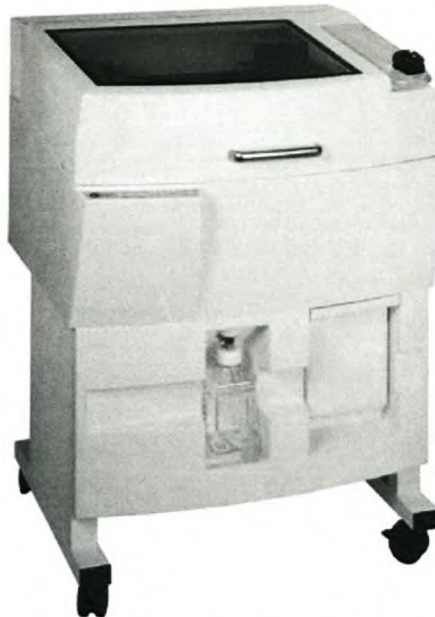


Figure 2.9: The ZPrinter 310 from Z Corporation [8]

The ZPrinter 310 is 50% to 100% faster than the Z400 which it replaced, and is half as fast as the Z406 machine. It is a monochrome printer, but it can process the full range of materials, which include the starch-based (zp14 and zp15e), the plaster powder (zp100), as well as the ZCast material.

ZCast material is a new material that was introduced in April 2002, and is a composite of plaster and ceramic powder. ZCast is a method of printing foundry tooling directly on the 3D printer and is then used to produce metal castings such as aluminium and other non-ferrous metals.

When parts are produced with Z Corporation's 3D printers, they emerge as fragile, "green" parts which need to be strengthened before further post-processing should be applied. Various infiltration materials (depending on the powder used) are available for this purpose. The starch-based powders are infiltrated by dipping the part into a container of melted surgical wax within an oven (shown in Figure 2.10).



Figure 2.10: Autowaxer oven from Z Corporation [8]

For the plaster-based powder (zp100), the parts are infiltrated with an epoxy resin called Zi580.

Recently in 2003, a new infiltrant material called Z-Max was introduced which is claimed to dramatically increase strength while reducing cost. Wohlers reports that on plaster prototypes, Z-Max offers 24 MPa tensile strength and 50 MPa flexural strength – a 100% improvement over the zi580's 14 MPa tensile strength and 25 MPa flexural strength, [2]. Concerning the cost, the Z-Max material is 32.6% cheaper than zi580, [2]. An added advantage is also its transparency, which will preserve the colour of parts produced on the Z406 machine.

2.2 RPM applications

A few of the significant applications of RP have already been mentioned in Chapter 1's introduction. Now a more thorough look will be taken at the different industries that are using these technologies, and how they are being applied.

The motor vehicle industry has been the leader in using RP systems since their development and acceptance into the market. As shown in Figure 2.11, the motor industry is still the chief user of RP technologies. Close behind them is the consumer products market, and combined, they constitute more than half of the total. Meanwhile, Wohlers mentions



that academic institutions have grown by nearly two percentage points over the past year, [2]. The “Other” category includes industries such as professional sporting goods, non-consumer and non-military marine products, and various other industries that do not fit into the named categories. He continues to state that the chart below has been constructed from estimates of 22 RP system manufacturers and 40 RP service providers, based on knowledge of their customers.

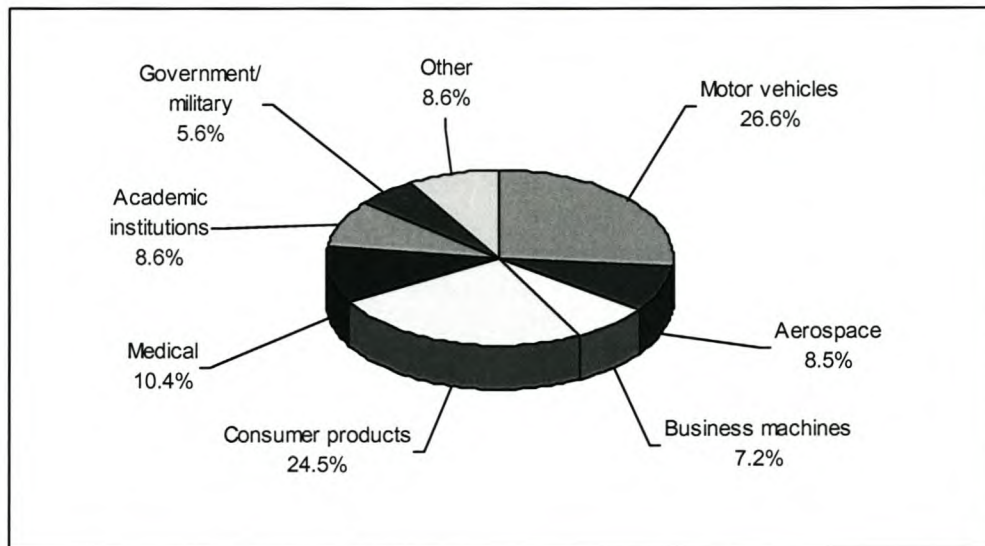


Figure 2.11: Major industrial sectors using RP technology [2]

Figure 2.12 shows how these different industries are applying the technology to their products and services. The length of each bar reflects the numerical responses from the industries surveyed by Wohlers. The significant applications are fit/assembly and the creation of functional models. These two categories together, constitute 37% of the total, while nearly 26% of all RP models are used as visual aids – for engineering, toolmaking, quote request, and proposals. What Figure 2.12 however does not show, is that a simple model is often used for two or more applications.

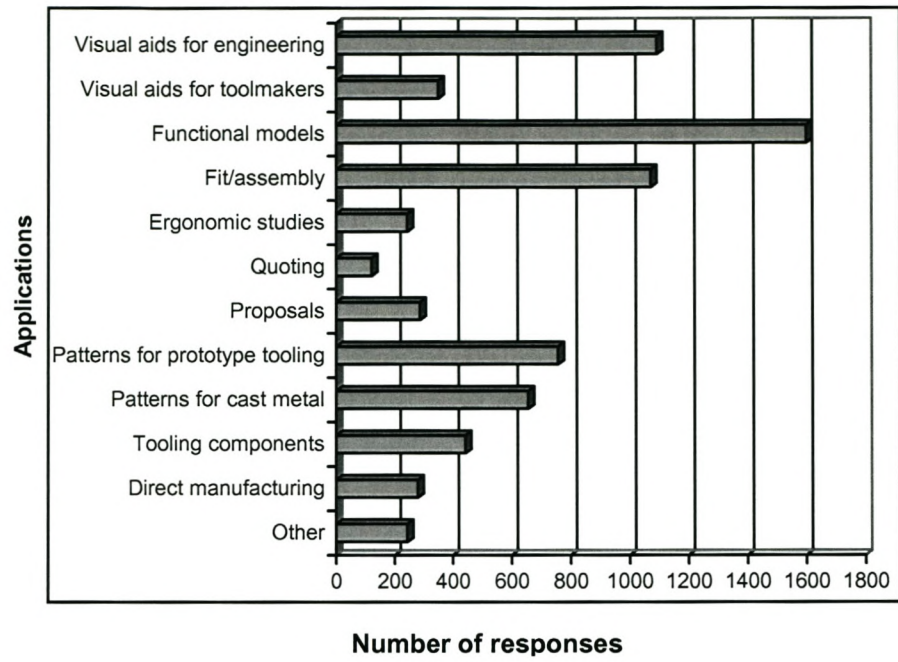


Figure 2.12: Distribution of RP applications in the market [2]

3. *Industry growth*

3.1 *Role players*

In an endeavour to identify the critical role players in industry that will provide the foundation and structure for continued growth, the following model (Figure 3.1) has been developed to describe their respective influences and contributions towards establishing the rapid manufacturing industry.

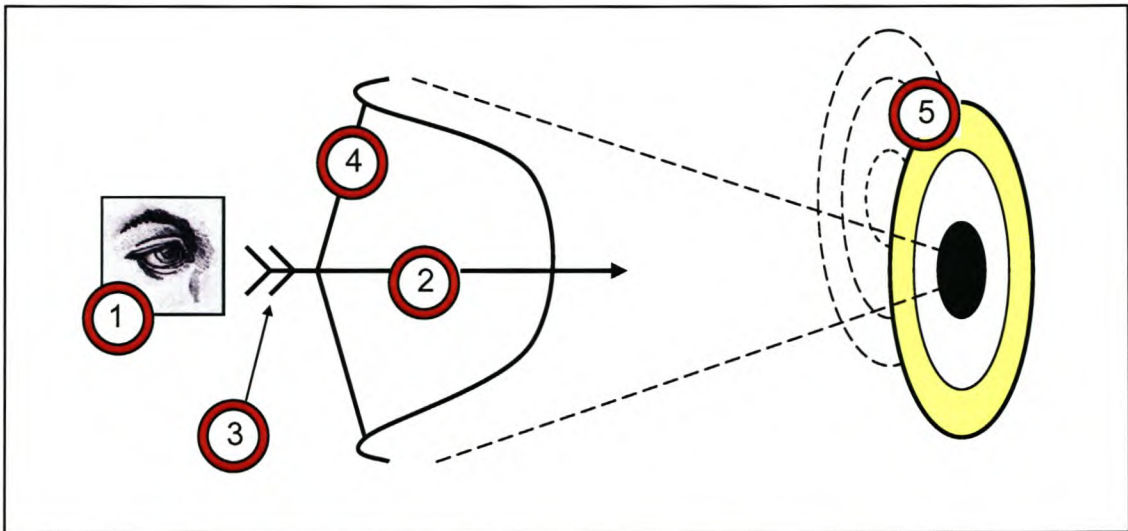


Figure 3.1: Model to describe critical role players for continued RP&M industry growth [9]

1 Industry surveyors

In any situation where one requires to move from point A to point B, it is necessary to determine where point A lies in relation to point B. In other words, one needs to know where one is, to be able to plan which route to take in reaching the end goal or destination. This then is true also in regard to the rapid prototyping and manufacturing (RP&M) industry.

Industry surveyors and analysts play a critical role in establishing perspective in the global surge for process improvement. Although they do not necessarily perform physical research themselves, they add invaluable support in shedding light upon areas where research is most



effectively needed. In essence, they determine which target to shoot the arrow at.

2 System, software and material developers

The system developers are regarded in this model as the organisations that are responsible for creating the technology of RP&M. At present, Stereolithography (SL), Selective Laser Sintering (SLS), Fused Deposition Modelling (FDM), Laminated Object Manufacturing (LOM) and 3DP form the five leading technologies of the industry [2]. A large number of new technologies are however already penetrating into the marketplace with innovative designs that will attract the attention of prospective system users.

System developers not only develop the hardware for these systems, but most also develop the required software and related materials. But for the new emerging technologies, there is still a wide scope for independent material scientists and software developers to take advantage in collaborating with prospective system developers and inventors.

This is however not such an easy process, and the focus should first be on collaboration between these different parties. By doing so, improvements to materials, hardware and software will be speeded up and they will continue to deliver prompt solutions for increased performance. They are the arrow – the vehicle that will transfer desires into results.



3 System users

The system users can be considered both in-house users and outsourced service providers. They are the feathers in the arrow. Besides being the ones that purchase RP systems, they are critical by the way in which they make processes more efficient. An arrow without any feathers will be unbalanced and will miss the target. In the same way, system users make the applications of these technologies more effective. While industry surveyors direct the thrust of the development effort, system users refine the applications of new technologies. By putting the technology into use, and grappling with unforeseen problems, innovatively developing new ways to overcome stumbling blocks – system users drive process improvement at its very core.

4 Government

The stimulating energy that is necessary to support continued growth for research and development is financial aid from government. In the model depicted in Figure 3.1, the government is represented by the bow that holds the arrow. It supports the development of new technology, and the amount of resources provided is represented by the distance the string is withdrawn – thereby determining the distance that results will reach. The government is most certainly not the only source of funding that will determine the success of research of a specific RP system or process – System developers also provide large quantities of funding that provides extra thrust. The role of government however, is not one that should be characterised by indifference or detached interest. Its active participation in assuring support will ultimately result in the development of solid infrastructures for stimulating industry growth and job creation.

5 Product developers

One should not disregard the influence that product developers themselves have on facilitating continued growth and inception of this technology into the marketplace. Product developers are regarded as



those individuals and organisations that produce products or provide services to the market. The model depicts these product developers as the target that is trying to be reached by the other role players. But as depicted by the use of dashed lines, the target is however, not a stationary one. This is so, because the demands of end-users are continually changing.

But this should not necessarily be regarded as a disadvantage. Once product developers become more aware of the capabilities that this technology can provide, they will become more specific in their demands to the industry. But the primary role that product developers can play at this stage is to exhibit an interest in the capabilities of these RP technologies. This should ignite innovative demands and applications, and ultimately enhance overall confidence for its acceptance into the marketplace.

3.2 *Market shares and unit sales*

The annual average growth of RP since its beginning until the year 2000 has been very positive. Figure 3.2 from Wohlers [2], gives estimated annual revenues (in millions of dollars) of services and products. The figures for 2003 and 2004 are forecasts. *Products* include RP systems, system upgrades, materials, and aftermarket products, such as third-party software and lasers. *Services* include revenues generated from RP models and patterns produced on RP systems by service providers, RP system maintenance contracts, training seminars, conferences, expositions, advertising, publications, contract research, and consulting. Although its initial growth has been very exciting, the last two years have unfortunately been disappointing. It can be seen from Figure 3.2 that the service sector has suffered the most. Something that is encouraging though, is the fact that machine unit sales were up, with 3D printer sales faring especially well, [2].

The numbers of these annual unit sales are presented in Figure 3.3. Again, the sales figures for 2003 and 2004 are forecasts. In 2002, 1482

machines were sold, compared to 1299 in 2001 – an increase of 14.1%. In 2003, Wohlers Associates expects annual unit sales to grow by 15.7% to 1715 units. In 2004, unit sales are forecast to grow by 16.3% to 1995 total units, [2].

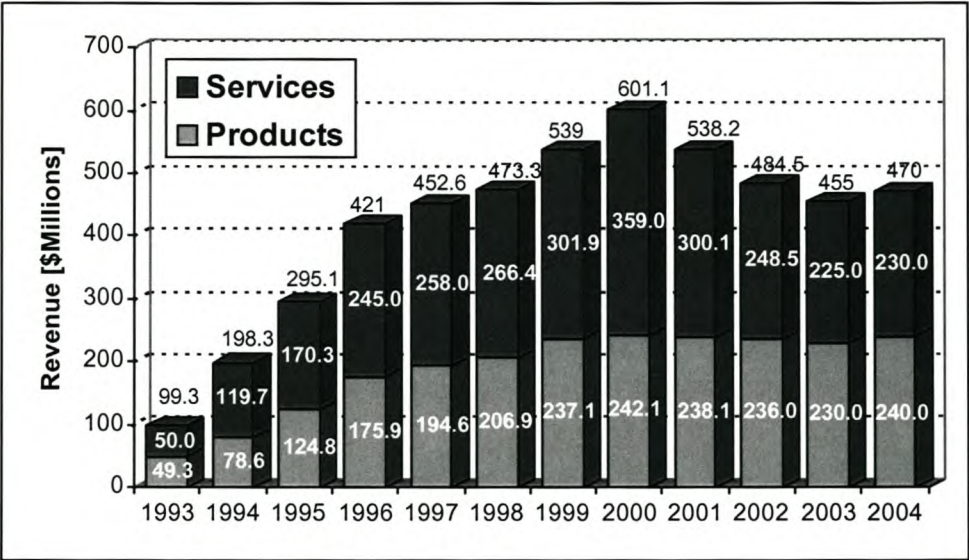


Figure 3.2: Annual revenues from products and services [2]

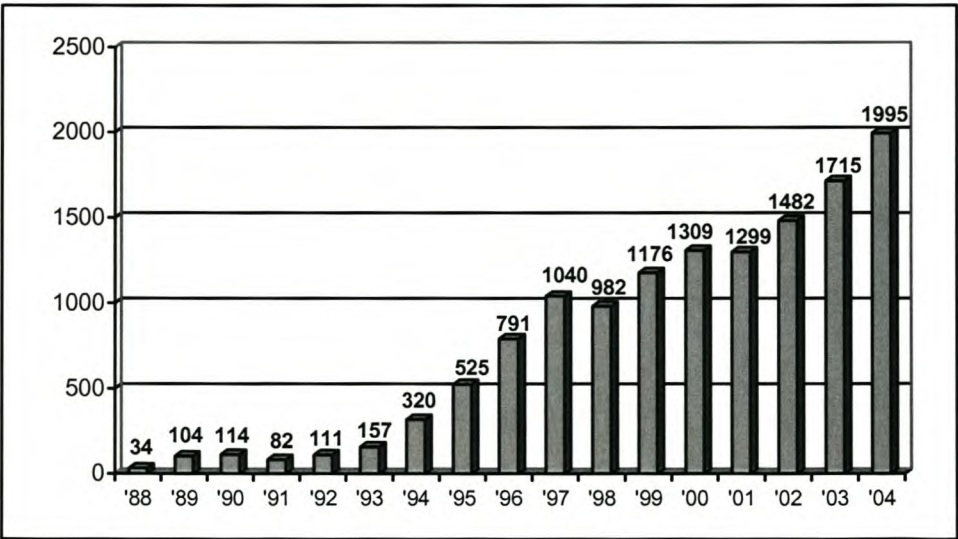


Figure 3.3: RP unit sales worldwide per year [2]

Wohlers Associates reports that the unit sales of 3D printers also showed a significant increase of 33.9% from 490 units in 2001 to 656 units in 2002 (see Table 3.1). With the increasing sales of 3D printers, the average RP system price continues to drop. This decline in average



system price is the reason unit sales can increase while revenues from sales decreased (Figure 3.2).

The cheaper sales-price of 3D printers is giving them a competitive edge in the fight for survival of new and existing system manufacturers.

Table 3.1: 3D printer sales by manufacturer and year [2]

Company	Machine	1996	1997	1998	1999	2000	2001	2002	Total
3D Systems	ThermoJet, Actua	14	113	90	155	227	182	88	869
Stratasys	Prodiy, Genisy, Dimension	90	40	60	75	115	95	305	780
Z Corp.	Z40X series, Z810	1	7	48	105	170	188	210	729
Objet	Quadra, QuadraTempo	-	-	-	-	-	24	51	75
Envisiontec	Perfactory, Bioplotter	-	-	-	-	-	-	2	2
Total		105	160	198	335	512	489	656	2455

Note: 1998 Actua and all Prodigy, Genisys, and Dimension figures are estimates from Wohlers Associates.

The total unit sales to date per manufacturer is shown in Figure 3.4. By comparing Table 3.1 with Figure 3.4, it is significant to note that 305 out of the 463 (65.9%) units sold by Stratasys in 2002 were their 3D printer machines.

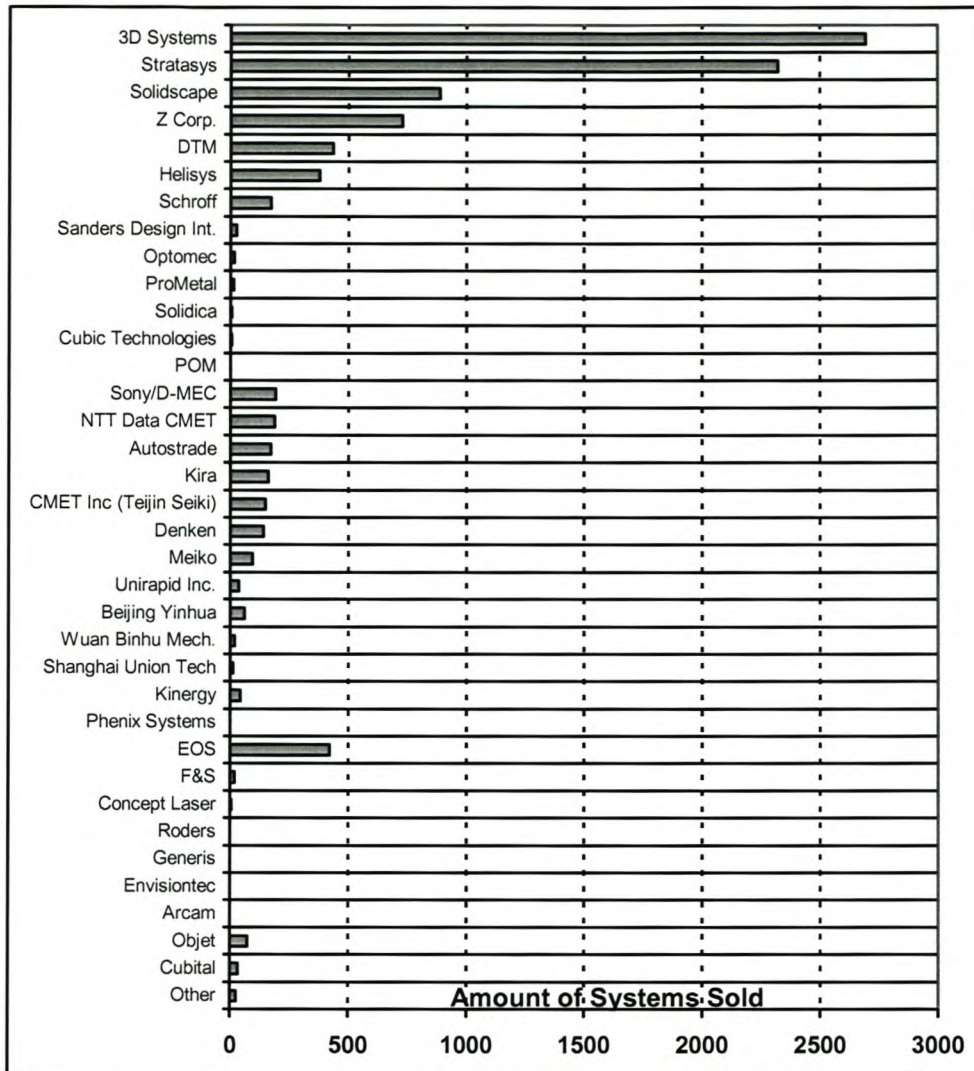


Figure 3.4: Cumulative market shares by manufacturer [2]

The tables and figures shown above present some conclusions, and can be summarized by:

- From Figure 3.2, it is interesting to note that the decline in revenue was mostly due to a decline in services rendered, while revenue contributions from products stayed relatively stable. So although an increase in unit sales (Figure 3.3) seems promising, because of cheaper product prices, it is having little effect on increasing total annual revenues. Reasons for the decline in the need for services should be investigated and properly addressed.



- The unit sales of the 3D printers all showed increases except for 3D Systems. Stratasys sold the most 3D printers in 2002 and showed an especially significant jump of 221.1% from their previous year.
- These industry growth trends seem to indicate that 3D printing is set to play an increasingly important role in the future of RP processes.

3.3 RPM in South Africa

RP has been actively applied in South Africa for the past twelve years, [2]. It is continuously growing as new developments are introduced and market confidence is won.

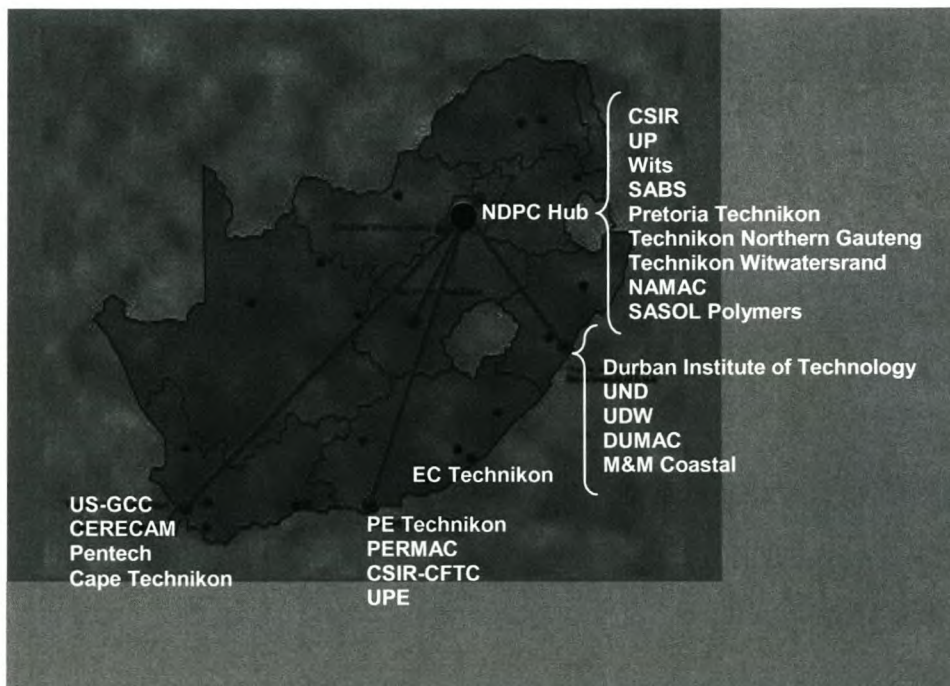
The Rapid Product Development Association of South Africa (RAPDASA) is a body that represents important academic and industrial organizations and has brought together the different RP contributors in South Africa into a collaborative network. By means of annual conferences and workshops, the network continues to be strengthened by the exchange of ideas and research.

South Africa currently possesses several centres that together employ the five leading RP technologies. Figure 3.5 below shows the distribution of the different centres. The main hub of collaboration between these different centres is the National Product Development Centre (NPDC) and is situated in Pretoria. The other collaborating centres are as follows:

- The Automotive Industry Development Centre (Pty) Ltd. in Gauteng,
- The Centre for Rapid Prototyping and Manufacturing (CRPM) in Bloemfontein,
- The Global Competitiveness Centre in Engineering in Stellenbosch,



- The Centre for Rapid Product Development at Peninsula Technikon in Bellville,
- The Centre for Engineering Research at the Durban Institute of Technology,
- The Automotive Components Technology Station at Port Elizabeth Technikon,
- The Centre for Design and Manufacturing at Potchefstroom University,
- The Materials Modelling Centre at the University of the North in Polokwane, and
- The Design Institute of the SABS in Pretoria.



Source: Willie du Preez - NDPC

Figure 3.5: Product development collaboration network of SA

The distribution of technologies that the combined network now occupies include the following:

- SLA 500 and FDM 1500 at NPDC Pretoria



- SLA 250 and ThermoJet with a private consortium (CLAM) in the north of the country.
- SLA 250, laser sintering (Sinterstation 2000 and EOS P 380), and ModelMaker II at the CRPM in Bloemfontein
- ZPrinter™ 310 System soon to replace existing Z402 3D printer at GCC in Stellenbosch, and
- LOM 1015 at Peninsula Technikon in Bellville.
- ThermoJet at the Technology Station for Automotive Components at the Port Elizabeth Technikon.

The continued and growing partnerships that already exist should continue to benefit the South African industry in general and its product developers and service providers.



4. Research Approach and Experimental Base

During this study, attention was given to the detail of every test procedure or experiment that was undertaken. Where possible existing standards and procedures were followed. In other cases, the steps that were followed are documented in this chapter.

Along with performing actual tests in accordance to specific standard procedures and under strict conditions, the importance of describing and reporting the results in acceptable formats should not be forgotten. Due to the variety in applications of RP systems, the author is aware that the results to these tests will be significant to different people for different reasons. Technically minded individuals who drive and lead the endeavours of system improvements typically desire to have their information delivered in statistical format, allowing them to make conclusions concerning bias and precision while also allowing them to determine the reliability of the reported numbers. Non-technical individuals in the RP&M industry who are experts in fields such as finance, corporate executives and salesmen also desire reliability of reported numbers. Their focus however, is usually on clear and straightforward conclusions concerning best- and worst-case scenarios. There decisions are usually also driven by financial considerations.

This chapter focuses on explaining the terminology applied in describing the results. It continues to discuss the concept and importance of selecting a benchmark part appropriate for the specific test being performed. All along, the relevant steps, procedures and test conditions that were followed during this study are described.

4.1 Terminology Useful for Interpreting Precision and Bias

Reporting on the results of tests usually require the use of concise statements that contain specific terminologies in order to prevent any possibility of ambiguity or misrepresentation of the results. This section gives definitions that have been quoted from ASTM International standard guides and practices [10],[11],[12],[13],[14],[15],[16],[17] to



these terminologies. ASTM standard guides and practices are well-accepted in South Africa too, as ASTM standards have been the basis for formulating many SABS standards.

4.1.1 Test Method

ASTM Standard E177 describes a test method as “a definitive procedure for the identification, measurement, and evaluation of one or more qualities, characteristics, or properties of a material, product, system or service that produces a test result.” [13]

For the purposes of this study, the above definition of a test method will apply, but with a narrower interpretation that does not include measurement or evaluation of any services.

4.1.2 Observation

For the purposes of this study, as also used in ASTM Standard Practice E177 [13], observation or observed value should be interpreted as the most elemental single reading or corrected reading obtained in the process of making a measurement. This statement is a narrower interpretation than is given in ASTM Terminology E456 [15] in that the latter applies to non-quantitative as well as quantitative test methods.

4.1.3 Test Determination

For a quantitative test method, a test determination may be described as (1) the process of calculating from one or more observations a property of a single test specimen, or as (2) the value obtained from the process. Thus, the test determination may summarize or combine one or more observations.

Examples:

- (1) The measurement of the density of a test specimen may involve the separate observation of the mass and the volume of the specimen and the calculation of the ratio mass/volume. The density calculated



from the ratio of one pair of mass and volume observations made on one specimen is a test determination.

- (2) The determination of the thickness of a tensile test specimen may involve averaging micrometer calliper observations taken at several points along the specimen. Each value obtained from averaging the different observations will result in one test determination.

4.1.4 Test Result

A test result is the value obtained by carrying out the complete protocol of the test method once, being either a single test determination or a specified combination of a number of test determinations.

In general, a test method describes not only the manner in which each test determination is to be made, but also the number of test determinations to be made and how these are to be combined to provide the test result.

4.1.5 Accuracy

Accuracy is a generic concept of exactness related to the closeness of agreement between the average of one or more test results and an accepted reference value. Unless otherwise qualified, the use of the word “accuracy” by itself is to be interpreted as the accuracy of a test result. The accuracy of a test result is the closeness of agreement between the test result and the accepted reference value. It depends on both the precision and the bias of the test method. According to ASTM Standard Practice E177 [13], referring to Mandel [18] and Murphy [19] in its document, there are two schools of thought on defining the accuracy of a measuring process. In either case, the measurement process must be in a state of statistical control, otherwise the accuracy of the process has no meaning:



- (1) The closeness of agreement between the accepted reference value and the average of a large set of test results obtained by repeated applications of the test method, preferably in many laboratories.
- (2) The closeness of agreement between the accepted reference value and the individual test result, [20],[21].

ASTM Standard Practice E177 [13] continues to state that in (1), the imprecision is largely eliminated by the use of a large number of measurements and the accuracy of the measuring process depends only on bias. In (2) the imprecision is not eliminated and the accuracy depends on both bias and imprecision. In order to avoid confusion resulting from use of the word “accuracy”, only the terms precision and bias should be used as descriptors of test methods.

The ASTM Guide C1215 [16] also agrees with the above, and since this study relies to a large extent on following ASTM standards, it will likewise prefer using separate bias and precision values in statements concerning accuracy. If however the term accuracy is used in text, it shall refer to the combined effects of precision and bias.

4.1.6 *Bias*

Bias is a constant positive or negative deviation of the method average from the correct value or accepted reference value. Bias represents a constant error as opposed to a random error [16]. The data from which the bias estimate is obtained, should be statistically analysed to establish bias in the presence of random error. In statistical terminology, an estimator is said to be unbiased if its expected value is equal to the true value of the parameter being estimated.

4.1.7 *Precision*

Precision is a generic concept related to the closeness of agreement between test results obtained under prescribed like conditions from the measurement process being evaluated. It ultimately describes the dispersion of a set of measured values. The greater the dispersion or



scatter of the test results, the poorer the precision. Measures of dispersion, usually used in statements about precision, are, in fact, direct measures of imprecision [13]. Precision is usually expressed as the standard deviation or some multiple of the standard deviation.

Other measures frequently used to express precision are relative standard deviation, variance, repeatability, reproducibility, confidence interval, and range. In addition to specifying the measure and the precision, it is important that the number of repeated measurements upon which the precision estimated is based also be given.

It is strongly recommended that a statement on precision of measurement procedure include the following [16]:

- a) A description of the procedure used to obtain the data,
- b) The number of repetitions, n , of the measurement procedure,
- c) The sample mean and standard deviation of the measurements,
- d) The measure of precision being reported,
- e) The computed value of that measure, and
- f) The applicable range or concentration.

This study will follow the above recommendation when reporting on the results obtained from various test methods employed.

4.1.8 Repeatability and Reproducibility

Repeatability relates to the closeness of agreement between test results obtained under repeatability conditions. These conditions are such that the test results are obtained with the same test method in the same laboratory, by the same operator with the same equipment, in the shortest practical period of time, using test units or test specimens taken at random, from a single quantity of material that is as nearly homogeneous as possible [13].

Reproducibility is a general term for a measure of precision applicable to the variability between single test results obtained in different



laboratories using test specimens taken at random from a single sample of material [13].

ASTM Standard C1215 [16] however, elaborates on these two definitions by quoting the following from Kendall and Buckland [22]:

"In some situations, especially interlaboratory comparisons, *precision* is defined by employing two additional concepts: *repeatability* and *reproducibility*. The general situation giving rise to these distinctions comes from the interest in assessing the variability *within* several groups of measurements. *Repeatability*, then, refers to the within-group dispersion of the measurements, while reproducibility refers to the between-group dispersion. In interlaboratory comparison studies, for example, the investigation seeks to determine how well each laboratory can repeat its measurements (repeatability) and how well the laboratories agree with each other (reproducibility). Similar discussions can apply to the comparison of laboratory technicians' skills, the study of competing types of equipment, and the use of particular procedures within a laboratory. An essential feature usually required, however, is that repeatability and reproducibility be measured as variances (or standard deviations in certain instances), so that both within- and between-group dispersions are modelled as a random variable. The statistical tool useful for the analysis of such comparisons is the analysis of variance."

4.1.9 *Repeatability Limit*

This is the value below which the absolute difference between two individual test results obtained under repeatability conditions may be expected to occur with a probability of approximately 95 % [15].

$$r = 1.96\sqrt{2}s_r \approx 2.8s_r \quad (\text{Eq. 4.1})$$

where:

r = 95 % repeatability limit,



s_r = repeatability standard deviation

4.1.10 Reproducibility Limit

Similar to repeatability limit, however this is the value below which the absolute difference between two test results obtained under reproducibility conditions may be expected to occur with a probability of approximately 95 % [15].

$$R = 1.96\sqrt{2}s_R \approx 2.8s_R \quad (\text{Eq. 4.2})$$

where:

R = 95 % reproducibility limit,

s_R = reproducibility standard deviation

4.1.11 Analysis of Variance (ANOVA)

ANOVA is the body of statistical theory, methods, and practices in which the variation in a set of data is partitioned into identifiable sources of variation. Sources of variation may include analysts, instruments samples, and laboratories. To use the analysis of variance, the data collection method must be carefully designed based on a model that includes all the sources of variation of interest [16].

4.1.12 Confidence Interval

This is an interval used to bound the value of a population parameter with a specified degree of confidence, known as the confidence level. The confidence interval has different values for different random samples.

When providing a confidence interval, analysts should give the number of observations on which the interval is based. The specified degree of confidence is usually 90, 95, or 99%. The form of a confidence interval depends on underlying assumptions and intentions. Usually, confidence intervals are taken to be symmetric, but this is not necessarily a prerequisite.



It is important to realize that a given confidence-interval estimate either does or does not contain the population parameter. The degree of confidence is actually in the procedure. For example, if the interval (9,13) is a 90% confidence interval for the mean, we are confident that the procedure (take a sample, construct an interval) by which the interval (9,13) was constructed will 90% of the time produce an interval that does indeed contain the mean. Likewise, we are confident that 10% of the time the interval estimate obtained will not contain the mean. Note that the absence of sample size information detracts from the usefulness of the confidence interval. If the interval were based on five observations, a second set of five might produce a very different interval. This would not be the case if 50 observations were taken, [16]

4.2 *Variability in Test Results*

Carrying out the steps set out in a test method to obtain final test results involves a number of known or unknown factors that could influence these results. The specifications in the test method try as far as possible to eliminate these sources of variability, but there always exists some element of change in the final test results that cannot be totally eliminated. This variability will ultimately be included as an inherent component of the test result.

4.2.1 *Sources of Variability*

Typical sources of variability involved with the actual application of a test method includes *interpretation* of the written document by a *specific test operator*, who uses a *specific unit and version of the specified test apparatus*, in the particular *environment* of his testing laboratory, to evaluate a *specified number of test specimens* of the material to be tested. These can be summarised as the following [13]:

- a) Operator variability
- b) Apparatus variability
- c) Environment variability



d) Sample variability

e) Time variability

The tests performed in this study also took into account several sources of variability. These will be discussed in Section 4.3 as well as in subsequent sections where the test method of each capability profile characteristic is presented.

4.2.2 *Error Model*

This is an algebraic expression that describes how a measurement is affected by error and other sources of variation. The model may or may not include a sampling error term [16].

A measurement error is an error attributable to the measurement process. The error may affect the measurement in many ways and it is important to correctly model the effect of the error on the measurement.

ASTM Standard C1215 [16] discusses two models, the additive and the multiplicative error models, which are regarded as common error models. In the additive model, the errors are independent of the value of the item being measured. Thus, for example, for repeated measurements under identical conditions, the additive error model might be:

$$X_i = \mu + b + \varepsilon_i \quad (\text{Eq. 4.3})$$

where:

X_i = the result of the i^{th} measurement,

μ = the true value of the item,

b = a bias, and

ε_i = a random error usually assumed to have a normal distribution with mean zero and variance σ^2 .



In the multiplicative model, the error is proportional to the true value. This type of error model is commonly used by analytical chemists to model percent recovery, and might be given as:

$$X_i = \mu b \varepsilon_i \quad (\text{Eq. 4.4})$$

where the meanings of the units are the same as above. There are many ways in which errors may affect a final measurement. The additive model is frequently assumed and is the basis for many common statistical procedures. The form of the model influences how the error components will be estimated and is very important, for example, in the determination of measurement uncertainties. In this study, the additive error model will be applied.



4.3 Factors Influencing Bias and Precision in 3DP

Apart from the unknown factors of variability mentioned previously, there are a number of (controllable) factors, which influence differently the achievable combination of precision and bias for the 3DP process. These include, firstly, the basic process parameters such as different scaling factors for X, Y and Z, and the core- and shell saturation values. These parameters are recommended by the system manufacturer with different values for different materials and purposes and should be checked for every new build. The impact on the accuracy of these factors as well as of the part location within the build platform has been investigated, and “optimal” values have been suggested [23]. The scaling factor employed per 3D build however, is also dependent on the particular environmental conditions and therefore cannot be declared as optimal in general. Scaling factors would typically differ not only for different laboratories, but may even differ for the same laboratory on different days if conditions such as temperature and humidity are not controlled. Based on experience and research results done at the Global Competitiveness Centre in Engineering (GCC), some other factors have been identified and have a much higher impact on accuracy. These include the following:

- Material used (MU);
- Nominal dimensions – small, medium, large (ND);
- Build orientation – in relation to the different axes (BO);
- Geometric features and their topology – e.g. open or closed contours (GF);
- Wall thickness – shell thickness, solid (WT);
- Post-treatment procedures (PT); and
- Infiltrating agent (IA).

The internal relationship among these factors is shown in a qualitative manner in Figure 4.1. The next step in research concerning these factors is to develop a mathematical model to quantify the interrelationships between them, and how they influence overall accuracy. The development of a mathematical model of the accuracy dependence is, however, an important task of the ongoing research and falls beyond the scope of this study.

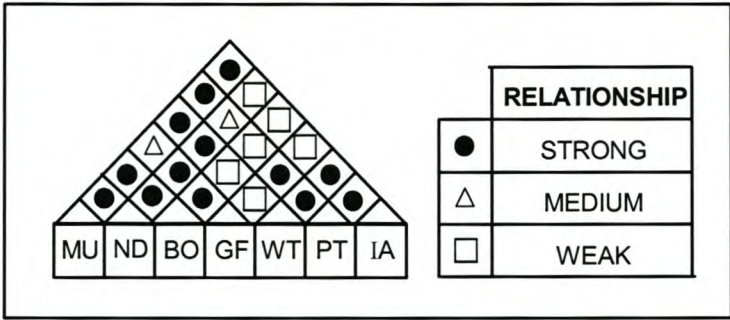


Figure 4.1: Factors and their interrelationships that influence accuracy [24]

One of the first tasks in developing a test method for determining the accuracy of the 3DP process, was to try and identify as many factors that could possibly influence the process, or create possible variability therein. This was accomplished through creating a flow diagram of the process as a whole, and at each stage speculate what these factors could be. Figure 4.2 on the following page shows this flow diagram that was developed.

After identifying the possible sources of variation, an attempt was made throughout this study, during the design and realisation of the relevant test methods, to control as many of these factors where possible.

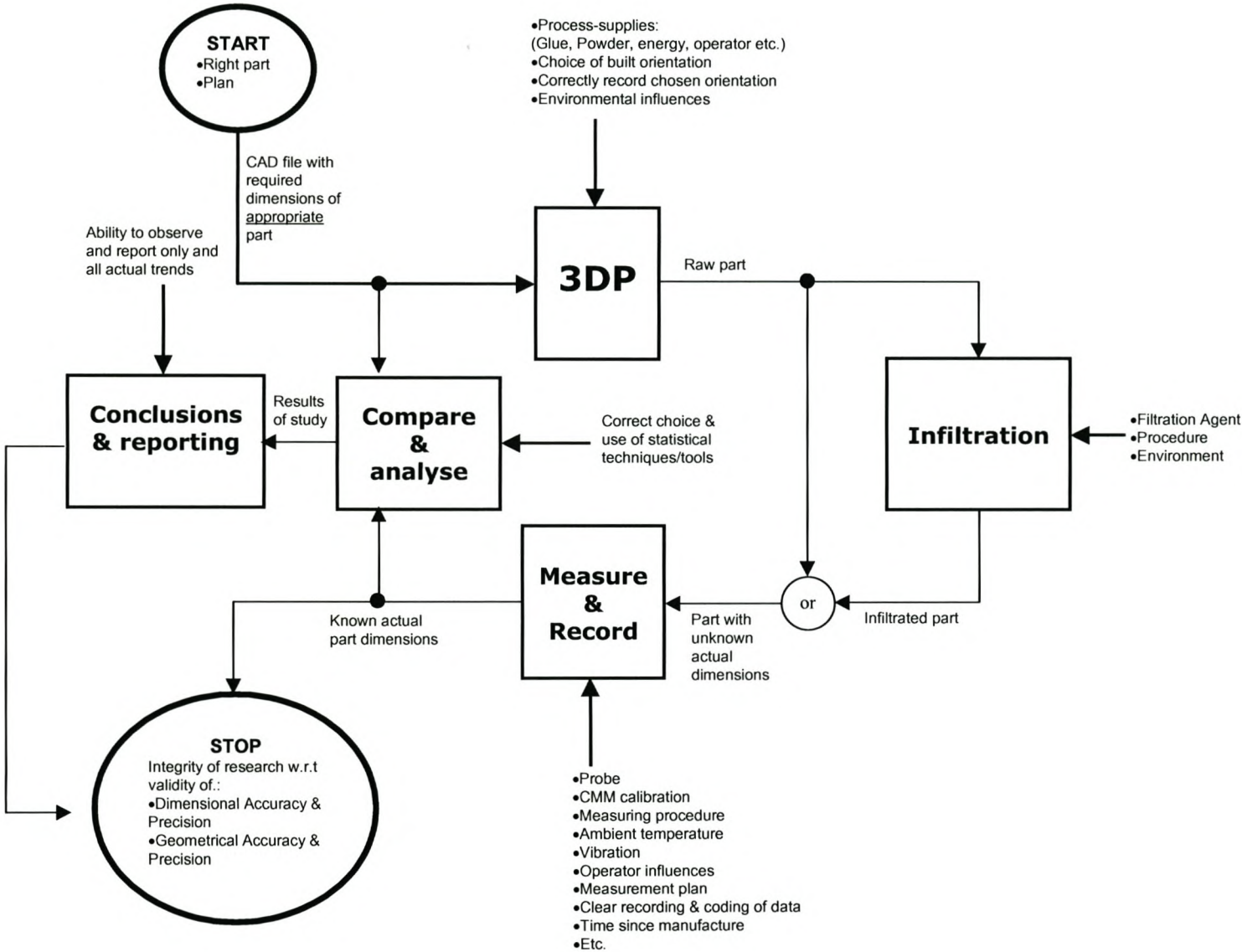


Figure 4.2: Process Flow Chart Indicating Sources of Variation [24]



4.4 Benchmark Approach and Procedure

4.4.1 Benchmarking Objectives

The execution of benchmarking tests is a traditional practice and necessary for all kinds of high productive and capital-intensive equipment. The objective of the benchmarking can however, differ substantially from case to case. In the case of this study, a benchmarking procedure was initially developed with the sole purpose to evaluate the performance capabilities regarding accuracy of the 3DP process as implemented by Z Corporation. The scope of the research later grew to incorporate a comparative study of other RP processes. The benchmark parts were essentially designed and chosen to try to accommodate all other potential RP processes that may possibly be evaluated in future comparative research studies. But reality proved that the benchmark designs required slight alterations to accommodate the LOM process (in order to facilitate de-blocking and post-printing paper removal).

4.4.2 Analysis of Existing Benchmarking Parts

There are several benchmark geometries presented and discussed in the relevant literature [25], [26], [27], [28], [29]. Jacobs [26] provides a list of properties for the ideal accuracy test part. Childs and Juster [28] undertook a critical analysis on existing benchmark geometries before they suggest another one. However, the most important observation that was deduced during this search for existing benchmarking parts, is that no adequately comparative investigation concerning the accuracy characteristics for large dimensions in all **three** axes was conducted. It has to be mentioned that with the exception of the "stereolithography user part" [26], all other benchmark parts were developed for comparison of different RP-processes.



4.4.3 *Benchmark Development*

Based on an extensive literature study as mentioned above, previous own research, and in-house experience, a series of conceptual designs were considered. It soon became apparent that one single design would not be adequate to describe all the features under investigation. Therefore an alternative approach was taken to use an actual component as a second benchmark [28]. In this way the ability of the process to create manufacturing features of real parts, such as free-form surfaces, fillets and draft angles, can be tested. It was therefore essentially decided to use one benchmark design to investigate the dimensional accuracy capability of the RP processes, and a second benchmarking part to characterize the geometric capabilities.

For dimensional accuracy a range of fine, small, medium and large distances were considered for measurement. For that purpose a special cube – 190 x 190 x 190 mm, reflecting the largest (theoretical) build capability in Y- and Z-directions, was designed (henceforth denoted Benchmark Cube). In order to describe the accuracy of the 3D printer with respect to all three build axes, and to compare the X, Y, and Z axes effectively, the same physical part features had to be repeated on at least three different faces that are perpendicular to the respective build directions. Figure 4.3 shows the Benchmark Cube that was used, as well as a sectioned view indicating a grid of inner support structures that was deemed necessary to aid with part and feature integrity.

The study further sought to identify if there would be a difference in the printer's capability to produce open features in comparison to solid features of the same dimensions. Thus the physical features that were chosen to describe distance measures were slots and protrusions of varying lengths. Three faces of the cube have protrusions, each with their features of nominal dimensions aligned along a positive build axis of the printer – while the remaining faces of the cube have slots with

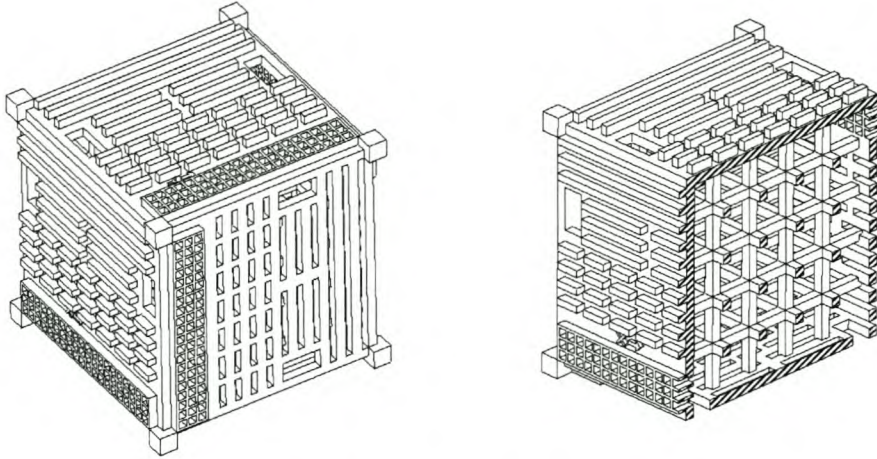


Figure 4.3: Benchmark Cube used for determining dimensional accuracy

their features also in line with the respective build axes of the printer. The nominal dimensions that were arbitrarily chosen were 2, 6, 18, 54, and 162 mm. These five nominal dimensions were chosen arbitrarily but still in such a way that they represent fine, small, medium and large dimensions. The following simple equation was used to derive these values:

$$\begin{aligned} X_0 &= 2 \\ X_i &= 3X_{i-1} \quad i = 1, 2, 3, 4 \end{aligned} \quad (\text{Eq. 4.5})$$

The next step was to determine the quantity of features required for statistical certainty. Using the t-distribution, combined with results from similar previous research, minimum sample quantities for each nominal dimension category was calculated according to the following set of equations from Walpole et. al. [30]:

Let Z be a standard normal random variable and V a chi-squared random variable with ν degrees of freedom. If Z and V are independent, then the distribution of the random variable T , where

$$T = \frac{Z}{\sqrt{V/\nu}}, \quad (\text{Eq. 4.6})$$

is given by



$$h(t) = \frac{\Gamma[(\nu+1)/2]}{\Gamma(\nu/2)\sqrt{\pi\nu}} \left(1 + \frac{t^2}{\nu}\right)^{-(\nu+1)/2}, \quad -\infty < t < \infty. \quad (\text{Eq. 4.7})$$

This is known as the t -distribution with ν degrees of freedom.

Now let X_1, X_2, \dots, X_n be independent random variables that are all normal with mean μ and standard deviation σ . Let

$$\bar{X} = \sum_{i=1}^n \frac{X_i}{n} \quad (\text{Eq. 4.8})$$

and

$$s^2 = \sum_{i=1}^n \frac{(X_i - \bar{X})^2}{n-1} \quad (\text{Eq. 4.9})$$

Then the random variable
$$T = \frac{\bar{X} - \mu}{s/\sqrt{n}} \quad (\text{Eq. 4.10})$$

has a t -distribution with $\nu = n - 1$ degrees of freedom.

Using Equation 4.10 an equation can be derived from which sample sizes can be determined, such that the calculated averages from each sample will not deviate more than a percentage K from the population mean.

$$P\left(-t_{\alpha/2} \leq \frac{\bar{X} - \mu}{s/\sqrt{n}} \leq t_{\alpha/2}\right) = 1 - \alpha \quad (\text{Eq. 4.11})$$

$$\therefore -t_{\alpha/2} \frac{s}{\sqrt{n}} \leq \bar{X} - \mu \leq t_{\alpha/2} \frac{s}{\sqrt{n}}$$

$$\therefore |\mu - \bar{X}| \leq \frac{s}{\sqrt{n}} t_{\alpha/2}$$

$$\Rightarrow K\bar{X} = \frac{s}{\sqrt{n}} t_{\alpha/2}$$



$$\Rightarrow n \geq \left(\frac{st_{\alpha/2}}{K \bar{X}} \right)^2 \quad (\text{Eq. 4.12})$$

where:

n = sample size,

s = standard deviation from known historical data,

$t_{\alpha/2}$ = t -value obtained from t -distribution at chosen values for α and historical sample value that historical standard deviation and average is based on,

K = chosen percentage variable. Average of measured values will not deviate by more than this percentage variable from the population mean μ ,

\bar{X} = average of known historical data.

From Equation 4.12, sample values were calculated for each of the nominal dimensions derived from Equation 4.5. Table 4.1 shows how these sample values were calculated for different values of the variable K . The sample amounts that were eventually used are indicated as shaded. The historical data used to estimate averages and standard deviations were taken from previous research [7] done using the zp100 powder.

**Table 4.1: Sample amounts for varying K -values**

Nominal Dimension [mm]	Historical Data			$t_{\alpha/2}$ $\alpha = 5 \%$	K	Sample Amount N
	\bar{X} [mm]	s [mm]	n			
2	1.836	0.341	72	2.000	1 %	1380
					5 %	56
					10 %	14
6	5.741	0.293	120	1.980	1 %	103
					1.5 %	46
					5 %	5
18	17.997	0.227	144	1.960	0.25 %	98
					0.5 %	25
					1 %	7
54	53.868	0.112	48	2.021	0.1 %	18
					0.2 %	5
					0.5 %	1
162 [†]	161.500	0.218	-	2.000	0.1 %	8
					0.2 %	3
					0.3 %	1

[†] This dimension had no specific historical average and standard deviation that could be used. For this study, a worst-case average was estimated while the average of previous historical standard deviations [7] (not all shown here) was used.

For geometric accuracy, the deviation with respect to the following features were considered for examination: freeform contour geometry, angularity, position of axes, manufacturing features (fillets), circularity, coaxiality and concentricity. These are very common geometric features found on many parts and, depending on its application, are also commonly required to have good levels of tolerance. Geometric features such as flatness and straightness were considered, but not included since in practice these recognised features are always machined onto any manufactured part, and would therefore be superfluous in this design. Following the alternative approach for describing geometric accuracy a very typical automotive component –

a differential housing (henceforth denoted Differential Housing Benchmark) – was chosen and is shown here in Figure 4.4. It is characterised by a rich selection of circular, angular, cylindrical and a range of different freeform features.



Figure 4.4: Benchmark part used for geometric accuracy

This specific part was further chosen since extensive experience in creating full-scale prototypes on the Z402 3D Printer had already been achieved prior to this study, [31]. This part had already been successfully built in a series of 15 patterns for investment casting, and were subsequently used by the client as commercially functional prototypes. Figure 4.5 shows how it was necessary to print the differential housing in four sections that would fit in the build volume of the Z402 printer.

Several iterations confirmed what was first suspected; that the ease with which separately printed parts are assembled is influenced by the way these parts are orientated in the printer. It was also found that parts are more easily assembled if they are created in the same orientation such that their mating faces are formed in the same plane. In this case, iterations were done by mostly experimenting with different orientations in the z-axis. The best results were obtained when the mating faces were the last layer that would be created in the z-direction for each build. Figure 4.5 shows how the parts were orientated in relation to the z-axis.

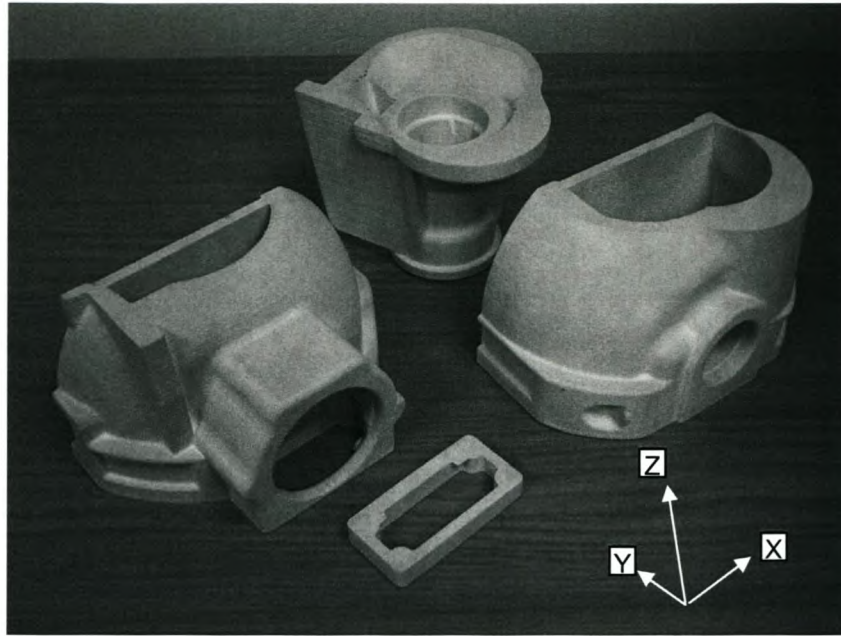


Figure 4.5: Different build sections to create full-scale parts [31]

Fitting into the build volume was not the only concern when sections were partitioned. The full-scale model needed to be partitioned with careful consideration of post-treatment procedures and especially, assembly of the parts. Figure 4.6 shows an illustration of the jig that was used to assemble the different components such that the axes of the drive- and wheel shaft holes were aligned and perpendicular to one another. Notice also, the web-supports that had been placed on

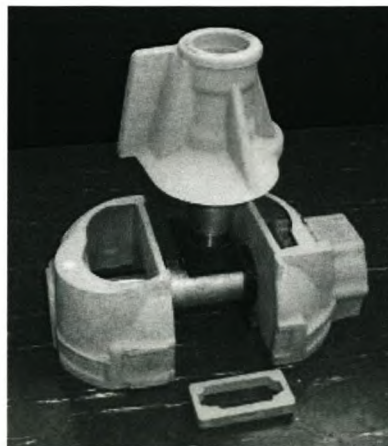


Figure 4.6: Illustration of jig used for assembly of sections [31]

two of the partitions. These were included on the sections after massive deformation (shown in Figure 4.7) occurred in the first parts created. During assembly, these webs were cut away and removed. Figure 4.8 shows the finished part assembled (a) before, and (b) after investment casting.

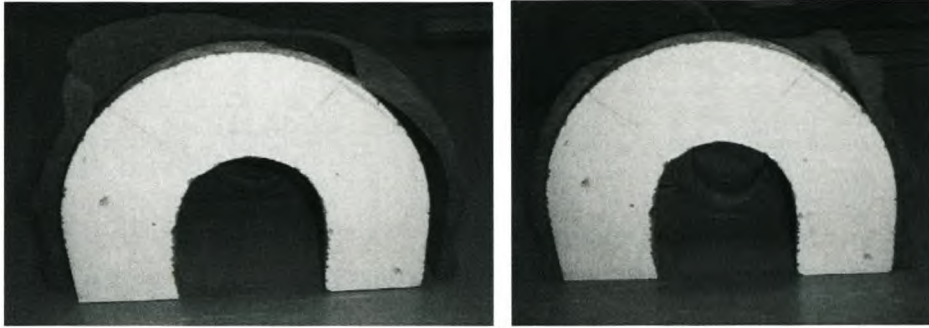


Figure 4.7: Deformation before and after use of web-supports [31]

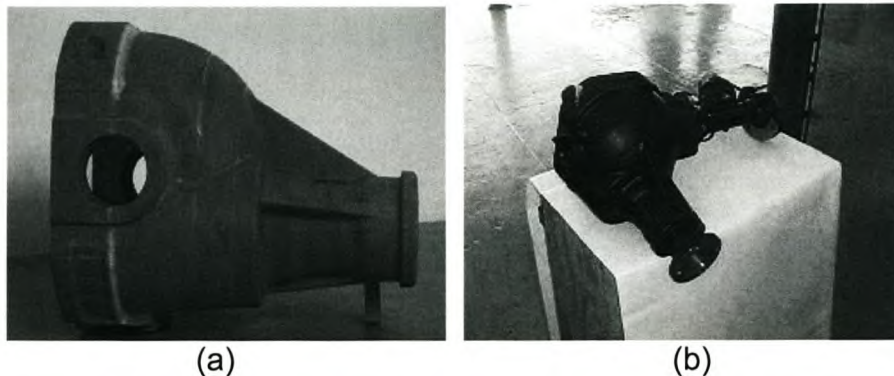


Figure 4.8: Differential housing before investment casting and after assembly [31]

In Section 4.3 and Figure 4.1, one of the factors that were mentioned that influence accuracy, was geometric features and their topology – e.g. open or closed contours. The experience gained through producing and assembling this differential housing strongly emphasized and proved this supposition. The importance of build orientation and its influence on accuracy was also observed during this case study. This experience also challenges the general belief that layer technologies remove the need of tooling and fixtures. For most parts, it may be accepted that the powder acts as support for overhanging and adjacent features – but where assembly or other



post-processing is involved that requires greater accuracy, experience has now shown that their lies wisdom in creating support structures to hold critical features to the tolerances desired. This important area of process development – i.e. design for assembly – is a significant part of ongoing research and is not specifically addressed further in this study.

For the purpose of this study, the Differential Housing Benchmark was scaled down to 60 % of its original size. This enabled the part to fit into the build platform of the Z402 printer, and therefore required no partitioning or assembly. The parts were not investment cast, but were only left infiltrated.

4.4.4 Benchmark Evaluation and Suggestions for Future Designs

Even though an extensive literature study was performed, with the guidelines and experience of other authors [25], [26], [27], [28] being followed during the design and selection of benchmark parts for this study, it was found that the designs used can still be improved upon. During the application of the test methods, a few shortcomings were observed. These will be discussed shortly for each benchmark part, with subsequent suggestions for future designs and related research.



a) *Size of Benchmark Cube*

The very first problem that was encountered occurred during the printing stage of the creation of the first part that was created using the zp14 material.

The prescribed scaling factors that were set as parameters during the print increased overall dimensions on the part. This is normally the case, with any part that is printed, and is done so purposely to accommodate shrinkage during post-procedural infiltration. In this case however, the dimensions increased to the point that not enough powder remained in the printer's feed box to supply the remaining layers. Even though the feed box had been filled to capacity, and the build platform had been raised to maximum height – this event showed that for the scaling factors applied and with zp100 powder, the demand to produce a part with nominal height dimension equal to 190 mm exceeded the printer's capability to produce such a part. The last few layers all had the same cross sectional area, and the result was that binder fluid was repeatedly sprayed onto the same surface. Without the addition of powder to the last layers being printed, the printed cross sectional area became saturated with binder fluid. The edges of the cross section being printed lost their definition because the over-saturation of binder fluid caused the edges to curl upward. Ultimately this made the top face of the Benchmark Cube, shown in Figure 4.9, unusable for measurements.

The other faces were not affected by this loss, and could still be measured successfully – so the decision was made to continue using this part because only one of the faces had been damaged. But a comparison between the protrusion-faces was now not possible, and the other two faces containing protrusions was not included further in the measurements. The exclusion of the protrusion-faces also, unfortunately made the objective of comparing same-size slots with protrusions unattainable. Therefore this study can make no conclusive statement yet concerning whether there is a severe difference in

accuracy when comparing slots and protrusions with the same cross-sectional geometry. But this study does reflect conclusive results about the accuracy capability of the printers to produce slot features of nominal lengths in all three build axes.

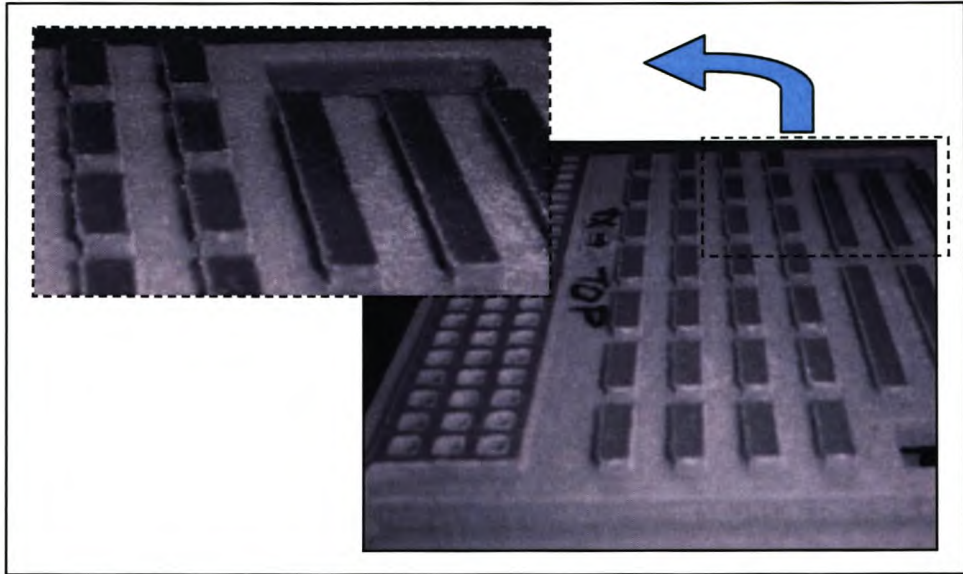


Figure 4.9: Powder deficient layers of top face of Benchmark Cube

b) Powder Removal from Benchmark Cube

A second problem that was encountered with the Benchmark Cube was during the process of powder removal.

Although rectangular holes were designed (two per cube-face), to facilitate the extraction of powder from in between the support structure grid inside the cube, these holes were not as large as may have been desired. This also forced a situation where powder was removed through the slots on three faces of the cube. This is highly undesirable, since it creates a potential for damage to occur to the very features that need to be measured. The part is at its most vulnerable to incur damage during powder removal since it is still brittle and fragile before being infiltrated. Recognizing this, great and meticulous care was taken to remove the powder without damaging the slots. Ultimately, all powder could still be removed, but with much effort and time.



c) *Paper Removal from Benchmark Cube*

The design of the Benchmark Cube was slightly altered for producing it on the LOM machine. It would be impossible to remove laminated strips of paper from the inside of the cube without creating it in (at least) two halves. Even then, removing the paper from in between the support grid structure would be virtually impossible without significant damage. Therefore it was decided to change the design so that the inside of the cube would be solid. The inside features of the cube are not as important as the outer features. The only purpose of the grid inside is to provide support. If the inside is created as solid for the LOM process it would be better. This would also enable the part to be printed in less time.

But the outer paper removal was very tedious and time consuming. It took longer than 50 hours to de-block both the Benchmark Cube and Differential. Again the importance of potential damage to the features was recognized, which contributed to the time used to post-process the parts. The areas that proved specifically challenging to remove paper from included:

- Any features that required layers of paper, when aligned with the feature, to be removed directly underneath it, or from within the feature. This can best be described by referring to Figure 4.10 (a) and (b) respectively, and Figure 4.11. Notice also the particular build orientations. Wherever there were open sections where a chisel blade could be easily applied, paper could be removed more easily. If trapped between two features however, it became very difficult to remove. As soon as some of the layers were removed, pressure between the features was relieved, and paper removal became possible. Without first removing this pressure, the excess paper would typically tare, but still remain on the part as can be seen in Figure 4.11 (b) and (c);
- In between the 6 mm slots (see Figure 4.11).

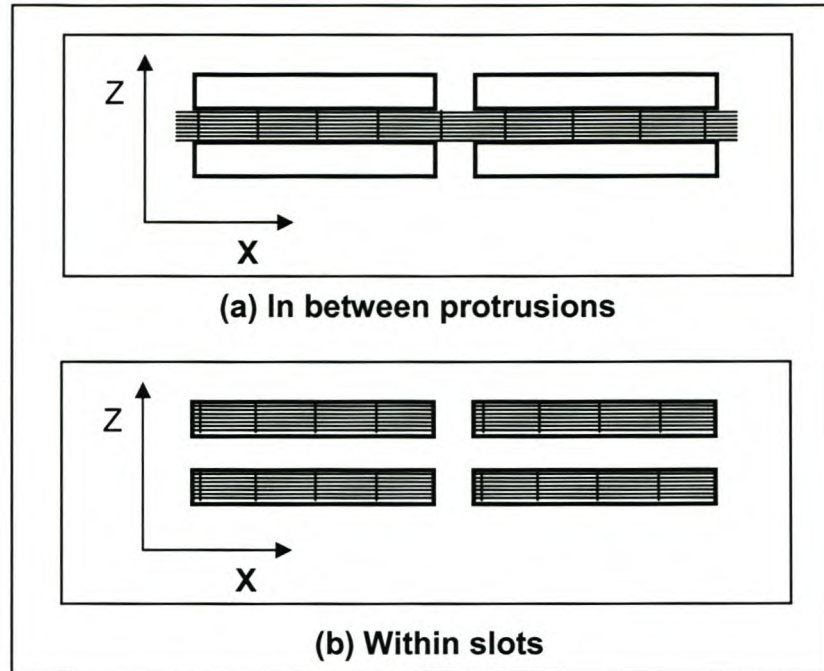


Figure 4.10: Features where paper removal was problematic

Several techniques were tried to remove this pressure, including the use of a fine drill (Figure 4.11 (d)). The task of paper removal was further hampered by the fact that in certain places, the laser had not completely penetrated and severed the paper properly into blocks. This forced the blocks of excess paper to be torn away from the main structure, instead of levering it away with chisels. Figure 4.12 show examples of this.

Although the geometry of the part made the paper removal process challenging and time consuming, this was not the only cause for the long time that was taken. Experienced users of the LOM technology indicated that the longer a printed block is exposed to the atmosphere before the process of de-blocking takes place, the more difficult it becomes to remove these outer layers of paper.

Circumstances unfortunately forced the researcher not to be available to de-block the printed block immediately after being printed. Precautions were taken to seal it from the atmosphere and keep it in a temperature-controlled environment. But the process of de-blocking still proved to be difficult despite these precautions.

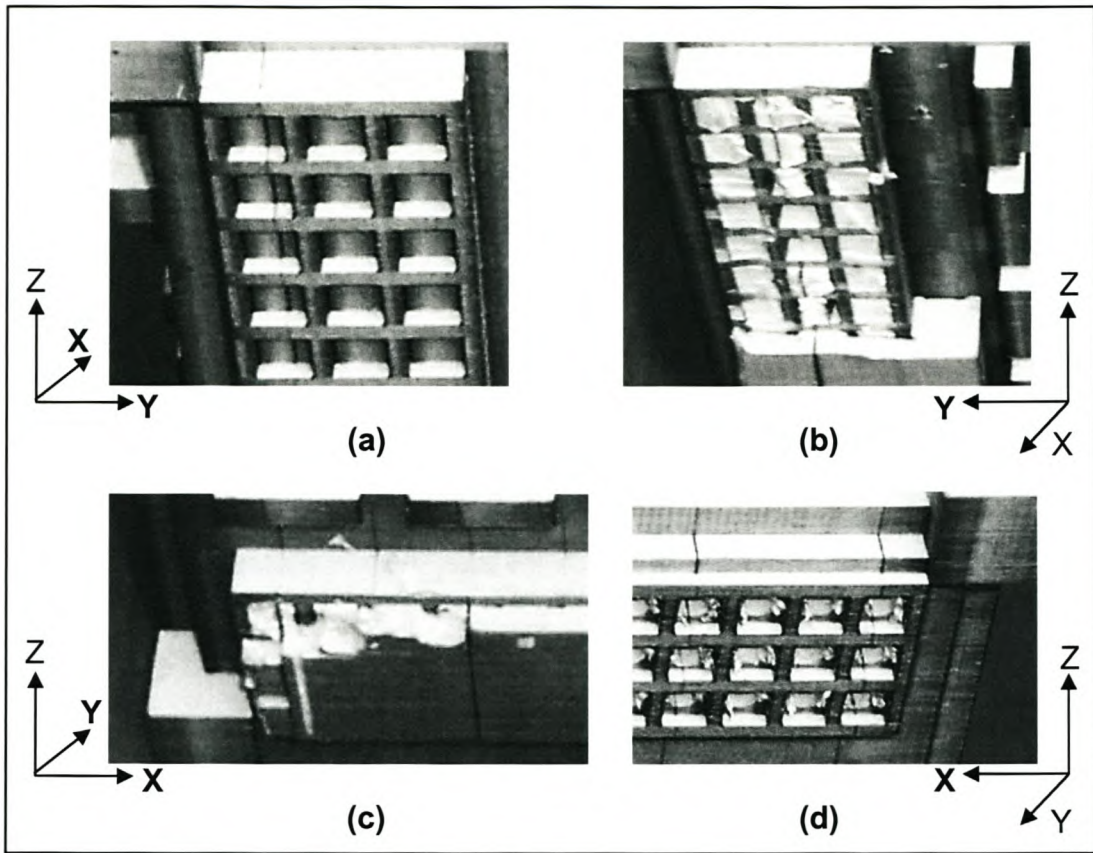


Figure 4.11: Paper removal difficulties with 6 mm slots

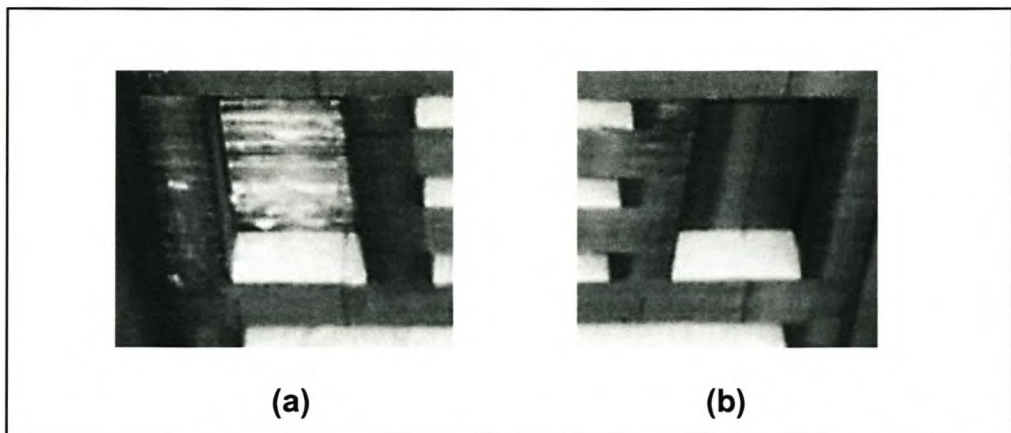


Figure 4.12: Paper not cut properly compared to a proper cut

In summary, the suggestions that are made for improving this particular benchmark design would include the following:

- Decrease overall part dimensions in order to fit the build volume
- Increase cavity sizes and quantities to facilitate powder removal.



- Design the part so that paper removal from the 6mm slots are easier to accomplish.
- De-block the support layers of paper as soon as possible in a controlled climatic environment. Infiltrate the part as soon as possible after de-blocking in order to seal and protect the paper from environmental influences.

d) *Differential Housing Benchmark*

The differential housing that was used as a benchmark for geometric accuracy proved to be a good benchmark selection. Almost no problems were encountered. The only real challenge with this part was in producing it with the LOM process. In order to still enable paper removal, the part needed to be produced in two sections (see Figure 4.13). This situation raised a very important point related to this study as a whole, i.e. research for characterizing a specific RP process versus research to compare different RP processes. How would the printing of this part in two sections with the LOM process influence its comparison with the other processes? The latter research objective would typically argue that for rigorous statistical correctness, each part essentially has to be the same – similar to the commonly used phrase: “comparing apples with apples”. Therefore changing the design could be regarded as “comparing apples with oranges”.

But in order to correctly compare different processes with one another, one cannot ignore the inherent differences in each process chain. Therefore slightly altering the benchmark can in some cases not be avoided, and should not be seen as incorrect. This study *does*, in effect, compare “apples with oranges”. Comparing the proverbial “apples with apples” would be more correctly associated with identifying the repeatability of a **single** process. It is also important to distinguish that this argument does not state that reproducibility is

being measured. Please refer back to Section 4.1.8, which describes the difference between repeatability and reproducibility.

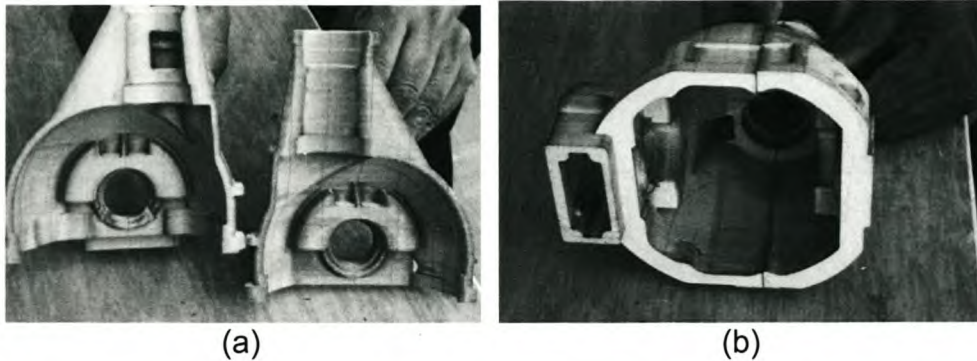


**Figure 4.13: Two halves of differential housing made with LOM
(a) held separately, and (b) held together**

4.5 Test Methods for Data Gathering

The following sub sections, describe the steps that were followed during actual data gathering for each of the characteristics of the capability profile.

4.5.1 Dimensional Accuracy

The Benchmark Cube was modelled in Pro/Engineer, and an STL-file was created. For the 3DP process, this part was built using both types of material – the zp14 and zp100 powders, and infiltrated with wax and Zi580 resin agent respectively. The layer thickness was 0.175 and 0.10 mm respectively. The Benchmark Cube was later also produced with the LOM and SLS processes.

The benchmarks were measured on a Mitutoyo Bright 710 CMM - Co-ordinate Measuring Machine. The quoted accuracy of the CMM and probe system is ± 0.006 mm for the size of measurements. A program was written in order to speed up and standardise the required measurements, [32]. The program contained approximately 3000 movement and/or measurement steps that were performed, and it took approximately 40 minutes to execute one cycle of the program. The measurements were processed into the sub-categories for each



nominal dimension. From these, average values and standard deviations for each nominal dimension were calculated. See Table 4.1 for the amounts of samples that were used during these calculations. The results of these measurements are discussed in the following chapter.

4.5.2 *Geometric Accuracy*

The Differential Housing Benchmark was also modelled in Pro/Engineer, and an STL-file was created. For the 3DP process, to examine the impact of the material on the geometric accuracy, this component was again built in the two available materials, zp14 and zp100, and infiltrated with wax and Zi580 resin agent respectively. The layer thickness was again 0.175 and 0.10 mm respectively. This part was later also produced with the LOM and SLS processes. As mentioned above in Sections (d), the difficulties associated with paper removal from the LOM parts forced the part to be built in two sections (see Figure 4.13). After de-blocking the LOM parts, both halves of the Differential Housing Benchmark were sealed with three coats of industrial wood sealer. Each coat was applied using a small paintbrush, and only applied after the previous one had dried. No further finishing such as sandpapering or painting was done. The only other post-processing that was done, was to fix the two halves together so that measurements could be done properly. Figure 4.14 shows the method by which the two halves were put together. The two halves were joined by first locating the bottom faces (A) together on a flatbed measuring block. A tight fitting cylinder (B), machined from plastic, was used to centre the two wheel shaft holes. Finally, two Alan-key screws and washers (C) hold the halves together. It was decided not to use glue, since the addition of any material between the two halves may influence its accuracy. An added benefit of using screws to hold the halves instead of glue is that they can still be separated again at a later stage if necessary – possibly for further measurements or even viewing or display purposes.

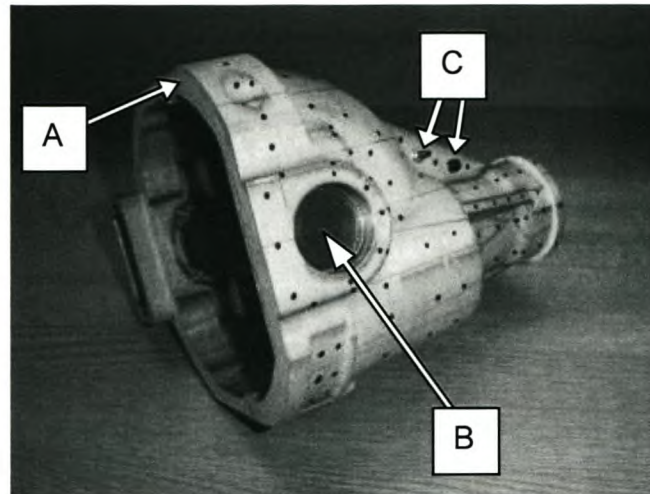


Figure 4.14: LOM Benchmark part showing fixtures of two halves

Steps concerning the measurements taken on the Differential Housing Benchmark are as follows.

Firstly, geometric accuracy categories that could be obtained from this part were identified. These were freeform contour geometry, circularity, concentricity, and angular tolerance, since they represent commonly encountered geometrical features on industry components that typically need to be created according to strict tolerances.

For freeform contour geometry, 290 evenly spaced points were measured using the same Mitutoyo Bright 710 CMM - Co-ordinate Measuring Machine. Figure 4.15 shows how these points have been distributed on the outside surface of the model.

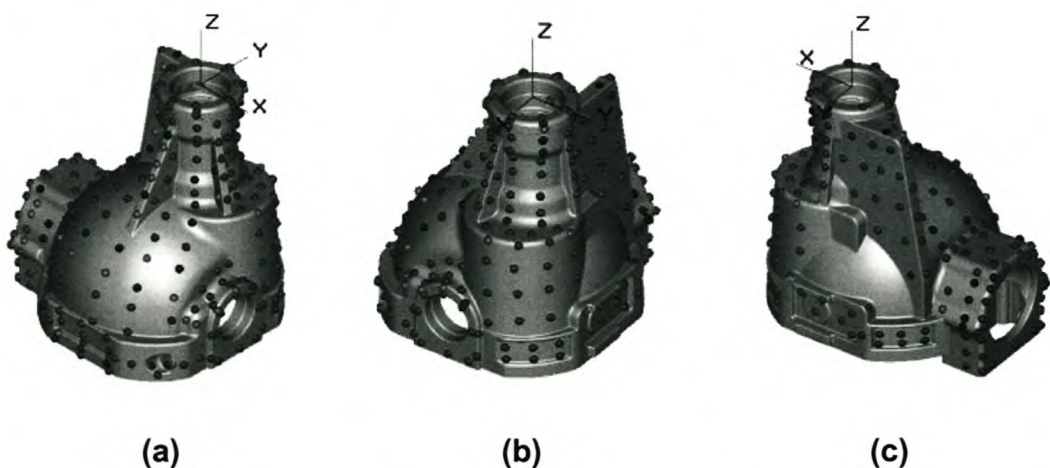


Figure 4.15: Distribution of measure points for freeform geometry



Through the use of Mitutoyo's software called 3DTol, the measured X, Y and Z values of each measurement were compared directly to the corresponding point on the CAD solid model. This is achieved by the following steps:

1. Define a coordinate system on the physical part in the same location and orientation as on the CAD model. A Cartesian coordinate system was used in this study.
2. Measure a few (20 will be enough) points at random over the surface of the physical part, which are compared by the software to the CAD model. These points define the starting condition that is necessary for the iterative step 3.
3. Perform a best-fit calculation by using these points in order to align the coordinate systems of the physical model with the CAD model before measurements are made. The software employs an algorithm that, through an iterative process, rotates and translates the coordinate system in such a way as to minimise all the deviations that have been measured.
4. Store the coordinate system, and restart the process of measuring points on the physical surface, now using the stored coordinate system.
5. Measure the desired amount of points over the profile of the surface. In this case, as mentioned above, 290 evenly spaced points were measured randomly over the surface of the part. During the course of taking a measurement, the software defines a normal vector on the surface of the part so that it can differentiate between the part material and empty space. With each measurement the software compares the measured point to the actual CAD model. From these comparisons, individual deviations are calculated accordingly. The sign associated with the deviation is determined by taking the normal vector into account – a positive deviation means that the actual part is



larger than its CAD counterpart and conversely, a negative error describes the part to be smaller than the CAD model. From the X, Y and Z deviations, a total volumetric deviation is calculated by adding the squared deviations of X, Y and Z – and then calculating the square root of this sum. Once again the sign of this total volumetric deviation is determined from the normal vector.

6. After measurements have been completed, the software executes another best-fit calculation. Averages and standard deviations of each data set per RP process (and for both materials of 3DP) are calculated and histogram graphs are drawn.

After freeform contour geometry was investigated, circularity and concentricity was looked at. For this purpose, seven circular features on the model were identified. In Figure 4.16, these seven circular features have been named and indicated. In the third column, each circular feature's nominal diameter as specified by the CAD design is also indicated.

Each hole was measured and defined with the CMM by eight points on its perimeter. Simmons et. al. [33] defines circularity as being the difference between the radii of the minimum inscribed circle and maximum circumscribed circle, both with the same centre points as the true circle.

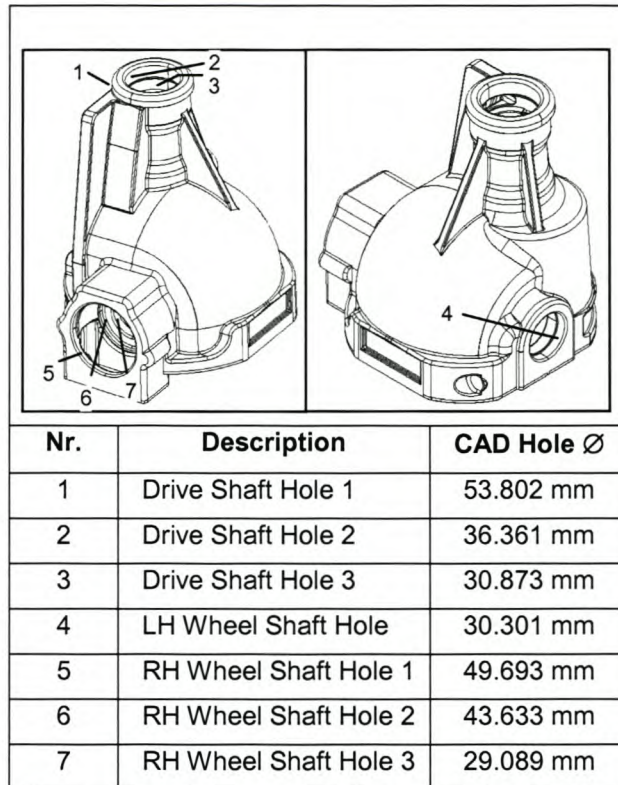


Figure 4.16: Circular features and their nominal diameters

The circularities were calculated for each circular feature as shown in Figure 4.17. This example is taken of the Drive Shaft Hole number 1 (refer to Figure 4.16). Notice thus, that the circularity has been calculated by subtracting the minimum distance radius from the maximum distance radius ($A - B = C$). The unit of circularity is measured in millimetres.

Figure 4.18 illustrates the elements of concentricity and can be stated as follows: Concentricity is value of the diameter of a small circle (Concentricity Tolerance) such that the centre of the measured circular feature (Actual Element) lies on the perimeter of the small circle. The small circle is centred at the same point as the centre of the circular feature to which the Actual Element is compared (i.e. the Reference Circle). The concentricity tolerance is used for both circles and cylinders, but in this study it will only refer to circles. As above, the unit of concentricity is millimetres.

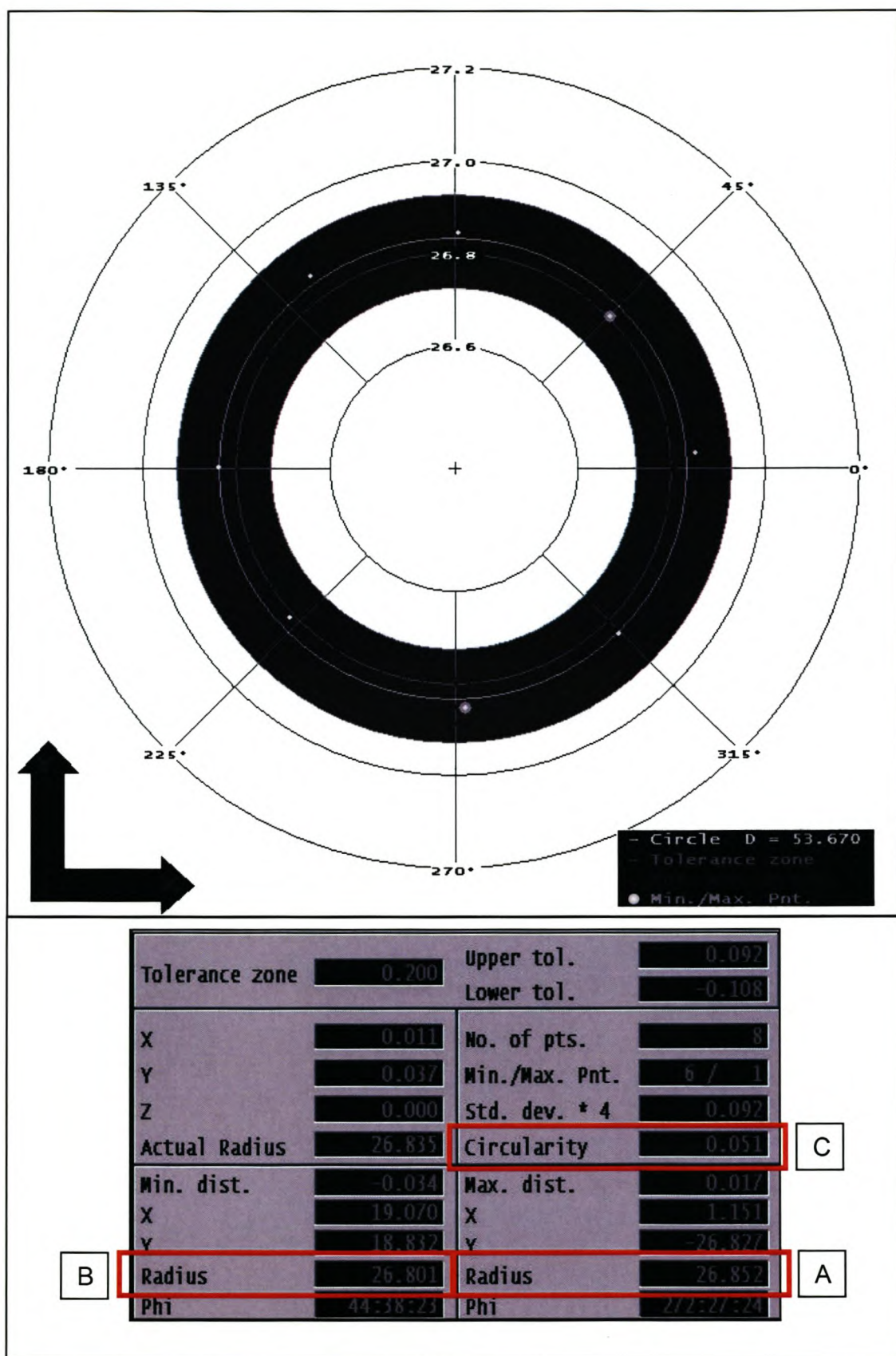


Figure 4.17: Example of circularity measures taken

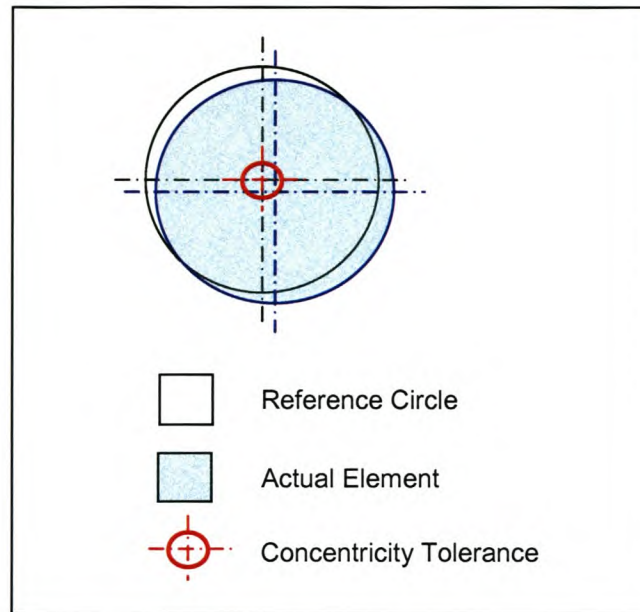


Figure 4.18: Diagram depicting the definition of concentricity

Finally, angular tolerance measures were made. Angular tolerance (as shown in Figure 4.19) is defined as the allowable deviation, in degrees, from a specified angle. In order to measure these deviations, a series of 10 points were measured with the CMM on specific surfaces by which a line was constructed. The angle that this line on the surface made with a reference plane was compared to the CAD design. The difference resulting from this comparison thus rendered the calculated angular tolerance deviations. The results of the collection of all geometric accuracy measures are discussed in the next chapter.

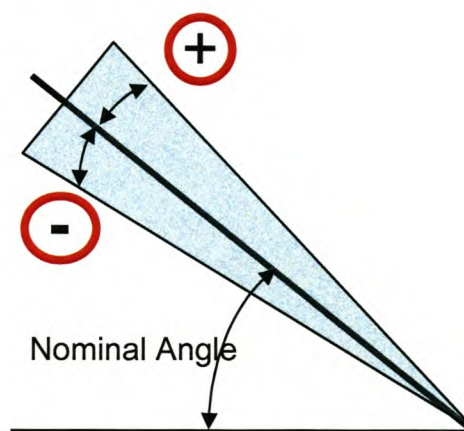


Figure 4.19: Illustration of Angular Tolerance

4.5.3 *Strength and Elongation*

Another characteristic that defines the capability profile of processes under investigation in this study, is their strengths and related elongations. To this point, only the tensile strength of the 3DP materials, zp100 and zp15e, have been investigated. The measurements relating to the other two processes, namely LOM and SLS, are still significant and now become part of ongoing research. The tests were performed according to the ASTM D638 method [34], which is the same standard that has been used in previous research to define the tensile strengths of materials associated with Stereolithography [3].

The test parts were modelled using Pro/Engineer with dimensions as stipulated in the ASTM D638 standard for a Type I test piece. The critical dimensions are as shown here in Figure 4.20.

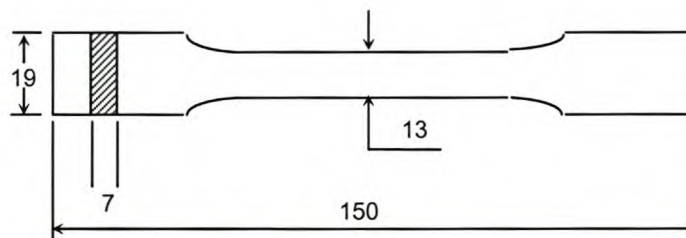


Figure 4.20: Dimensions of Type I test piece for tensile testing

Twenty samples of each material were produced according to the printing parameters that are shown for each material in Table 4.2. After the parts were printed and cleaned, their critical dimensions were measured and they were each weighed. Figure 4.21 shows where on each specimen the critical dimensions were measured and noted down. After measurements were taken, zp100 specimens were placed in a 70°C oven for approximately 30 minutes to dry. A temperature of 70°C is used because this is warm enough to remove moisture from the part while not causing any damage to the material. From experience this temperature has also proven to show moderate drying



times, while still allowing a person to control the process sufficiently by checking critical dimensions at intervals while drying takes place. After their drying time, the specimens were measured and weighed again. Hereafter, they were infiltrated by hand with Zi580 epoxy resin. The specimens were then placed in a vacuum chamber for 10 minutes, after which they were again placed in the 70°C oven for final drying.

Table 4.2: Printing parameters for test part used in tensile testing

Parameter		Material	
		zp100	zp15e
Anisotropic Scaling	X	1	1
	Y	1	1
	Z	1	1
Layer Thickness		0.100 mm	0.175 mm
Binder/Volume Ratio	Shell	35 %	35 %
	Core	17.5 %	17.5 %
Saturation Level	Shell	100 %	100 %
	Core	100 %	100 %
Saturation	Shell	2	2
	Core	1	1

Zp15e specimens were produced two days after zp100 specimens. The same post-processing and measuring procedure was followed, except they were placed in a 40°C oven for approximately one hour. In this case a 40°C oven was used because the previous 70°C oven was unavailable for use. This lower temperature would not influence the process other than prolonging the drying time. After drying, they too, were measured and weighed a second time before being infiltrated with melted surgical wax.

After all specimens of both materials had been infiltrated, their critical dimensions and individual weights were measured a third time to monitor the effect of the infiltration agent.

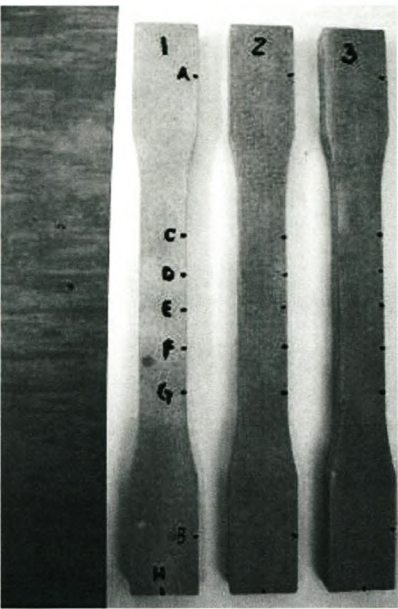


Figure 4.21: Points where dimensions of test parts were measured



Figure 4.22: Illustration of infiltrations with epoxy resin



4.5.4 Surface Roughness

Another measure of part quality lies in the roughness of the surface finish. The industry standard used for reporting quality of surface roughness is according to R_a (roughness average) values [35]. The R_a value is the arithmetic mean of the absolute values of the profile deviation, from the centre line, within the evaluation length (L_e) (also referred to as cut-off length).

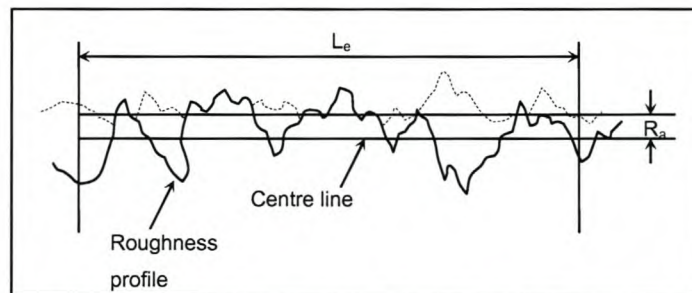


Figure 4.23: Representation of roughness average (R_a)

Due to the limitations of the measuring instrument, only flat surfaces were considered in this study to describe surface quality measurements. Due to their long flat surfaces, the specimens used for determining tensile strengths of the materials were ideal to use for investigating surface roughness too. A Mitutoyo Surftest – 211 was used as the measuring instrument and is quoted to be able to gather surface roughness measurements up to $160\text{ }\mu\text{m}$. Ten R_a values (over a cut-off length of 0.25mm each) were measured and then averaged for resin-infiltrated zp100 material. The same was done for the wax-infiltrated zp15e material. For the sake of comparison, some parts underwent post-processing with sanding and painting to produce very smooth surfaces. These were also measured and compared in the same way as was mentioned above for zp100 and zp15e.



5. Discussion of Results

This chapter is dedicated to bring forth and discuss the analytical results that have been obtained from measurements taken according to the procedures and test methods described in the previous chapter.

5.1 Dimensional Accuracy

Table 5.1 contains a high level summary of all the important statistics that were measured and calculated for dimensional bias and precision. Some of the results in Table 5.1 have been further summarized in Figure 5.1 and Figure 5.2, showing the average errors and standard deviations respectively, of the different processes for each of their build axes.

From inspection, the following is observed from Figure 5.1:

1. Deviations in the z-axis for zp100 material indicate a downward trend as nominal dimension increase. In other words, errors become negatively larger as the nominal dimension increases.
2. The same is observed for zp14 material, but with the z-axis errors becoming *positively* larger as the nominal dimension increases.
3. While the LOM process shows small errors for small nominal dimensions, the largest error (4.228 mm) observed is at 162 mm nominal dimension in the z-axis direction. The average errors in the Z direction of each nominal dimension for the LOM process are much larger than those for X- and Y average. This discrepancy between the directional errors, points to a massive expansion in the Z direction that may have been caused by atmospheric moisture. This value should therefore be regarded as an outlier and not taken into further account. Since the de-blocking of the LOM parts took such a long time and could not be infiltrated sooner, swelling between the layers may have occurred. This also explains the growth trend of error values that is also observed in the z-axis direction as nominal dimensions increase.

4. The dispersion in zp100 material in its x-axis build direction (Figure 5.2) remains relatively constant around 0.1 mm for fine and small nominal dimensions, but becomes larger for medium and large nominal dimensions – growing to approximately 0.15 mm and 0.225 mm respectively.
5. Zp14 Material surprisingly shows smaller bias for fine, small and medium dimensions than zp100 material. The dispersion of zp14 material however, is not as consistent and as small as zp100.
6. The best performer in terms of bias and precision is the SLS process. It shows small negative bias, and standard deviation ranging between approximately 0.05 mm for fine nominal dimensions and approximately 0.15 mm for large nominal dimensions.

Table 5.1: Measured Bias and Precision of Different Processes.

Nominal dimension (mm)		2			6			18			54			162		
		Axis			X			Y			Z			X		
		63	63	63	60	60	60	28	28	28	6	6	6	3	3	3
zp100	Average measurement	2.559	2.639	2.235	5.464	5.361	5.750	17.557	17.172	17.670	53.696	53.321	53.431	161.931	161.780	161.134
	Average error	0.559	0.639	0.235	-0.537	-0.639	-0.250	-0.444	-0.828	-0.330	-0.304	-0.679	-0.569	-0.069	-0.220	-0.866
	Standard deviation of error	0.117	0.075	0.087	0.119	0.068	0.105	0.099	0.091	0.083	0.143	0.121	0.078	0.223	0.029	0.066
	6 Std. Dev's of error	0.705	0.448	0.520	0.713	0.408	0.631	0.594	0.549	0.499	0.857	0.726	0.466	1.335	0.172	0.397
	3 Std. Dev's of error	0.352	0.224	0.260	0.356	0.204	0.316	0.297	0.274	0.249	0.428	0.363	0.233	0.668	0.086	0.198
	IT grade	IT15	IT14	IT15	IT15	IT14	IT15	IT14	IT14	IT13	IT13	IT13	IT12	IT14	IT9	IT11
zp14	Average measurement	2.240	2.434	2.068	5.796	5.567	6.030	17.856	17.663	18.168	54.100	53.798	54.608	162.482	162.787	163.675
	Average error	0.240	0.434	0.068	-0.204	-0.433	0.030	-0.144	-0.337	0.168	0.100	-0.202	0.608	0.482	0.787	1.675
	Standard deviation of error	0.089	0.084	0.124	0.094	0.078	0.135	0.097	0.130	0.129	0.230	0.100	0.198	0.030	0.284	0.090
	6 Std. Dev's of error	0.534	0.503	0.743	0.566	0.468	0.809	0.580	0.782	0.775	1.379	0.601	1.188	0.181	1.705	0.541
	3 Std. Dev's of error	0.267	0.251	0.372	0.283	0.234	0.405	0.290	0.391	0.387	0.690	0.301	0.594	0.090	0.853	0.270
	IT grade	IT15	IT15	IT15	IT14	IT14	IT15	IT14	IT14	IT14	IT14	IT13	IT14	IT9	IT14	IT12
SLS	Average measurement	2.015	2.003	2.152	5.959	5.971	5.880	17.895	17.899	17.933	53.711	53.844	53.964	161.575	161.824	162.324
	Average error	0.015	0.003	0.152	-0.041	-0.029	-0.120	-0.105	-0.102	-0.067	-0.289	-0.156	-0.036	-0.425	-0.176	0.324
	Standard deviation of error	0.045	0.061	0.085	0.050	0.053	0.057	0.043	0.059	0.060	0.084	0.048	0.045	0.140	0.126	0.079
	6 Std. Dev's of error	0.273	0.364	0.509	0.298	0.319	0.344	0.260	0.352	0.359	0.504	0.287	0.272	0.842	0.756	0.476
	3 Std. Dev's of error	0.136	0.182	0.255	0.149	0.160	0.172	0.130	0.176	0.180	0.252	0.144	0.136	0.421	0.378	0.238
	IT grade	IT13	IT14	IT15	IT13	IT13	IT13	IT12	IT12	IT12	IT12	IT11	IT11	IT13	IT12	IT11
LOM	Average measurement	1.990	1.971	2.205	6.025	6.062	5.989	18.064	18.060	18.298	53.886	54.160	55.102	162.274	162.489	166.228
	Average error	-0.010	-0.029	0.205	0.025	0.062	-0.011	0.064	0.060	0.298	-0.114	0.160	1.102	0.274	0.489	4.228
	Standard deviation of error	0.052	0.052	0.113	0.072	0.049	0.135	0.043	0.024	0.179	0.541	0.029	0.345	0.010	0.036	0.045
	6 Std. Dev's of error	0.313	0.310	0.679	0.432	0.295	0.813	0.256	0.144	1.075	3.244	0.172	2.069	0.060	0.217	0.269
	3 Std. Dev's of error	0.156	0.155	0.339	0.216	0.148	0.406	0.128	0.072	0.538	1.622	0.086	1.035	0.030	0.109	0.134
	IT grade	IT14	IT14	IT15	IT14	IT13	IT15	IT12	IT11	IT15	IT16	IT10	IT15	IT7	IT10	IT10

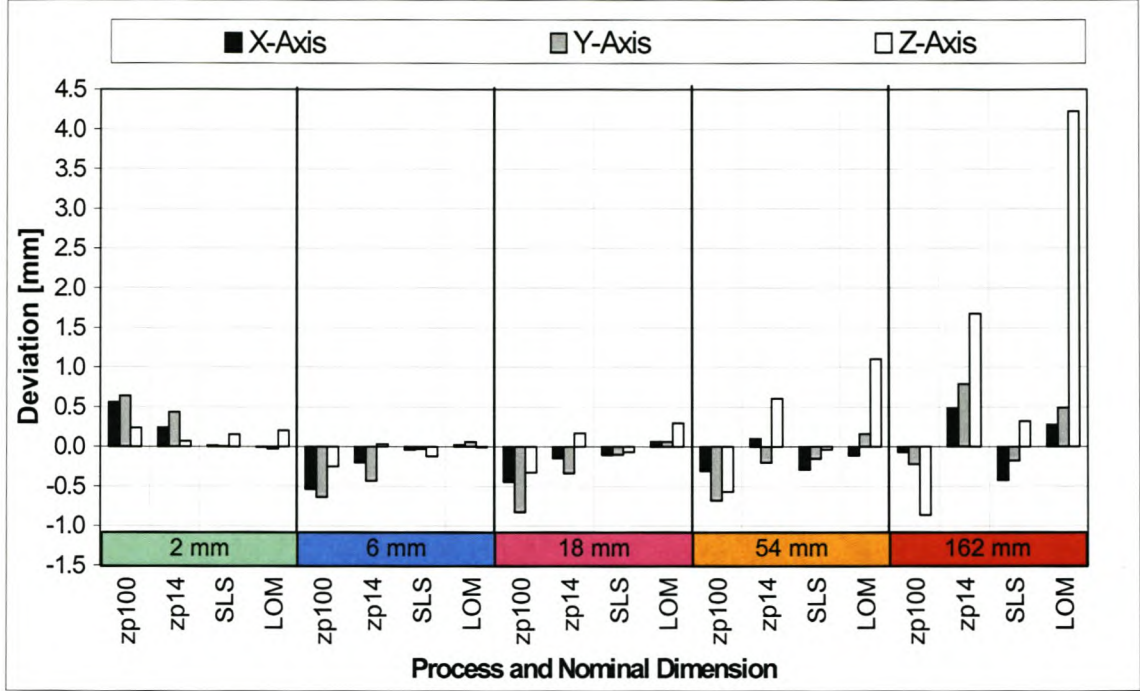


Figure 5.1: Average Errors for Different Processes

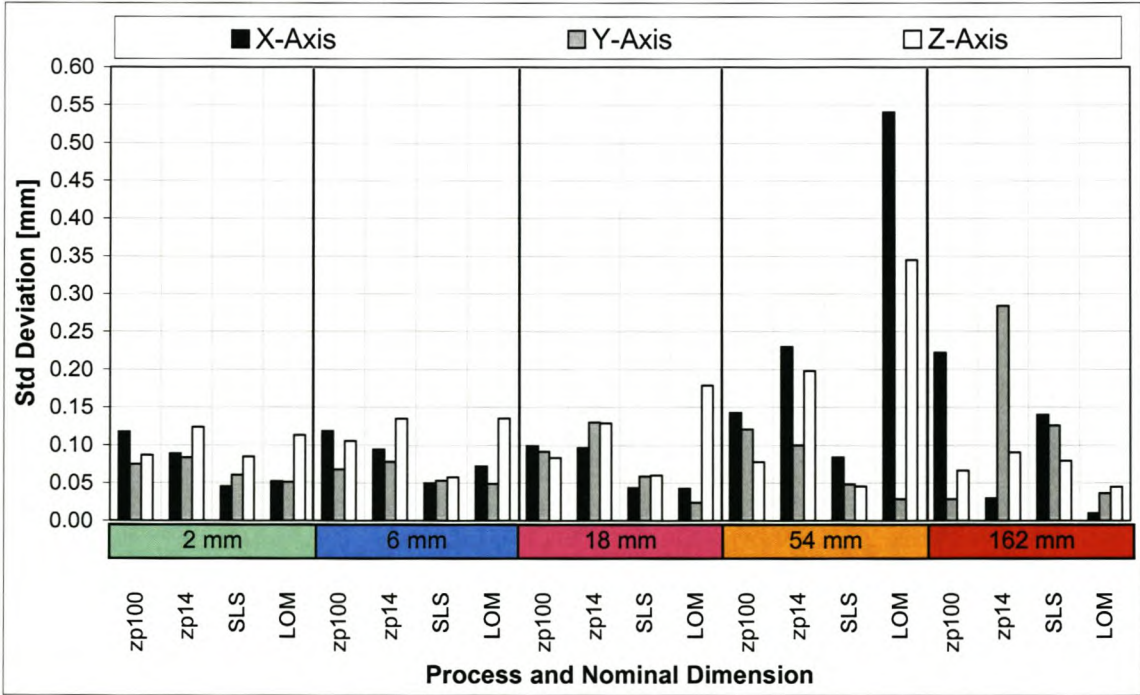


Figure 5.2: Standard Deviations for Different Processes

5.2 Geometric Accuracy

Section 4.5.2 discussed the methods that were followed and which geometric accuracy tolerances were investigated. The test determinations of these test methods are presented in the following subsections.

5.2.1 Profile of a Surface

Figure 5.3, Figure 5.4, Figure 5.5, and Figure 5.6 are error distribution charts that show the volumetric deviations measured between the physical benchmark parts and the CAD design.

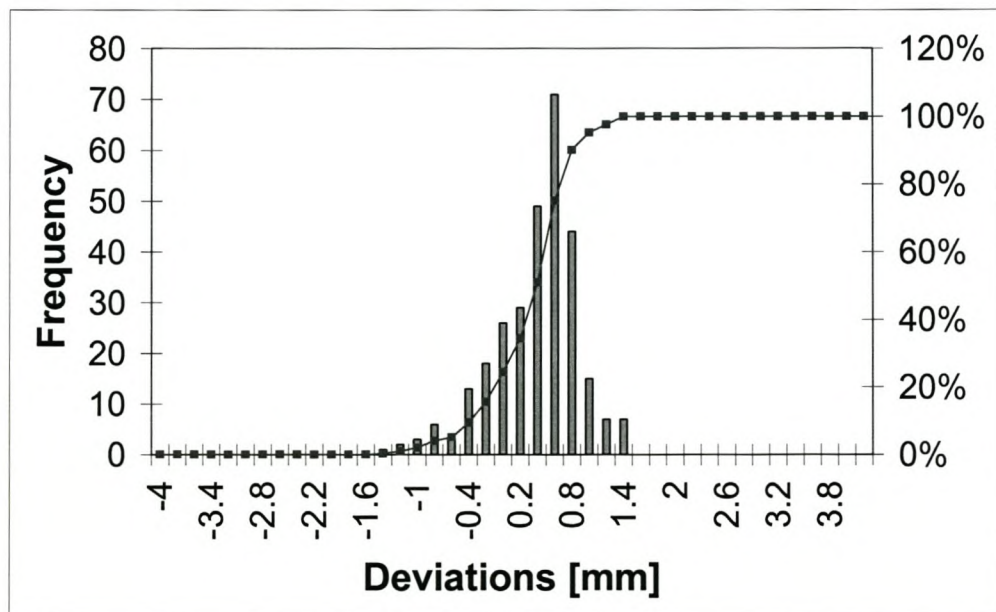


Figure 5.3: Error Distribution of 3D Geometric Features Using zp100 Powder.

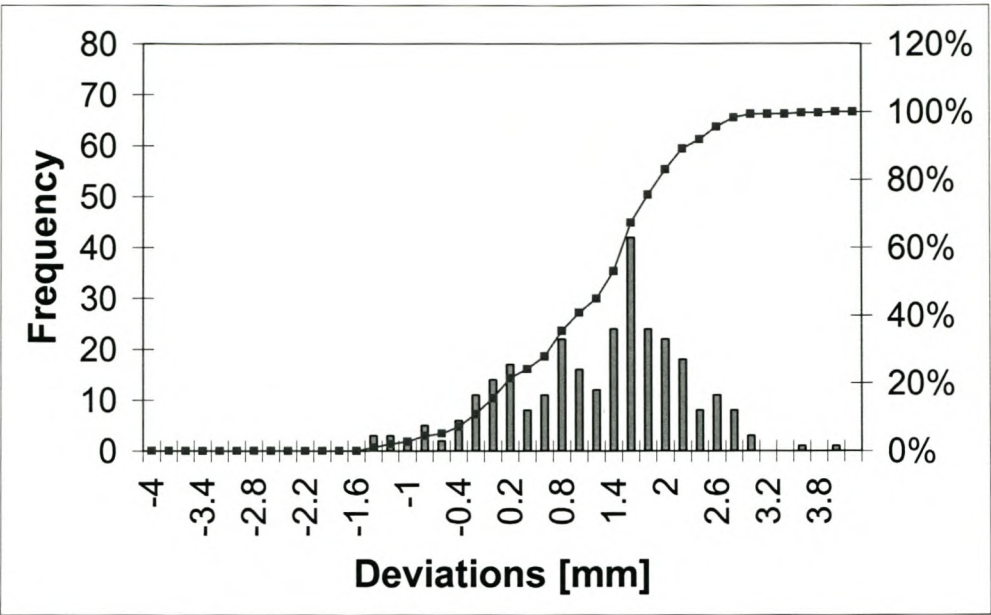


Figure 5.4: Error Distribution of 3D Geometric Features Using zp14 Powder.

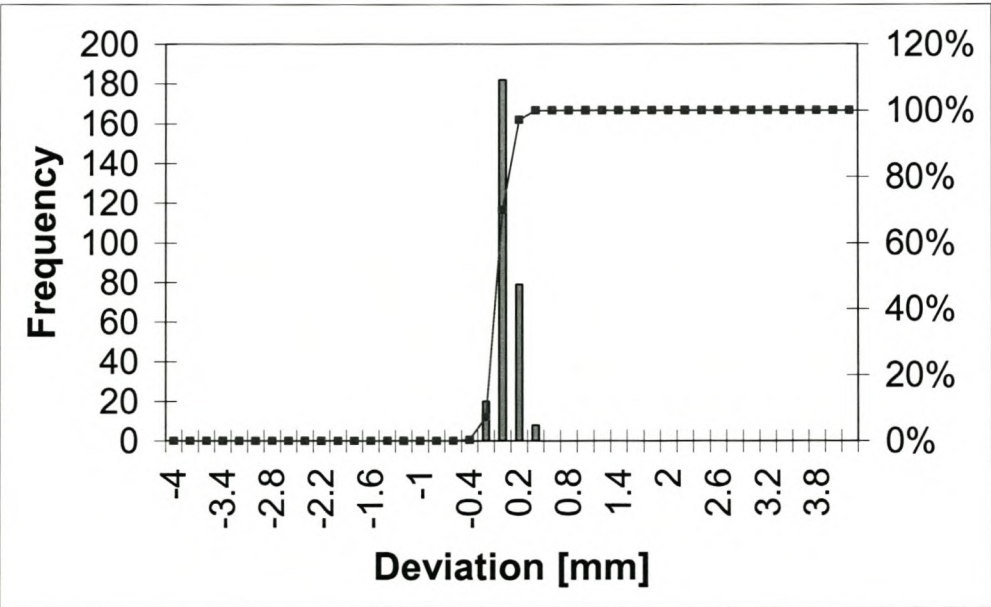


Figure 5.5: Error Distribution of SLS Process.

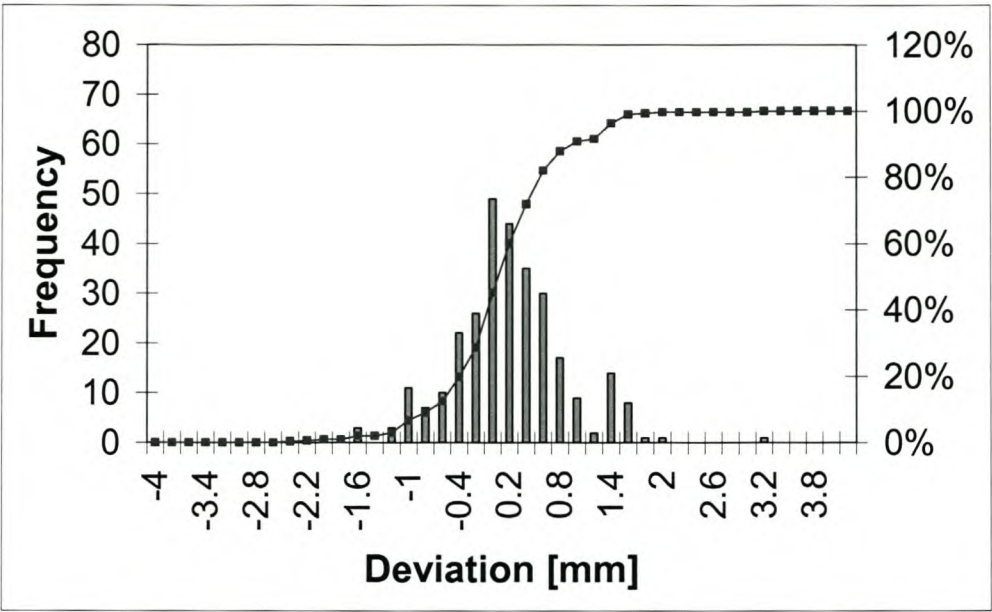


Figure 5.6: Error Distribution of the LOM Process.

These figures give a good visual comparison of the bias and dispersion of the different processes being considered in this study. As with the dimensional accuracy, the zp100 powder demonstrated smaller dispersion than zp14 powder. In this case however, the zp100 powder also achieved less bias, indicating that the printer parameters and post-processing techniques are close to achieving zero bias. Continued studies of repeatability should help in reaching this goal. The specific values are shown here in Table 5.2, along with the other most relevant characteristics of the error distribution charts.

Table 5.2: Important Values of Error Distribution of Different Processes

Process	Sample Amount	Max [mm]	Min [mm]	Avg [mm]	Std Dev [mm]
3DP (zp100)	294	1.39	-1.50	0.29	0.49
3DP (zp14)	294	3.81	-1.57	1.11	0.98
SLS	296	0.30	-0.45	-0.04	0.11
LOM	290	3.17	-2.42	0.08	0.70

Again the SLS process shows very good geometric accuracy capability, with small bias and dispersion. The LOM process also shows very good bias, being centred at only 0.08mm average error. Unfortunately however, its dispersion is disappointingly large. Two related points are important to mention in this regard. First, the differential housing created with LOM was de-blocked much sooner than its Benchmark Cube counterpart. Being infiltrated sooner, there was less chance for influence from moisture. Second, the part was created in two halves as shown in Figure 4.13 and Figure 4.14. The process of joining them together would have created a source of variation.

5.2.2 *Circularity*

The graphs below (Figure 5.7, Figure 5.8, Figure 5.9 and Figure 5.10) indicate three issues:

- a) The value of the circularity of seven circles measured on the chosen benchmarking part.
- b) The difference between the measured diameter and the true diameter (see Figure 4.16).
- c) The diameter error shown as a percentage of the true diameter.

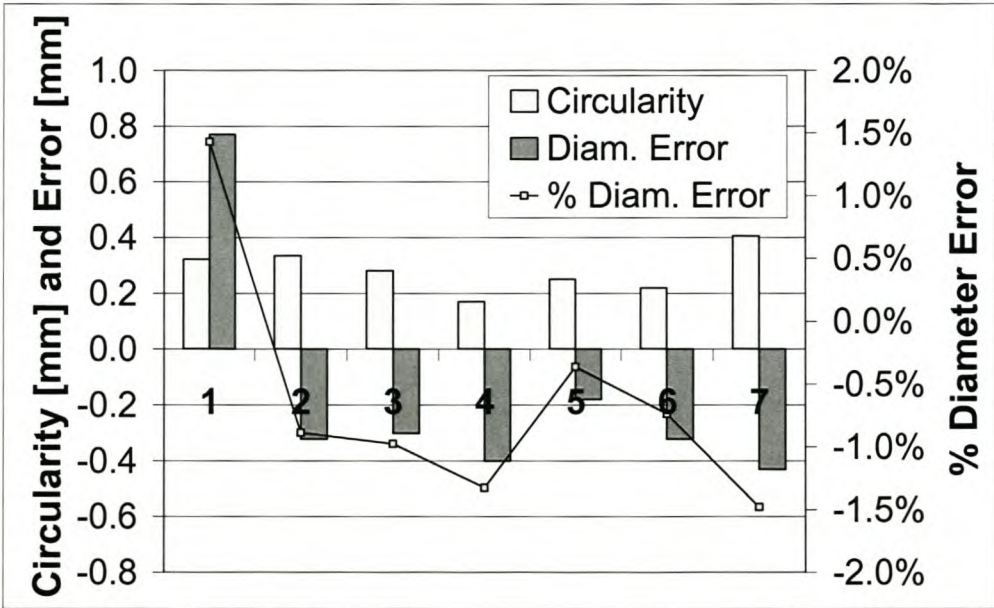


Figure 5.7: Circularity of 3DP with zp100 Powder.

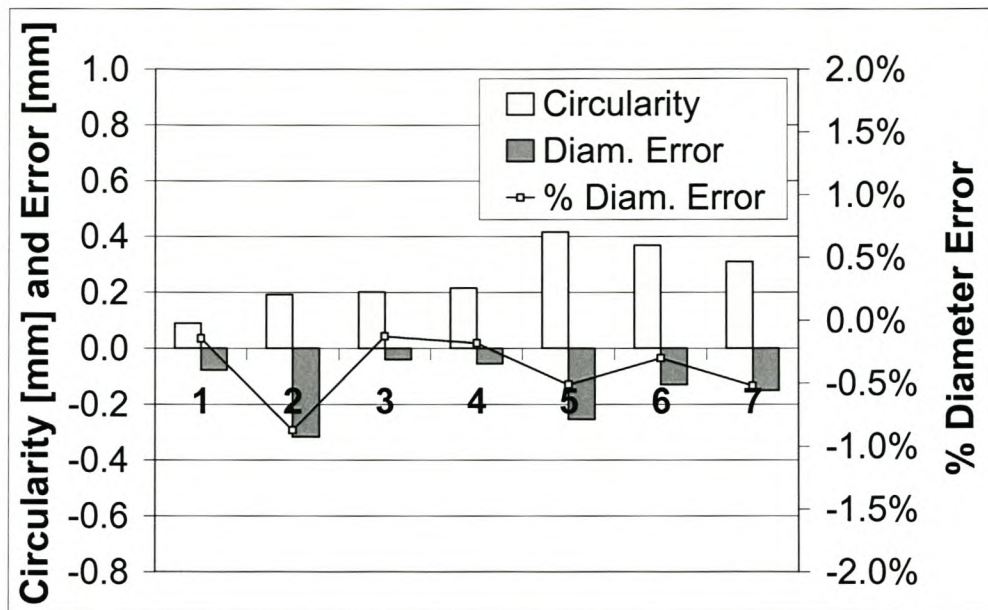


Figure 5.8: Circularity of 3DP with zp14 Powder.

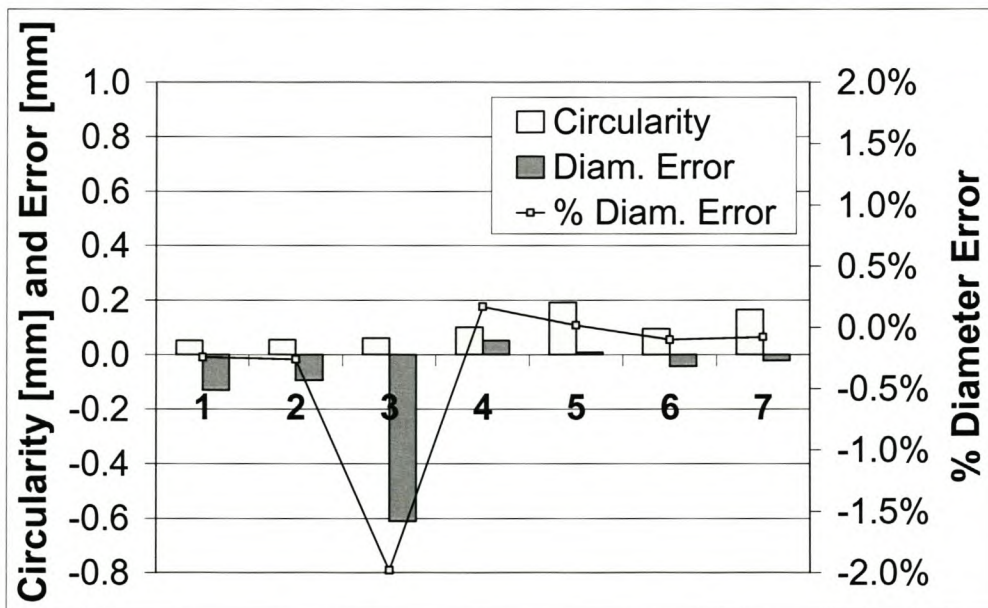


Figure 5.9: Circularity of the SLS Process.



Figure 5.10: Circularity of the LOM Process.

The diameter errors are consistent with dimensional tolerances shown in Table 5.1. The negative diameter errors, with the one exception for the zp100 powder, are consistent with the observation that the part expanded, in fact it seems that the wall thickness increased. A possible reason for this may be hygroscopic effects. Note that the circle marked “1” (Figure 4.16) is an outer diameter measure. Zp14 powder shows better circularity values than zp100 powder.

SLS results of circularity are better for circular features that are created in the XY plane (holes 1, 2 and 3). This is expected because the stair-step effect of the layers should deteriorate circularity. The diameters of holes however, are better controlled in these layered planes (holes 4 – 7).

The LOM results are surprising by the fact that those circular features 1, 2 and 3 where the split line passes through (see Figure 4.14), show better circularity and diameter errors than holes 4 – 7. This could be because the orientation of holes 4 – 7 were built perpendicular to the z-axis of the LOM machine resulting in the familiar stair-stepping effect of subsequent layers.



5.2.3 Concentricity

The concentricity of circular elements on the benchmark parts were measured and are presented in Figure 5.11 below. Please refer back to Section 4.5.2 and Figure 4.18 for the definition of concentricity. Table 5.3 shows the categories that define the different combinations of circular features that were compared to one another. For each measure of concentricity therefore, a circular feature is measured (actual element) and compared to another circular feature (reference element). The reader is referred also again back to Figure 4.16 for identifying the placement of each circular feature mentioned in this table.

Table 5.3: Categories defining reference and actual elements for concentricity

Category	Reference Element	Actual Element
1	Drive Shaft H1	Drive Shaft H2
2	Drive Shaft H1	Drive Shaft H3
3	Drive Shaft H2	Drive Shaft H3
4	RH Wheel Shaft H1	RH Wheel Shaft H2
5	RH Wheel Shaft H1	RH Wheel Shaft H3
6	RH Wheel Shaft H2	RH Wheel Shaft H3
7	LH Wheel Shaft	RH Wheel Shaft H1
8	LH Wheel Shaft	RH Wheel Shaft H2
9	LH Wheel Shaft	RH Wheel Shaft H3

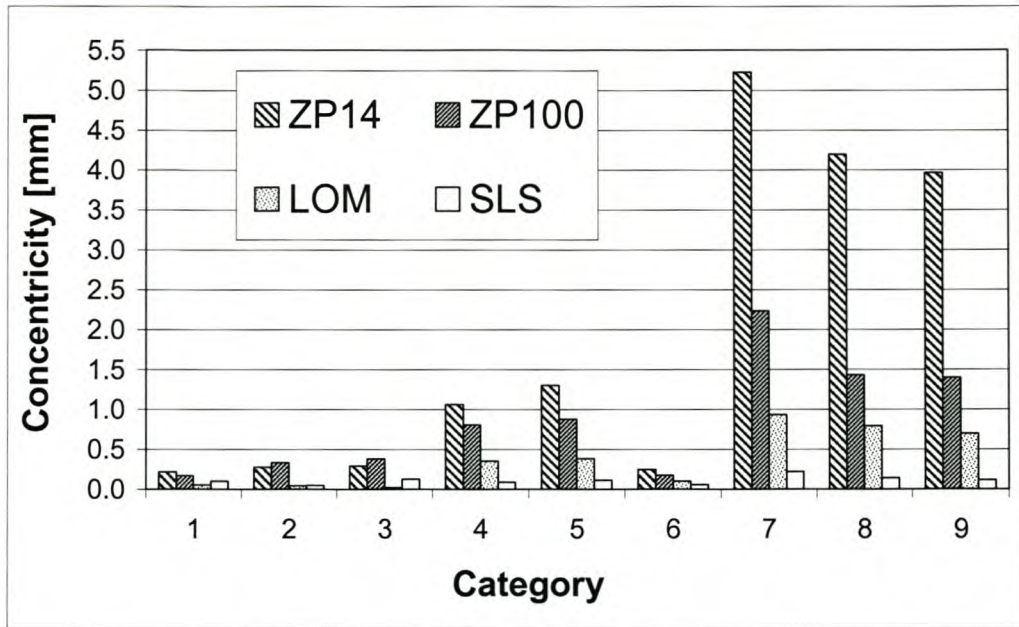


Figure 5.11: Concentricity of the different processes considered

Categories 1, 2, 3 and 6 exhibit the lowest concentricity values for each material. The results in Figure 5.11 seem to form three distinct groups. Categories 1-3, 4-5 and 7-9 seem (with the exception of category 6) to display the same magnitudes of concentricity. Considering the geometry of the benchmark part, and the location of each of these circular features thereon, concentricity is very dependent on the form of surrounding geometry to circular features. Categories 1-3 involve circular features that are in the same vicinity, and are surrounded and supported by rigid geometry such as the fillets. Categories 4-9 on the other hand, are close to the large open section at the bottom of the model.

Despite the process of assembling the two halves of the model for the LOM process, its values again shows better-than-expected results. Consider especially categories 1-3 where the split line passes directly through the circles being examined.

SLS exhibits the most consistent concentricity, while the wax-infiltrated starch models produced with 3DP, vary extensively with a maximum of 5.2 mm. The zp100 material seems to show the same form of results, but with more promising values.



When looking at the values of the concentricity, the definition of concentricity must be remembered. It means that the centre of one circles lies within a certain diameter from the centre of the reference circle. In other words the distance between the centres of the two circles is half the measured concentricity. In the case of the approximate 5mm concentricity measured for zp14 powder, the centres lie approximately 2.5mm apart. This deviation is in line with the surface tolerances given in Figure 5.4.

All of these observations indicate that a very rigid geometry is a precondition for narrow concentricity tolerances if required.

5.2.4 *Angular Tolerance*

Three angles were measured and the results of each of the RP processes are given in Figure 5.12. Note the consistency of the signs of the angles for the different types of materials. From the small amount of data it is not possible to explain the reason for this since both form and growing direction can have an influence. The growing direction determines which section of the component cures the longest in the printer while the upper sections are still being printed. This requires deeper investigation. It becomes risky to make any further concrete inferences from the limited data, but these measured values remain within at least one degree of the nominal angles.

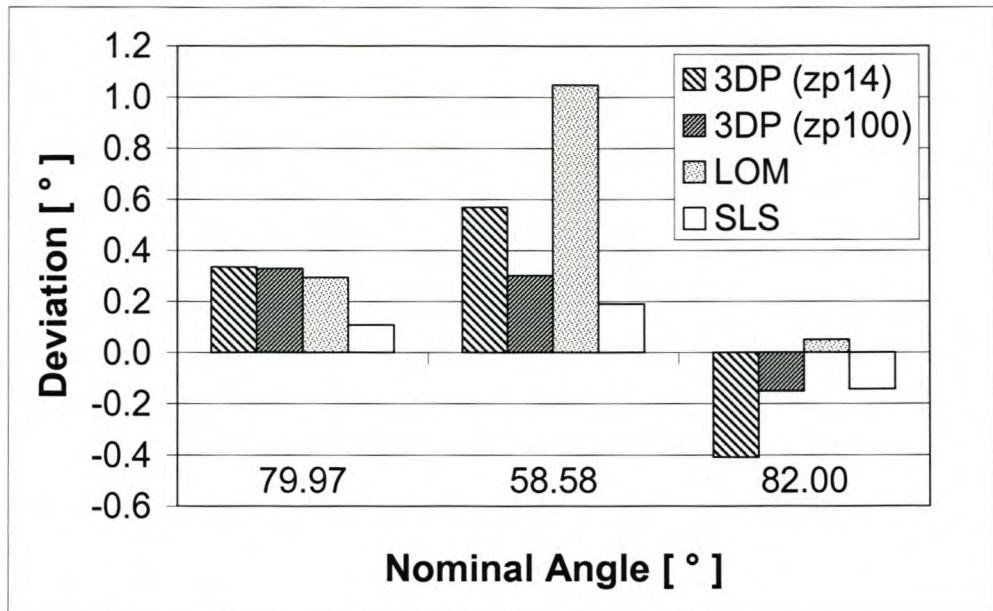


Figure 5.12: Angular deviations measured per process

5.3 Strength and Elongation

ASTM standard method D638 [34] was used to investigate the strength characteristics of parts created using the Z402 3D printer. This is the same standard that has been used with previous research to characterize the Stereolithography process [3]. To this point, only the tensile strength of the 3DP materials, zp100 and zp15e, have been investigated. The comparison of measurements relating to the other two processes, namely LOM and SLS, are still significant and now become part of ongoing research.

Figure 5.13 and Figure 5.14 shows the results obtained for zp100 and zp15e materials respectively. Those samples that have been encircled show the samples that have been disqualified due to breakage occurring too close to the clamp jaws of the tensile testing machine. These samples have been omitted from all calculations. The average tensile strength reached by the resin-infiltrated zp100 was 126.7 kPa. The wax-infiltrated zp15e material measured almost 38 % stronger, with an average tensile strength of 202.8 kPa. Both materials are very brittle and showed almost negligible elongation. The elongation that occurred at

break averaged 0.081 mm and 0.223 mm for the zp100 and zp15e materials respectively.

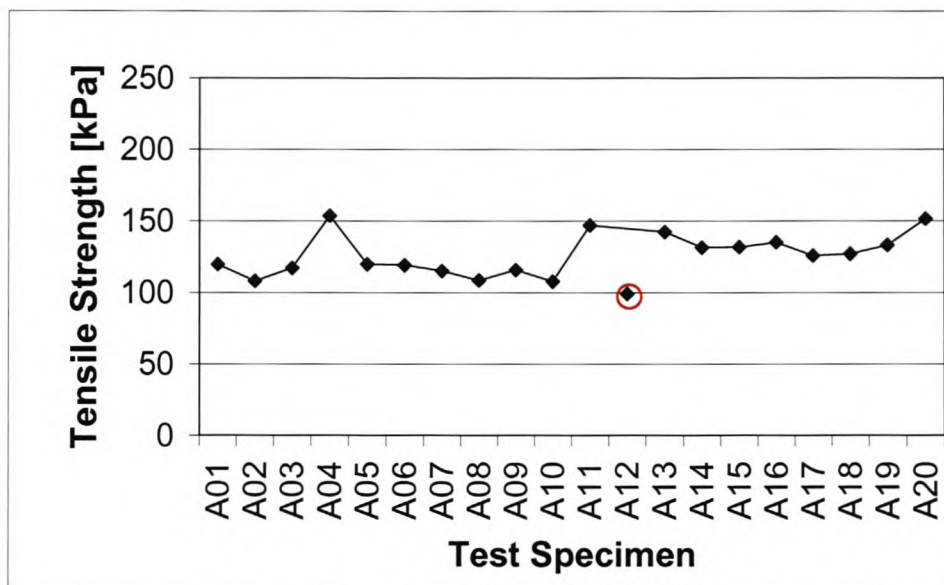


Figure 5.13: Maximum Tensile Strengths of zp100

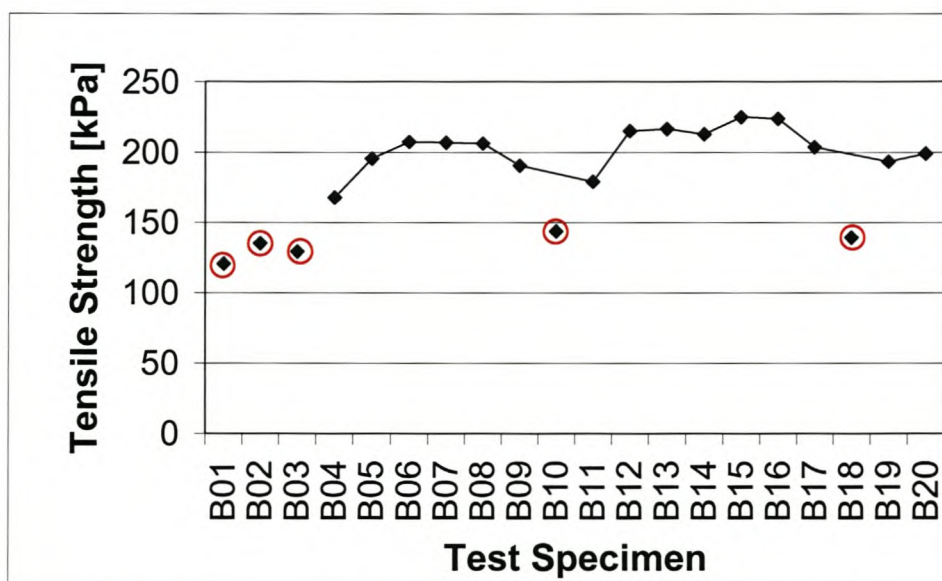


Figure 5.14: Maximum Tensile Strengths of zp15e

These tensile strengths are quite low when compared to tensile strengths that are reported by Wohlers [2] for other process. Depending on their materials,

- SL exhibits between 23 MPa to 77 MPa,



- SLS exhibits between 5MPa to 48 MPa, and
- FDM is quoted to show between 3.5 MPa to 69 MPa.
- LOM tensile strengths are not available yet.

It is interesting and disconcerting to note that the values measured for the 3DP process in this study do not correspond with the values reported by Wohlers [2]. Table 5.4 shows the values quoted by Wohlers in comparison to those found in this study. Note that the tensile strength column on the right has units in KPa. Even though the same ASTM Standard D638 was used in both cases, there is a very large difference between these values and the values measured in this study. The reason for this is still to be investigated further.

Table 5.4: Tensile strengths reported by Wohlers [2]

Wohlers [2]			This Study		
Material	Infiltrant Material	Tensile Strength [MPa]	Material	Infiltrant Material	Tensile Strength [KPa]
zp14	-	4	zp15e	-	Did not measure
zp14	Zi580	10.8 – 15	zp15e	Wax	202.8
zp100	-	10	zp100	-	Did not measure
zp100	Zi580	8.6 – 14.8	zp100	Zi580	126.7



5.4 Surface Roughness

The surface roughness measured results were as follows:

- The Zi580 resin-infiltrated zp100 material gave an average R_a value of $10.38 \mu\text{m}$ while
- The wax-infiltrated zp15e material gave R_a readings that averaged $12.64 \mu\text{m}$.

With the help of post-processing techniques such as sanding and painting, R_a values of at least $1.35 \mu\text{m}$ were obtained.

5.5 Build Time and Cost

The cost and time that it takes to produce models are an integral part of characterizing an RP process. It is most certainly one of the main areas where competitive advantage is obtained between competing RP processes or organizations. Table 5.5 shows a breakdown summary of the costs and times that were required to produce the benchmark parts used in this study. The costs quoted includes both the cost to produce as well as the cost of post-processing. Although the SLS process has given most favourable accuracy results, it is also the most expensive. Because of difficulties experienced during paper removal, the LOM process took the longest to produce the parts. It should however be mentioned that if correctly done, the de-cubing time could be reduced substantially. All post-processing times also include the time necessary for parts to cure or set in the printer before removal.

Table 5.5: Cost and Time Involved per Process

Process	Cost (To produce + post processing)	Time [hrs]		
		Build	Post- Process	Total
3DP (zp100)	R11 403.41	30.52	20.12	50.64
3DP (zp14)	R7 189.55	14.40	15.65	30.05
SLS	R18 300.00	18.55	3.42	21.97
LOM	R11 300.00	47.50	56.50	104.0

5.6 Part Design Influence on Accuracy

A further interesting characteristic that is under investigation, is the influence that design has on part accuracy and part integrity over time. As already discussed in Section 4.4.3, experience has shown that geometric features such as open or closed sections strongly influence the accuracy of the build process in 3DP. Continuing along this investigation, this study has sought to look at the influence that different wall thicknesses have on part accuracy. Two cubes (50 mm in dimension) were designed with 4 mm and 10 mm wall thicknesses. A third cube with the same dimensions was designed solid. These three cube designs were created in zp100 and zp14. Therefore, altogether six cubes were generated, and infiltrated with Zi580 epoxy resin and wax respectively.

Figure 5.15 to Figure 5.20 show results of contour plots of different wall thickness cubes for the two materials. The contour plots were made on the top, XY plane of the cube. Similar graphs of all the other cube-faces were made, but these have been selected because they reveal the most prominent deviations and differences between the materials. One can clearly see that the sagging occurs most for the cubes that are solid and for the zp14 material. This corresponds with normal foundry experience, where internal material solidifies at a slower rate than outer material, and



therefore solid designs are avoided. The top face of the cube also showed the most deviation, because of the effect of gravity. Figure 5.21 gives further values of maximum deviations that occurred per plane of each cube. The X-axis of the graph shows each of the planes that were measured along with the direction of the contour plot taken on the specific plane. The first two letters are the plane and the third letter after the hyphen, the direction. Negative deviations mean that the measurement was below the original plane of measurement.

In addition to investigating the influence of different wall thicknesses, the degree to which parts change over time was also looked at. The parts were measured twice with a four month interval between measurements. The amount of deviation between measurements can also be seen in Figure 5.15 to Figure 5.20 below.

Both materials show good integrity over time, with only very small movement being observed. For zp100 material, average movement ranged from 0.013 mm to 0.118 mm. For zp14 material, the average movement was a little bit more, ranging between 0.022 mm and 0.136 mm.

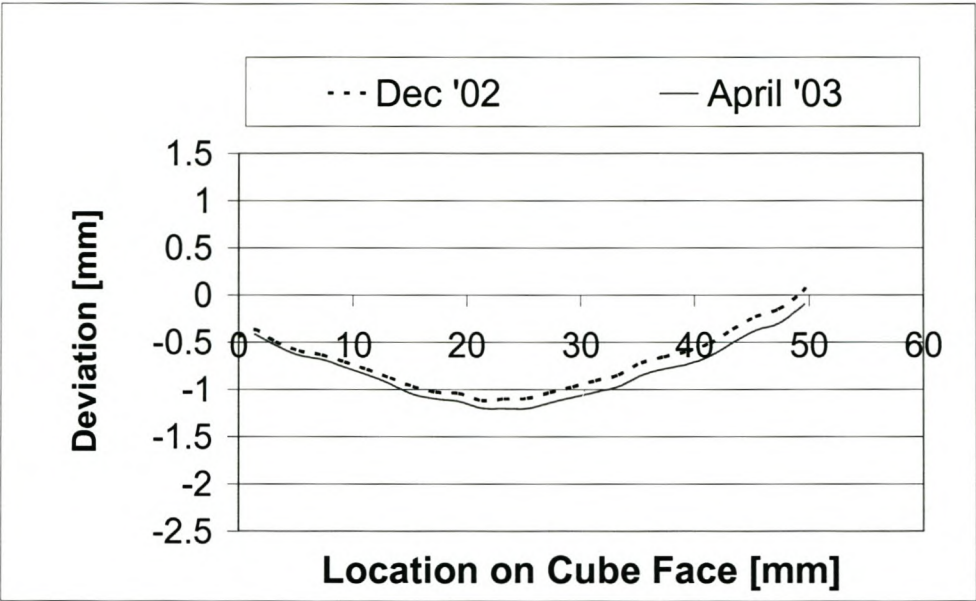


Figure 5.15: XY Face of zp14 Cube with 4mm Wall Thickness

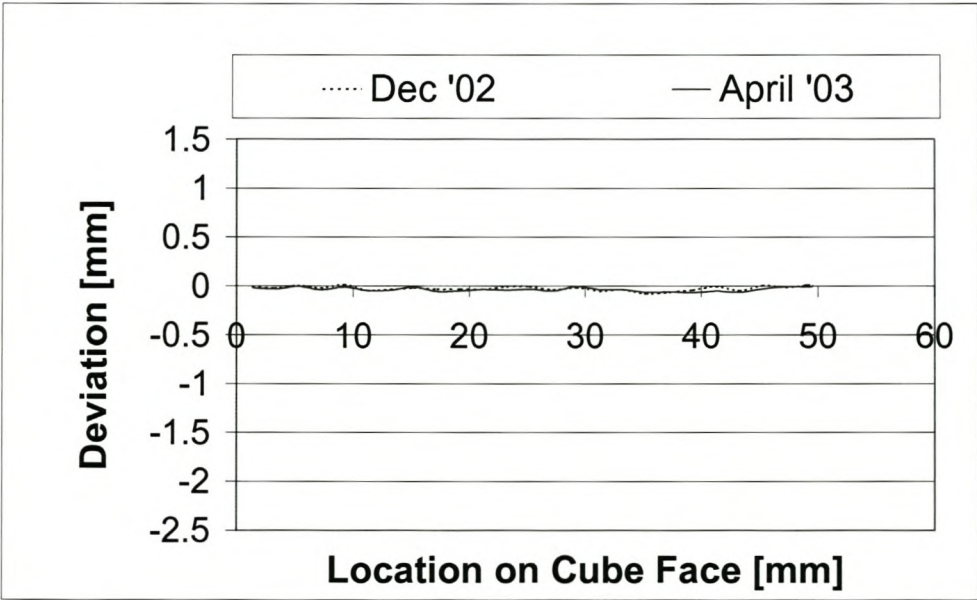


Figure 5.16: : XY Face of zp100 Cube with 4mm Wall Thickness

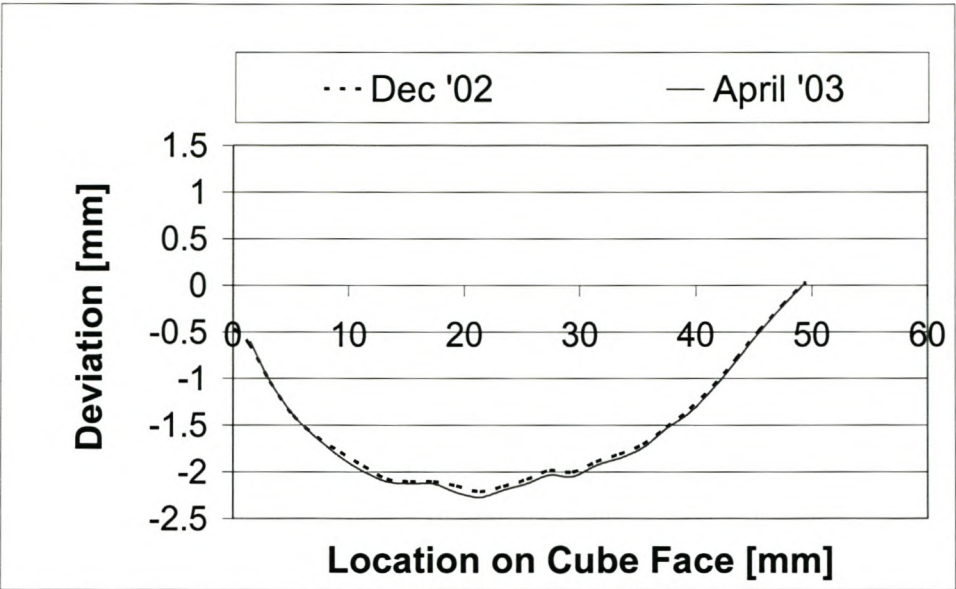


Figure 5.17: XY Face of zp14 Cube with 10mm Wall Thickness

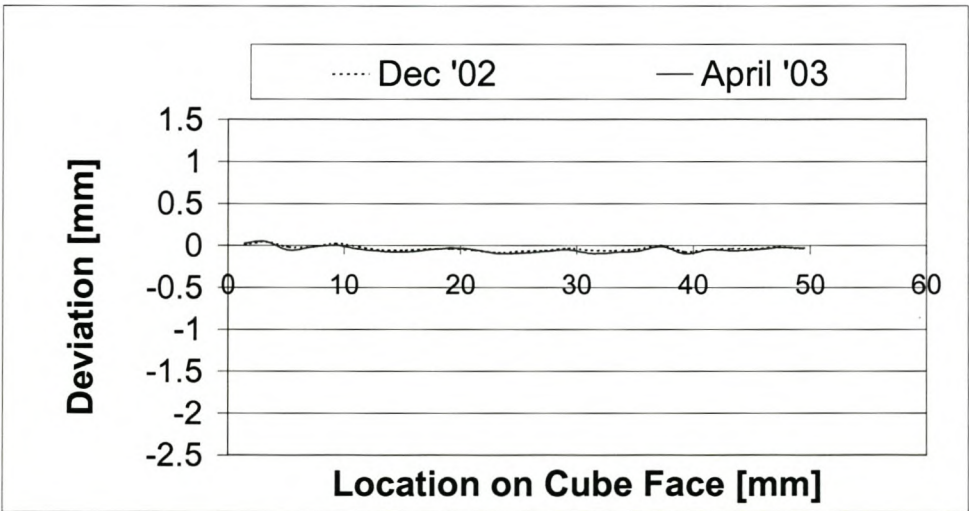


Figure 5.18: XY Face of zp100 Cube with 10mm Wall Thickness

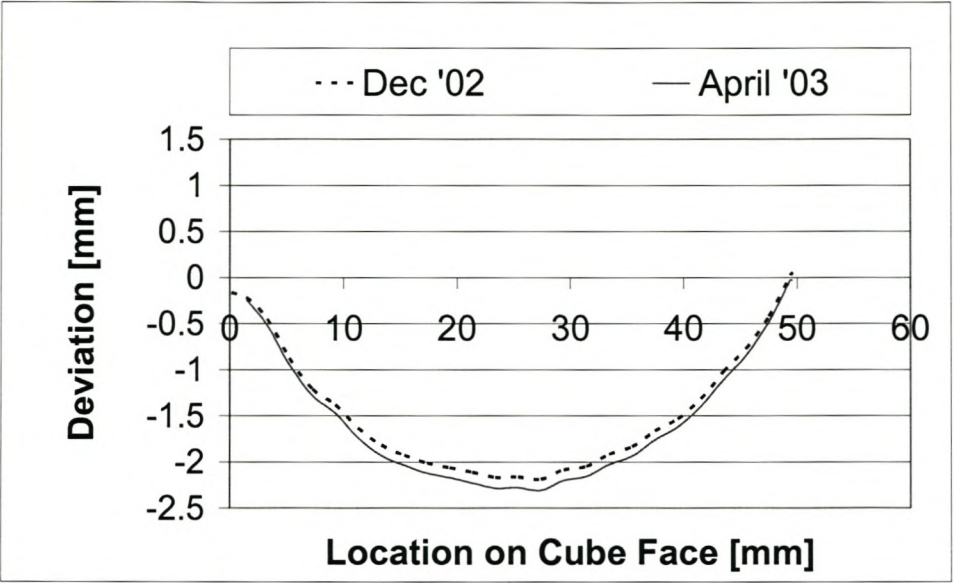


Figure 5.19: XY Face of zp14 Cube as Solid Part

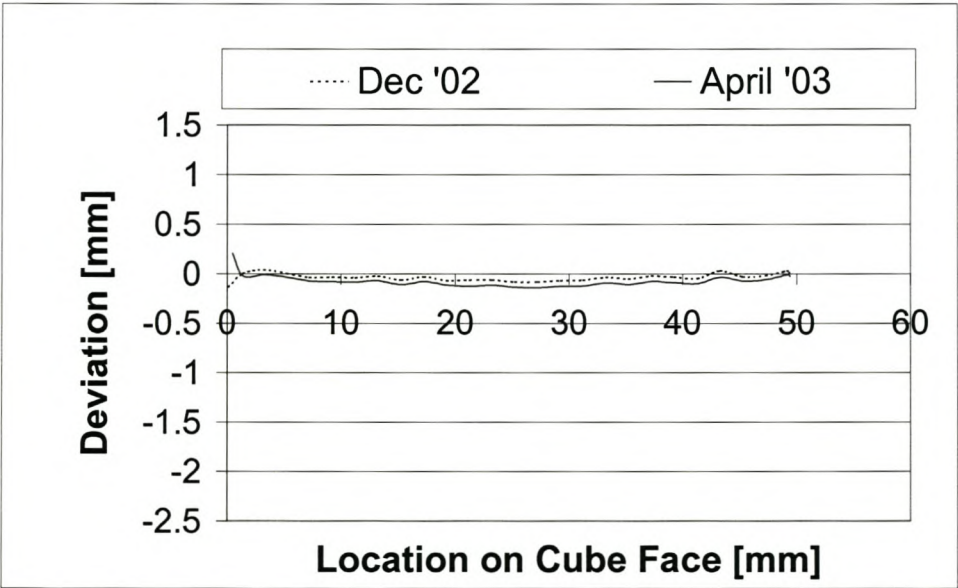


Figure 5.20: XY Face of zp100 Cube as Solid Part

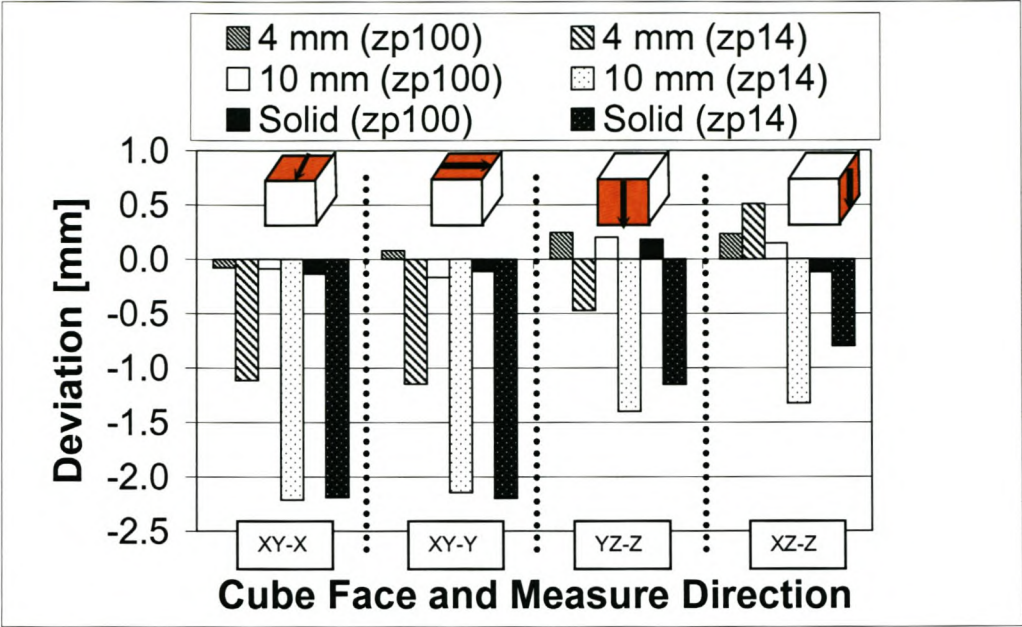


Figure 5.21: Maximum Deviations for Different Wall Thicknesses and Materials



6. *Conclusions and Recommendations*

This study has defined a set of characteristics (accuracy, surface roughness, build time, strength and elongation, and cost) that collectively describe the capability profile of an RP process. The study focussed on investigating the capability profile of the 3DP process, but also included the SLS and LOM processes as comparison.

Measuring procedures were designed for determining accuracy and surface roughness while the ASTM D638 standard procedure [34] was used to determine part strengths and elongations. Build times and costs were calculated for each process and compared on the basis of the time and cost it took to produce the benchmarking parts.

An extensive literature study was done to investigate previous benchmarking parts. Learning from these previous designs, subsequent benchmarking parts were designed and created where needed for the relevant measuring procedures of this study. From these procedures, a large set of measured data was accumulated that will contribute to the existing knowledge of the characteristics of the SLS, LOM and 3DP technologies.

The reported experimental results can be summarised by the following:

- Both the accuracy and the precision of the processes are influenced by the following three factors:
 1. The material (powder) used to produce the item.
 2. The 3D printer axis responsible for the particular dimension, and
 3. The magnitude of the nominal dimension.
- For dimensional accuracy, a trend is observed that bias grows (either negative or positive depending on the process) as the nominal dimension is enlarged – especially in the z-axis build direction.
- Zp14 Material surprisingly showed smaller bias for fine, small and medium dimensions than zp100 material. The dispersion of zp14 material however, is not as consistent and as small as zp100.



- The SLS process performed better than the other processes in terms of bias and precision.
- The capability of this specific 3D printing process in terms of IT grades, ranges from IT9 to IT16.
- Geometric accuracy depends on the type of material that is used. In general zp100 produced significantly better results than zp14. In some cases, LOM results were very promising and were close to the values measured for SLS. But SLS consistently showed very good tolerances on features that were measured.
- Zp14's distribution of deviations has a much greater dispersion than that of zp100, but both powders resulted in parts that were bigger in size than the CAD model (positive bias). Figure 5.3, Figure 5.4, Figure 5.5 and Figure 5.6 give good visual confirmation and comparison of the bias and dispersion of the different processes. See also Table 5.2 for exact values of these distributions.
- Circularity results of the SLS process were better than the other processes considered. Zp14 material also performed better than zp100 material.
- Concentricity results of the processes are in the following order (from best to worst): SLS, LOM, 3DP (zp100), 3DP (zp14).
- For the angles that were measured, the maximum angular deviation that was measured was approximately 1° positive for the LOM process. The other processes' angular deviations were within 0.6°.
- The average tensile strength reached by the zp100 (infiltrated with zi580 epoxy resin) was 126.7 kPa. The wax-infiltrated zp15e material measure almost 38% stronger, with an average tensile strength of 202.8 kPa. Both materials are very brittle and showed almost negligible elongation. The elongation that occurred at break averaged 0.081 mm and 0.223 mm for the zp100 and zp15e materials respectively.



- The Zi580 resin-infiltrated zp100 material gave an average R_a value of $10.38 \mu\text{m}$ while the wax-infiltrated zp15e material gave R_a readings that averaged $12.64 \mu\text{m}$. A cut-off length of 0.25 mm was used.
- Concerning the cost and build times of the processes, the SLS process took the shortest time (22 hours) to produce the benchmarking parts – but also proved to be the most expensive at R18 300. On the other hand, the 3DP process using zp14 material took the second shortest time (30 hours) to produce and was also the cheapest at approximately R7 200.
- Finally, it was shown that wall thickness influences part accuracy by the amount with which deformation occurs on a flat surface. It was shown that by increasing wall thicknesses up to the point of having a solid part the amount of deviation observed is also increased. Both zp14 and zp100 materials show good integrity over time, with only very small movement being observed. For zp100 material, the average movement ranged from 0.013 mm to 0.118 mm . For zp14 material, the average movement was a little bit more, ranging between 0.022 mm and 0.136 mm .

The results from this study have succeeded in obtaining values that now contribute toward characterising the 3DP, LOM and SLS processes, but still forms part of an ongoing research endeavour to quantify the effects of different factors of influence. Therefore, the following recommendations are made for future-related studies:

1. Values for bias and precision have been identified in this study. The next step is to identify how to eliminate or compensate for this bias. The precision is an inherent property of the process. Scaling factors may be considered for the compensation of the bias but careful attention must be given to the fact that different bias scaling is required for different build axes as well as for different nominal dimensions. Therefore, the situation poses an interesting software challenge that



should be attempted – ie. that of programmed dynamic scaling factors [24].

2. Further research is warranted to quantify the internal relationships between the factors that have been identified that influence variability as described in Section 4.3. The approach should be to produce a mathematical model by which results can be simulated and verified.
3. Research should be continued to include other prominent RP processes in the attempt to classify them in the same way using similar capability profiles. In doing so, this will contribute and form part of the larger research objective in designing decision support systems that aid in deciding which is the most appropriate RPM process chain to use.



References

- [1] Levy, G.N., Schindel, R., Kruth, J.P., 2003, *Rapid Manufacturing and Rapid Tooling with Layer Manufacturing (LM) Technologies, State of the Art and Future Perspectives*, Keynote Paper from the Annals of the CIRP Vol 52/2/2003, pp.1-23.
- [2] Wohlers, T., 2003, *Wohlers Report 2003, Rapid Prototyping, Tooling & Manufacturing State of the Industry*, Annual Worldwide Progress Report, Wohlers Associates Inc., Colorado, USA.
- [3] Jacobs, P.F., 1996, *Stereolithography and other RP&M Technologies*, ASME Press, American Society of Mechanical Engineers, New York.
- [4] Website: *What is Solid Freeform Manufacturing*, <http://www.msoe.edu/reu/ssf.shtml>
- [5] Kruth, J.P., Mercelis, P., Van Vaerenbergh, J., Froyen, L., Rombouts, M., 2003, *Advances in Selective Laser Sintering*, Proceedings of the 1st International Conference on Advanced Research in Virtual and Rapid Prototyping (VRAP), pp 59-70.
- [6] Website: *An explanation of & free help with selective laser sintering process / SLS models*, <http://www.toolcraft.co.uk/helpslsproc.htm>
- [7] De Beer, N., 2001, *Investigations towards a wider utilization of the 3D-Printing technology for rapid prototyping*, Unpublished report, Department of Industrial Engineering, University of Stellenbosch.
- [8] Website: *Z Corporation*, <http://www.zcorp.com>
- [9] Dimitrov, D., De Beer, N., 2002, *Advances in the 3D-Printing Technology for Rapid Prototyping & Manufacturing and Critical Role Players for Continued Growth*, Proceedings from the 17th Annual Conference of the Southern African Institute for Industrial Engineering, September 2002, Stellenbosch, South Africa, pp. 43-53.



- [10] ASTM Standards, E 105 – 58 (Reapproved 1996), Standard Practice for Probability Sampling of Materials.
- [11] ASTM Standards, E 122 – 00, Standard Practice for Calculating Sample Size to Estimate, With a Specified Tolerable Error, the Average for a Characteristic of a Lot or Process.
- [12] ASTM Standards, E 141 – 91 (Reapproved 1997), Standard Practice for Acceptance of Evidence Based on the Results of Probability Sampling.
- [13] ASTM Standards, E 177 – 90a (Reapproved 2002), Standard Practice for Use of the Terms Precision and Bias in ASTM Test Methods.
- [14] ASTM Standards, E 178 – 02, Standard Practice for Dealing With Outlying Observations.
- [15] ASTM Standards, E 456 – 02, Standard Terminology Relating to Quality and Statistics.
- [16] ASTM Standards, C1215-92 (Reapproved 1997), Standard Guide for Preparing and Interpreting Precision and Bias Statements in Test Method Standards Used in the Nuclear Industry.
- [17] ASTM Standards, E 1488 – 02, Standard Guide for Statistical Procedures to Use in Developing and Applying Test Methods.
- [18] Mandel, J., 1984, *The Statistical Analysis of Experimental Data*, Dover Publishers, New York, NY, p. 105.
- [19] Murphy, R.B., April 1961, “*On the Meaning of Precision and Accuracy*”, Materials Research and Standards, ASTM, pp. 264-267.
- [20] Eisenhart, C., June 1952, “The Reliability of Measured Values – Part I: Fundamental Concepts”, Photogrammetric Engineering, pp 542-561.
- [21] Eisenhart, C., 1963, “*Realistic Evaluation of the Precision and Accuracy of Instrument Calibration Systems*”, Journal of Research of the National Bureau of Standards, 67C, pp. 161-187.



- [22] Kendall, M.G., Buckland, W.R., 1971, *A Dictionary of Statistical Terms*, 3rd Edition, Hafner Publishing Co., Inc., New York, NY.
- [23] Yao A., Tseng Y., 2002, *A Robust Process Optimisation for a Powder Type Rapid Prototyper*, *Rapid Prototyping Journal*, Vol. 8, No. 3, pp 180-189.
- [24] Dimitrov, D., Van Wijck, W., Schreve, K., De Beer, N., 2003, *On the Achievable Accuracy of the Three Dimensional Printing Process for Rapid Prototyping*, *Proceedings of the 1st International Conference on Advanced Research in Virtual and Rapid Prototyping (VR@P 2003)*, pp 575-582.
- [25] Byun, H-S., Shin, H-J., Lee, K.H., 2002, *Design of Benchmarking Part and Selection of Optimal Rapid Prototyping Processes*, *Proceedings of the Second International Conference on Rapid Prototyping and Manufacturing 2002*, Beijing, China, pp 469-477.
- [26] Jacobs, P.F., 1992, *Rapid Prototyping and Manufacturing. Fundamentals of Stereolithography*, SME, Dearborn, MI.
- [27] Kruth, J.P., 1991, *Material Incess Manufacturing by Rapid Prototyping Techniques*, *Annals of the CIRP*, Vol. 40/2: pp 603-614.
- [28] Childs, T.H.C., Juster, N.P., 1994, *Linear and Geometric Accuracies from Layer Manufacturing*, *Annals of the CIRP*, Vol. 43/1: pp163-166.
- [29] Ippolito, R., Iuliano, L., 1995, *Benchmarking of Rapid Prototyping Techniques in Terms of Dimensional Accuracy and Surface Finish*, *Annals of the CIRP*, Vol. 44/1: pp 157-160.
- [30] Walpole, R.E., Myers, R.H., Myers, S.L., 1998, *Probability and Statistics for Engineers and Scientists*, 6th Edition, Prentice Hall International, Inc., New Jersey.
- [31] Dimitrov, D., Schreve, K., 2002, *Rapid Prototyping of a Differential Housing Using 3D Printing Technology*, *Proceedings of the International*



Conference on Manufacturing Automation, December 2002, Hong Kong, China, pp. 483-490.

- [32] De Beer, N., 2003, Computer Measuring Machine (CMM) Program for Conducting Measurements on Benchmarking Parts for Dimensional Accuracy, Unpublished report, Department of Industrial Engineering, University of Stellenbosch.
- [33] Simmons, C.H., Maguire, D.E., 1995, Manual of Engineering Drawing, Edward Arnold, London.
- [34] ASTM Standards, D638 – 02a, Standard Test Method for Tensile Properties of Plastics
- [35] Website: *Quality Gaging Tips: Surface Texture From Ra to Rz*, <http://www.mmsonline.com/articles/1102gage.html>

.



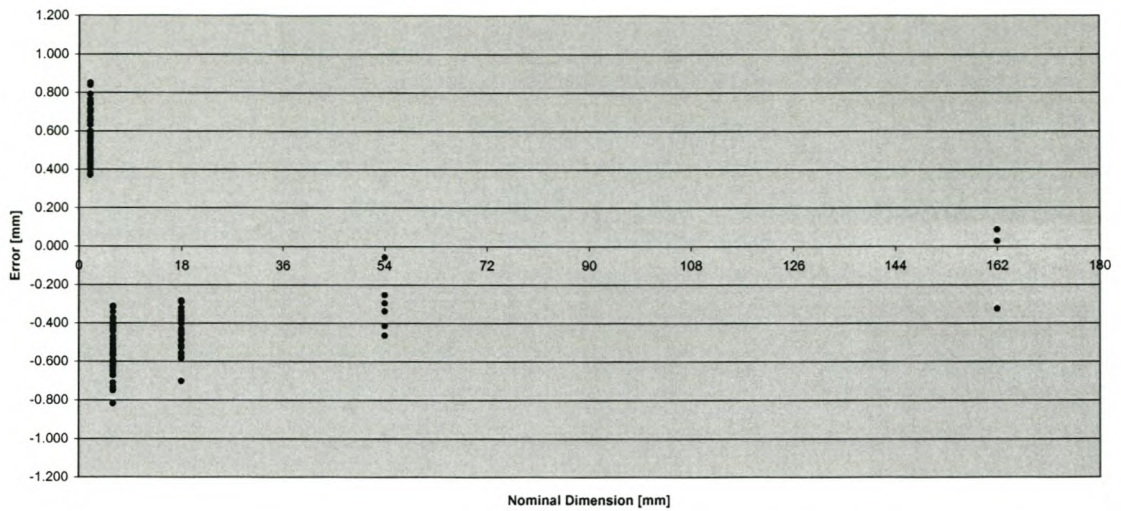
Appendix A *Dimensional Accuracy Data
Sheets and Graphs for 3DP
Process – Using Plaster
Powder*



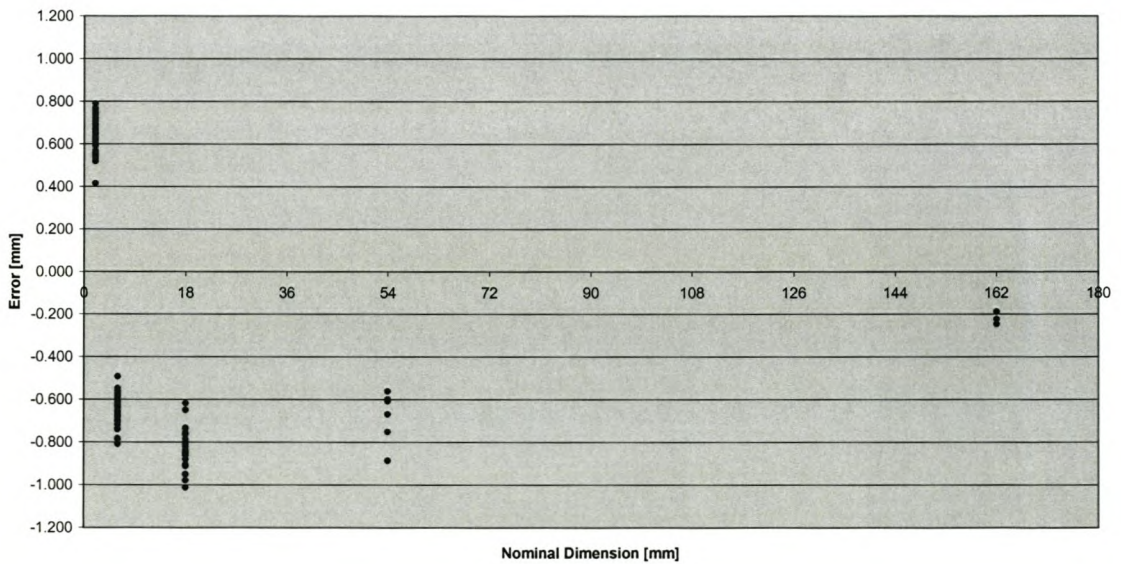
Category	A		B		C		D		E	
Nominal Value	162	mm	54	mm	18	mm	6	mm	2	mm
Sample Count	3	mm	6	mm	28	mm	60	mm	63	mm
Average Error	-0.069	mm	-0.304	mm	-0.444	mm	-0.537	mm	0.559	mm
Std Dev	0.223	mm	0.143	mm	0.099	mm	0.119	mm	0.117	mm
Average Error	-0.220	mm	-0.679	mm	-0.828	mm	-0.639	mm	0.639	mm
Std Dev	0.029	mm	0.121	mm	0.091	mm	0.068	mm	0.075	mm
Average Error	-0.866	mm	-0.569	mm	-0.330	mm	-0.250	mm	0.235	mm
Std Dev	0.066	mm	0.078	mm	0.083	mm	0.105	mm	0.087	mm



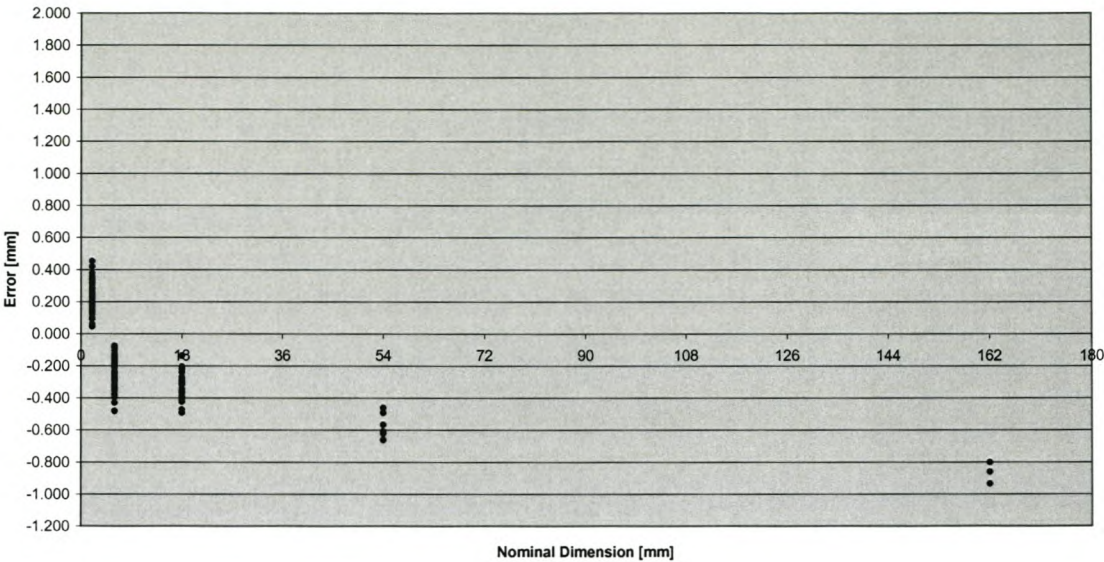
Scatterplot of Measured Errors
ZP100 (Microstone)
X-Direction



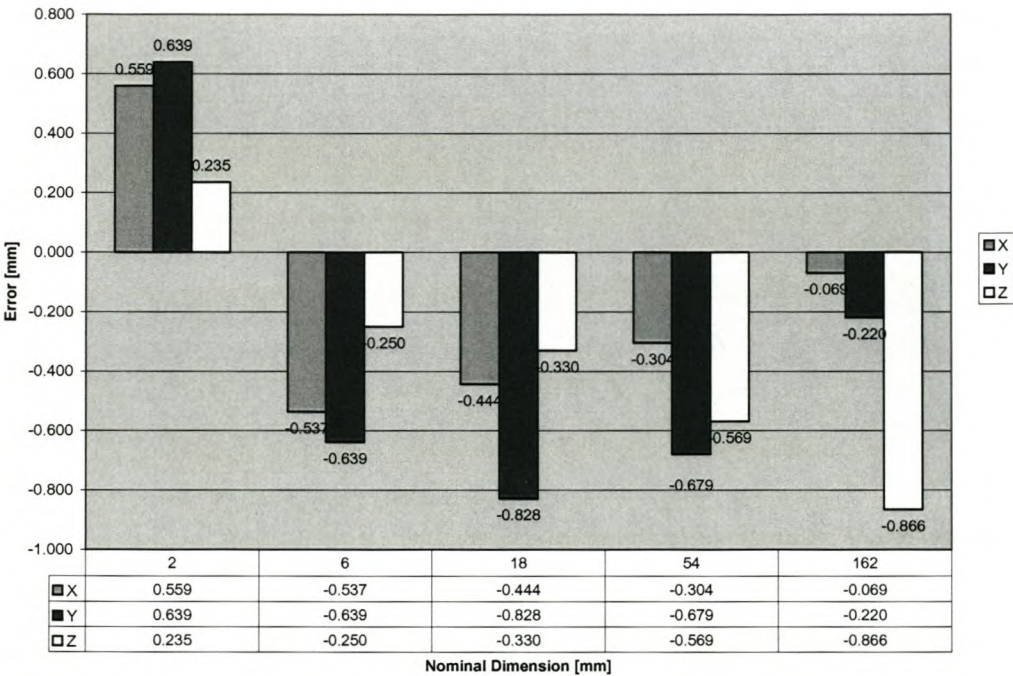
Scatterplot of Measured Errors
ZP100 (Microstone)
Y-Direction



Scatterplot of Measured Errors
ZP100 (Microstone)
Z-Direction



Measured Errors per Nominal Dimension for ZP100 (Microstone) Powder



Category A (162mm)

Measurement ID	Measured Value	Error	% Error
XA1	162.088	0.088	0.05%
XA2	162.028	0.028	0.02%
XA3	161.676	-0.324	-0.20%
YA1	161.776	-0.224	-0.14%
YA2	161.811	-0.189	-0.12%
YA3	161.754	-0.246	-0.15%
ZA1	161.198	-0.802	-0.50%
ZA2	161.066	-0.934	-0.58%
ZA3	161.139	-0.861	-0.53%

Category B (54mm)

Measurement ID	Measured Value	Error	% Error
XB1	53.746	-0.254	-0.47%
XB2	53.586	-0.414	-0.77%
XB3	53.942	-0.058	-0.11%
XB4	53.662	-0.338	-0.63%
XB5	53.536	-0.464	-0.86%
XB6	53.703	-0.297	-0.55%
YB1	53.331	-0.669	-1.24%
YB2	53.114	-0.886	-1.64%
YB3	53.249	-0.751	-1.39%
YB4	53.438	-0.562	-1.04%
YB5	53.401	-0.599	-1.11%
YB6	53.392	-0.608	-1.13%
ZB1	53.433	-0.567	-1.05%
ZB2	53.507	-0.493	-0.91%
ZB3	53.539	-0.461	-0.85%
ZB4	53.379	-0.621	-1.15%
ZB5	53.339	-0.661	-1.22%
ZB6	53.391	-0.609	-1.13%

**Category C (18mm)**

Measurement ID	Measured Value	Error	% Error
XC1	17.484	-0.516	-2.87%
XC2	17.552	-0.448	-2.49%
XC3	17.423	-0.577	-3.21%
XC4	17.638	-0.362	-2.01%
XC5	17.708	-0.292	-1.62%
XC6	17.678	-0.322	-1.79%
XC7	17.538	-0.462	-2.57%
XC8	17.472	-0.528	-2.93%
XC9	17.561	-0.439	-2.44%
XC10	17.632	-0.368	-2.04%
XC11	17.542	-0.458	-2.54%
XC12	17.505	-0.495	-2.75%
XC13	17.516	-0.484	-2.69%
XC14	17.444	-0.556	-3.09%
XC15	17.416	-0.584	-3.24%
XC16	17.439	-0.561	-3.12%
XC17	17.547	-0.453	-2.52%
XC18	17.61	-0.390	-2.17%
XC19	17.616	-0.384	-2.13%
XC20	17.717	-0.283	-1.57%
XC21	17.624	-0.376	-2.09%
XC22	17.569	-0.431	-2.39%
XC23	17.655	-0.345	-1.92%
XC24	17.658	-0.342	-1.90%
XC25	17.637	-0.363	-2.02%
XC26	17.595	-0.405	-2.25%
XC27	17.507	-0.493	-2.74%
XC28	17.299	-0.701	-3.89%
YC1	17.136	-0.864	-4.80%
YC2	17.244	-0.756	-4.20%
YC3	17.135	-0.865	-4.81%
YC4	17.162	-0.838	-4.66%
YC5	17.149	-0.851	-4.73%
YC6	17.049	-0.951	-5.28%
YC7	17.149	-0.851	-4.73%



YC8	17.261	-0.739	-4.11%
YC9	17.35	-0.650	-3.61%
YC10	17.143	-0.857	-4.76%
YC11	17.159	-0.841	-4.67%
YC12	17.261	-0.739	-4.11%
YC13	17.095	-0.905	-5.03%
YC14	17.177	-0.823	-4.57%
YC15	17.199	-0.801	-4.45%
YC16	17.382	-0.618	-3.43%
YC17	17.189	-0.811	-4.51%
YC18	17.234	-0.766	-4.26%
YC19	17.153	-0.847	-4.71%
YC20	17.119	-0.881	-4.89%
YC21	17.213	-0.787	-4.37%
YC22	17.02	-0.980	-5.44%
YC23	17.237	-0.763	-4.24%
YC24	17.048	-0.952	-5.29%
YC25	17.266	-0.734	-4.08%
YC26	17.087	-0.913	-5.07%
YC27	17.201	-0.799	-4.44%
YC28	16.988	-1.012	-5.62%
ZC1	17.682	-0.318	-1.77%
ZC2	17.628	-0.372	-2.07%
ZC3	17.6	-0.400	-2.22%
ZC4	17.682	-0.318	-1.77%
ZC5	17.527	-0.473	-2.63%
ZC6	17.782	-0.218	-1.21%
ZC7	17.692	-0.308	-1.71%
ZC8	17.864	-0.136	-0.76%
ZC9	17.699	-0.301	-1.67%
ZC10	17.611	-0.389	-2.16%
ZC11	17.731	-0.269	-1.49%
ZC12	17.64	-0.360	-2.00%
ZC13	17.645	-0.355	-1.97%
ZC14	17.509	-0.491	-2.73%
ZC15	17.711	-0.289	-1.61%
ZC16	17.715	-0.285	-1.58%
ZC17	17.576	-0.424	-2.36%



ZC18	17.684	-0.316	-1.76%
ZC19	17.589	-0.411	-2.28%
ZC20	17.703	-0.297	-1.65%
ZC21	17.759	-0.241	-1.34%
ZC22	17.795	-0.205	-1.14%
ZC23	17.657	-0.343	-1.91%
ZC24	17.598	-0.402	-2.23%
ZC25	17.605	-0.395	-2.19%
ZC26	17.709	-0.291	-1.62%
ZC27	17.777	-0.223	-1.24%
ZC28	17.59	-0.410	-2.28%

Category D (18mm)

Measurement ID	Measured Value	Error	% Error
XD1	5.391	-0.609	-10.15%
XD2	5.183	-0.817	-13.62%
XD3	5.574	-0.426	-7.10%
XD4	5.452	-0.548	-9.13%
XD5	5.377	-0.623	-10.38%
XD6	5.565	-0.435	-7.25%
XD7	5.571	-0.429	-7.15%
XD8	5.354	-0.646	-10.77%
XD9	5.688	-0.312	-5.20%
XD10	5.582	-0.418	-6.97%
XD11	5.438	-0.562	-9.37%
XD12	5.525	-0.475	-7.92%
XD13	5.626	-0.374	-6.23%
XD14	5.379	-0.621	-10.35%
XD15	5.447	-0.553	-9.22%
XD16	5.587	-0.413	-6.88%
XD17	5.446	-0.554	-9.23%
XD18	5.403	-0.597	-9.95%
XD19	5.588	-0.412	-6.87%
XD20	5.571	-0.429	-7.15%
XD21	5.374	-0.626	-10.43%
XD22	5.39	-0.610	-10.17%
XD23	5.594	-0.406	-6.77%



XD24	5.353	-0.647	-10.78%
XD25	5.29	-0.710	-11.83%
XD26	5.524	-0.476	-7.93%
XD27	5.484	-0.516	-8.60%
XD28	5.351	-0.649	-10.82%
XD29	5.529	-0.471	-7.85%
XD30	5.628	-0.372	-6.20%
XD31	5.399	-0.601	-10.02%
XD32	5.27	-0.730	-12.17%
XD33	5.562	-0.438	-7.30%
XD34	5.459	-0.541	-9.02%
XD35	5.4	-0.600	-10.00%
XD36	5.556	-0.444	-7.40%
XD37	5.329	-0.671	-11.18%
XD38	5.354	-0.646	-10.77%
XD39	5.604	-0.396	-6.60%
XD40	5.62	-0.380	-6.33%
XD41	5.409	-0.591	-9.85%
XD42	5.382	-0.618	-10.30%
XD43	5.582	-0.418	-6.97%
XD44	5.399	-0.601	-10.02%
XD45	5.366	-0.634	-10.57%
XD46	5.657	-0.343	-5.72%
XD47	5.682	-0.318	-5.30%
XD48	5.433	-0.567	-9.45%
XD49	5.492	-0.508	-8.47%
XD50	5.47	-0.530	-8.83%
XD51	5.51	-0.490	-8.17%
XD52	5.25	-0.750	-12.50%
XD53	5.466	-0.534	-8.90%
XD54	5.259	-0.741	-12.35%
XD55	5.343	-0.657	-10.95%
XD56	5.327	-0.673	-11.22%
XD57	5.367	-0.633	-10.55%
XD58	5.429	-0.571	-9.52%
XD59	5.592	-0.408	-6.80%
XD60	5.578	-0.422	-7.03%
YD1	5.217	-0.783	-13.05%



YD2	5.322	-0.678	-11.30%
YD3	5.38	-0.620	-10.33%
YD4	5.334	-0.666	-11.10%
YD5	5.316	-0.684	-11.40%
YD6	5.212	-0.788	-13.13%
YD7	5.347	-0.653	-10.88%
YD8	5.417	-0.583	-9.72%
YD9	5.371	-0.629	-10.48%
YD10	5.282	-0.718	-11.97%
YD11	5.303	-0.697	-11.62%
YD12	5.302	-0.698	-11.63%
YD13	5.316	-0.684	-11.40%
YD14	5.431	-0.569	-9.48%
YD15	5.422	-0.578	-9.63%
YD16	5.374	-0.626	-10.43%
YD17	5.414	-0.586	-9.77%
YD18	5.418	-0.582	-9.70%
YD19	5.398	-0.602	-10.03%
YD20	5.344	-0.656	-10.93%
YD21	5.191	-0.809	-13.48%
YD22	5.452	-0.548	-9.13%
YD23	5.399	-0.601	-10.02%
YD24	5.316	-0.684	-11.40%
YD25	5.413	-0.587	-9.78%
YD26	5.36	-0.640	-10.67%
YD27	5.419	-0.581	-9.68%
YD28	5.37	-0.630	-10.50%
YD29	5.216	-0.784	-13.07%
YD30	5.395	-0.605	-10.08%
YD31	5.295	-0.705	-11.75%
YD32	5.301	-0.699	-11.65%
YD33	5.389	-0.611	-10.18%
YD34	5.411	-0.589	-9.82%
YD35	5.4	-0.600	-10.00%
YD36	5.262	-0.738	-12.30%
YD37	5.259	-0.741	-12.35%
YD38	5.451	-0.549	-9.15%
YD39	5.377	-0.623	-10.38%



YD40	5.452	-0.548	-9.13%
YD41	5.364	-0.636	-10.60%
YD42	5.384	-0.616	-10.27%
YD43	5.507	-0.493	-8.22%
YD44	5.441	-0.559	-9.32%
YD45	5.376	-0.624	-10.40%
YD46	5.28	-0.720	-12.00%
YD47	5.387	-0.613	-10.22%
YD48	5.416	-0.584	-9.73%
YD49	5.385	-0.615	-10.25%
YD50	5.302	-0.698	-11.63%
YD51	5.319	-0.681	-11.35%
YD52	5.433	-0.567	-9.45%
YD53	5.338	-0.662	-11.03%
YD54	5.34	-0.660	-11.00%
YD55	5.326	-0.674	-11.23%
YD56	5.325	-0.675	-11.25%
YD57	5.422	-0.578	-9.63%
YD58	5.389	-0.611	-10.18%
YD59	5.436	-0.564	-9.40%
YD60	5.452	-0.548	-9.13%
ZD1	5.825	-0.175	-2.92%
ZD2	5.803	-0.197	-3.28%
ZD3	5.759	-0.241	-4.02%
ZD4	5.752	-0.248	-4.13%
ZD5	5.653	-0.347	-5.78%
ZD6	5.702	-0.298	-4.97%
ZD7	5.658	-0.342	-5.70%
ZD8	5.653	-0.347	-5.78%
ZD9	5.654	-0.346	-5.77%
ZD10	5.668	-0.332	-5.53%
ZD11	5.712	-0.288	-4.80%
ZD12	5.709	-0.291	-4.85%
ZD13	5.761	-0.239	-3.98%
ZD14	5.809	-0.191	-3.18%
ZD15	5.842	-0.158	-2.63%
ZD16	5.922	-0.078	-1.30%
ZD17	5.848	-0.152	-2.53%



ZD18	5.846	-0.154	-2.57%
ZD19	5.925	-0.075	-1.25%
ZD20	5.831	-0.169	-2.82%
ZD21	5.767	-0.233	-3.88%
ZD22	5.803	-0.197	-3.28%
ZD23	5.684	-0.316	-5.27%
ZD24	5.814	-0.186	-3.10%
ZD25	5.519	-0.481	-8.02%
ZD26	5.665	-0.335	-5.58%
ZD27	5.57	-0.430	-7.17%
ZD28	5.702	-0.298	-4.97%
ZD29	5.702	-0.298	-4.97%
ZD30	5.602	-0.398	-6.63%
ZD31	5.623	-0.377	-6.28%
ZD32	5.644	-0.356	-5.93%
ZD33	5.801	-0.199	-3.32%
ZD34	5.8	-0.200	-3.33%
ZD35	5.817	-0.183	-3.05%
ZD36	5.913	-0.087	-1.45%
ZD37	5.853	-0.147	-2.45%
ZD38	5.86	-0.140	-2.33%
ZD39	5.865	-0.135	-2.25%
ZD40	5.826	-0.174	-2.90%
ZD41	5.813	-0.187	-3.12%
ZD42	5.796	-0.204	-3.40%
ZD43	5.72	-0.280	-4.67%
ZD44	5.743	-0.257	-4.28%
ZD45	5.658	-0.342	-5.70%
ZD46	5.705	-0.295	-4.92%
ZD47	5.617	-0.383	-6.38%
ZD48	5.729	-0.271	-4.52%
ZD49	5.652	-0.348	-5.80%
ZD50	5.57	-0.430	-7.17%
ZD51	5.647	-0.353	-5.88%
ZD52	5.65	-0.350	-5.83%
ZD53	5.922	-0.078	-1.30%
ZD54	5.765	-0.235	-3.92%
ZD55	5.786	-0.214	-3.57%



ZD56	5.81	-0.190	-3.17%
ZD57	5.663	-0.337	-5.62%
ZD58	5.895	-0.105	-1.75%
ZD59	5.876	-0.124	-2.07%
ZD60	5.838	-0.162	-2.70%

Category E (2mm)

Measurement ID	Measured Value	Error	% Error
XE1	2.488	0.488	24.40%
XE2	2.791	0.791	39.55%
XE3	2.569	0.569	28.45%
XE4	2.568	0.568	28.40%
XE5	2.654	0.654	32.70%
XE6	2.454	0.454	22.70%
XE7	2.472	0.472	23.60%
XE8	2.559	0.559	27.95%
XE9	2.516	0.516	25.80%
XE10	2.435	0.435	21.75%
XE11	2.489	0.489	24.45%
XE12	2.543	0.543	27.15%
XE13	2.481	0.481	24.05%
XE14	2.475	0.475	23.75%
XE15	2.712	0.712	35.60%
XE16	2.494	0.494	24.70%
XE17	2.487	0.487	24.35%
XE18	2.673	0.673	33.65%
XE19	2.500	0.500	25.00%
XE20	2.579	0.579	28.95%
XE21	2.409	0.409	20.45%
XE22	2.513	0.513	25.65%
XE23	2.695	0.695	34.75%
XE24	2.542	0.542	27.10%
XE25	2.431	0.431	21.55%
XE26	2.851	0.851	42.55%
XE27	2.555	0.555	27.75%
XE28	2.517	0.517	25.85%
XE29	2.630	0.630	31.50%



XE30	2.497	0.497	24.85%
XE31	2.478	0.478	23.90%
XE32	2.475	0.475	23.75%
XE33	2.648	0.648	32.40%
XE34	2.715	0.715	35.75%
XE35	2.401	0.401	20.05%
XE36	2.748	0.748	37.40%
XE37	2.515	0.515	25.75%
XE38	2.598	0.598	29.90%
XE39	2.740	0.740	37.00%
XE40	2.517	0.517	25.85%
XE41	2.457	0.457	22.85%
XE42	2.456	0.456	22.80%
XE43	2.448	0.448	22.40%
XE44	2.661	0.661	33.05%
XE45	2.534	0.534	26.70%
XE46	2.459	0.459	22.95%
XE47	2.765	0.765	38.25%
XE48	2.422	0.422	21.10%
XE49	2.371	0.371	18.55%
XE50	2.381	0.381	19.05%
XE51	2.595	0.595	29.75%
XE52	2.590	0.590	29.50%
XE53	2.441	0.441	22.05%
XE54	2.631	0.631	31.55%
XE55	2.737	0.737	36.85%
XE56	2.573	0.573	28.65%
XE57	2.839	0.839	41.95%
XE58	2.706	0.706	35.30%
XE59	2.558	0.558	27.90%
XE60	2.700	0.700	35.00%
XE61	2.505	0.505	25.25%
XE62	2.555	0.555	27.75%
XE63	2.401	0.401	20.05%
YE1	2.414	0.414	20.70%
YE2	2.695	0.695	34.75%
YE3	2.734	0.734	36.70%
YE4	2.623	0.623	31.15%



YE5	2.692	0.692	34.60%
YE6	2.75	0.750	37.50%
YE7	2.719	0.719	35.95%
YE8	2.627	0.627	31.35%
YE9	2.61	0.610	30.50%
YE10	2.655	0.655	32.75%
YE11	2.767	0.767	38.35%
YE12	2.613	0.613	30.65%
YE13	2.788	0.788	39.40%
YE14	2.676	0.676	33.80%
YE15	2.566	0.566	28.30%
YE16	2.659	0.659	32.95%
YE17	2.531	0.531	26.55%
YE18	2.604	0.604	30.20%
YE19	2.651	0.651	32.55%
YE20	2.59	0.590	29.50%
YE21	2.631	0.631	31.55%
YE22	2.55	0.550	27.50%
YE23	2.746	0.746	37.30%
YE24	2.544	0.544	27.20%
YE25	2.709	0.709	35.45%
YE26	2.665	0.665	33.25%
YE27	2.653	0.653	32.65%
YE28	2.539	0.539	26.95%
YE29	2.644	0.644	32.20%
YE30	2.766	0.766	38.30%
YE31	2.722	0.722	36.10%
YE32	2.645	0.645	32.25%
YE33	2.648	0.648	32.40%
YE34	2.67	0.670	33.50%
YE35	2.666	0.666	33.30%
YE36	2.568	0.568	28.40%
YE37	2.739	0.739	36.95%
YE38	2.707	0.707	35.35%
YE39	2.617	0.617	30.85%
YE40	2.685	0.685	34.25%
YE41	2.607	0.607	30.35%
YE42	2.519	0.519	25.95%



YE43	2.558	0.558	27.90%
YE44	2.623	0.623	31.15%
YE45	2.552	0.552	27.60%
YE46	2.553	0.553	27.65%
YE47	2.602	0.602	30.10%
YE48	2.735	0.735	36.75%
YE49	2.619	0.619	30.95%
YE50	2.612	0.612	30.60%
YE51	2.608	0.608	30.40%
YE52	2.757	0.757	37.85%
YE53	2.657	0.657	32.85%
YE54	2.595	0.595	29.75%
YE55	2.655	0.655	32.75%
YE56	2.65	0.650	32.50%
YE57	2.712	0.712	35.60%
YE58	2.721	0.721	36.05%
YE59	2.595	0.595	29.75%
YE60	2.536	0.536	26.80%
YE61	2.626	0.626	31.30%
YE62	2.594	0.594	29.70%
YE63	2.522	0.522	26.10%
ZE1	2.090	0.090	4.50%
ZE2	2.264	0.264	13.20%
ZE3	2.216	0.216	10.80%
ZE4	2.245	0.245	12.25%
ZE5	2.223	0.223	11.15%
ZE6	2.281	0.281	14.05%
ZE7	2.326	0.326	16.30%
ZE8	2.311	0.311	15.55%
ZE9	2.340	0.340	17.00%
ZE10	2.246	0.246	12.30%
ZE11	2.277	0.277	13.85%
ZE12	2.277	0.277	13.85%
ZE13	2.147	0.147	7.35%
ZE14	2.190	0.190	9.50%
ZE15	2.159	0.159	7.95%
ZE16	2.045	0.045	2.25%
ZE17	2.184	0.184	9.20%



ZE18	2.180	0.180	9.00%
ZE19	2.145	0.145	7.25%
ZE20	2.166	0.166	8.30%
ZE21	2.451	0.451	22.55%
ZE22	2.133	0.133	6.65%
ZE23	2.257	0.257	12.85%
ZE24	2.318	0.318	15.90%
ZE25	2.210	0.210	10.50%
ZE26	2.250	0.250	12.50%
ZE27	2.375	0.375	18.75%
ZE28	2.354	0.354	17.70%
ZE29	2.311	0.311	15.55%
ZE30	2.264	0.264	13.20%
ZE31	2.233	0.233	11.65%
ZE32	2.344	0.344	17.20%
ZE33	2.333	0.333	16.65%
ZE34	2.239	0.239	11.95%
ZE35	2.170	0.170	8.50%
ZE36	2.234	0.234	11.70%
ZE37	2.060	0.060	3.00%
ZE38	2.166	0.166	8.30%
ZE39	2.176	0.176	8.80%
ZE40	2.101	0.101	5.05%
ZE41	2.264	0.264	13.20%
ZE42	2.321	0.321	16.05%
ZE43	2.119	0.119	5.95%
ZE44	2.178	0.178	8.90%
ZE45	2.306	0.306	15.30%
ZE46	2.228	0.228	11.40%
ZE47	2.236	0.236	11.80%
ZE48	2.285	0.285	14.25%
ZE49	2.284	0.284	14.20%
ZE50	2.247	0.247	12.35%
ZE51	2.260	0.260	13.00%
ZE52	2.357	0.357	17.85%
ZE53	2.320	0.320	16.00%
ZE54	2.417	0.417	20.85%
ZE55	2.057	0.057	2.85%



ZE56	2.162	0.162	8.10%
ZE57	2.227	0.227	11.35%
ZE58	2.197	0.197	9.85%
ZE59	2.322	0.322	16.10%
ZE60	2.188	0.188	9.40%
ZE61	2.138	0.138	6.90%
ZE62	2.164	0.164	8.20%
ZE63	2.243	0.243	12.15%



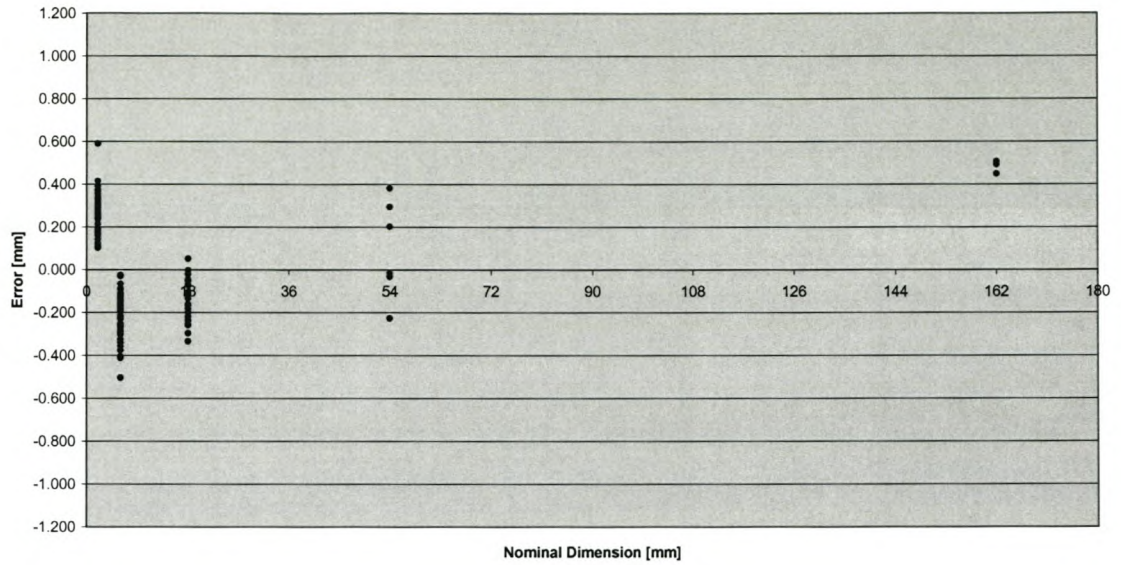
Appendix B *Dimensional Accuracy Data
Sheets and Graphs for 3DP
Process – Using Starch
Powder*



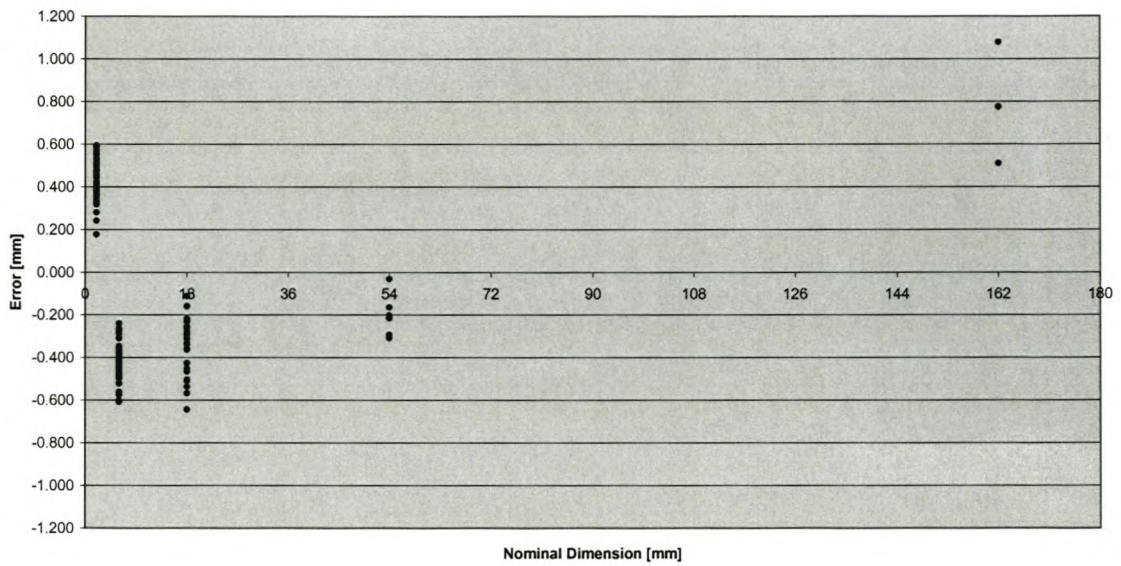
Category	A		B		C		D		E	
Nominal Value	162	mm	54	mm	18	mm	6	mm	2	mm
Sample Count	3	mm	6	mm	28	mm	60	mm	63	mm
Average Error	0.482	mm	0.100	mm	-0.144	mm	-0.204	mm	0.240	mm
Std Dev	0.030	mm	0.230	mm	0.097	mm	0.094	mm	0.089	mm
Average Error	0.787	mm	-0.202	mm	-0.337	mm	-0.433	mm	0.434	mm
Std Dev	0.284	mm	0.100	mm	0.130	mm	0.078	mm	0.084	mm
Average Error	1.675	mm	0.608	mm	0.168	mm	0.030	mm	0.068	mm
Std Dev	0.090	mm	0.198	mm	0.129	mm	0.135	mm	0.124	mm



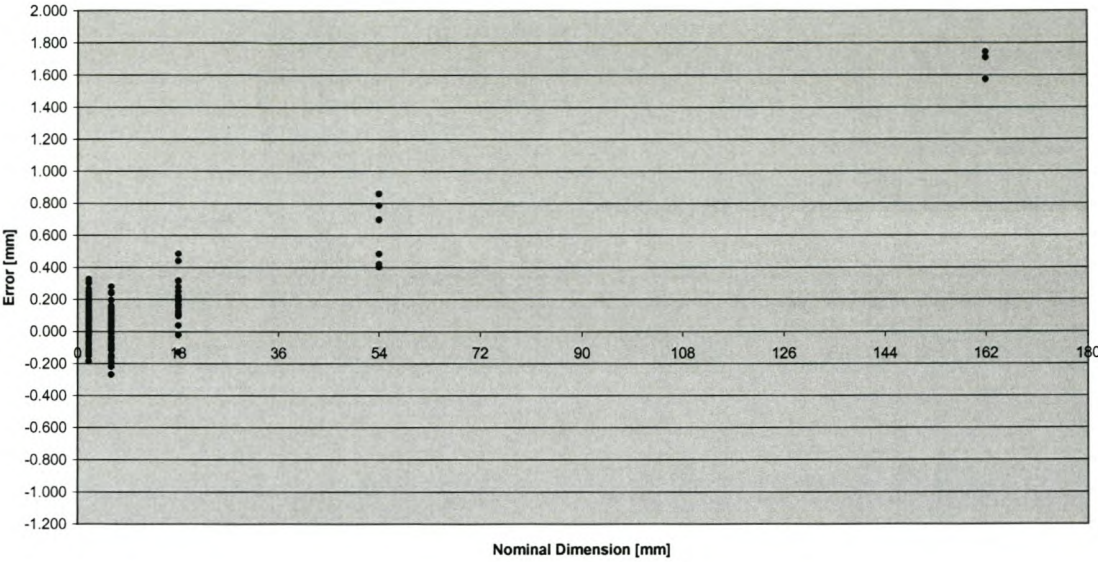
Scatterplot of Measured Errors
ZP14 (Starch)
X-Direction



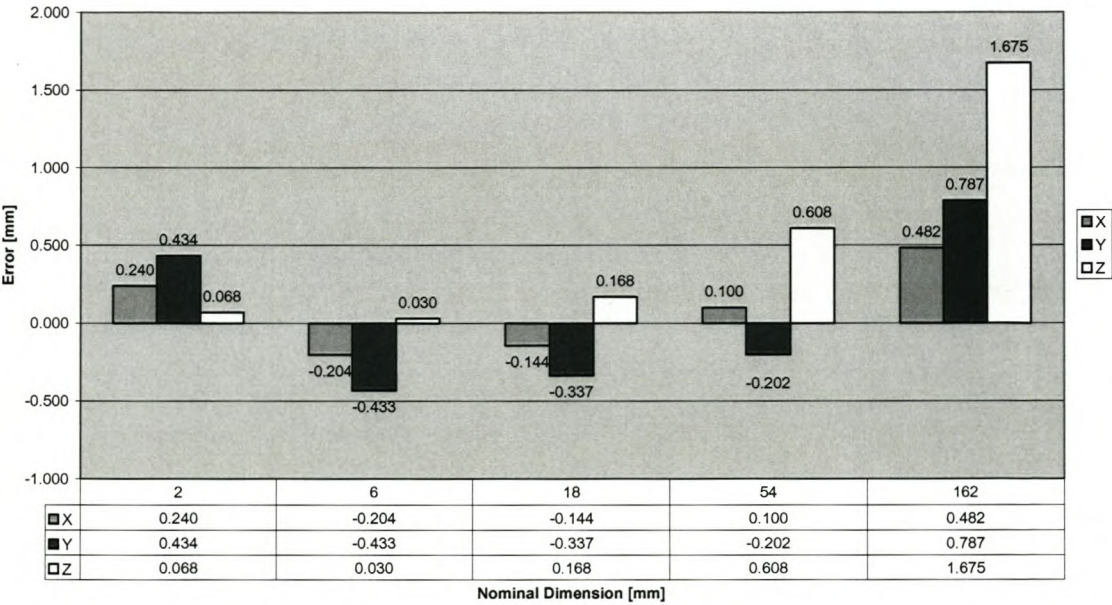
Scatterplot of Measured Errors
ZP14 (Starch)
Y-Direction



Scatterplot of Measured Errors
ZP14 (Starch)
Z-Direction



Measured Errors per Nominal Dimension for ZP14 (Starch) Powder



**Category A (162mm)**

Measurement ID	Measured Value	Error	% Error
XA1	162.506	0.506	0.31%
XA2	162.491	0.491	0.30%
XA3	162.448	0.448	0.28%
YA1	163.078	1.078	0.67%
YA2	162.51	0.510	0.31%
YA3	162.774	0.774	0.48%
ZA1	163.573	1.573	0.97%
ZA2	163.744	1.744	1.08%
ZA3	163.708	1.708	1.05%

Category B (54mm)

Measurement ID	Measured Value	Error	% Error
XB1	54.201	0.201	0.37%
XB2	53.968	-0.032	-0.06%
XB3	53.774	-0.226	-0.42%
XB4	53.983	-0.017	-0.03%
XB5	54.381	0.381	0.71%
XB6	54.294	0.294	0.54%
YB1	53.799	-0.201	-0.37%
YB2	53.708	-0.292	-0.54%
YB3	53.692	-0.308	-0.57%
YB4	53.785	-0.215	-0.40%
YB5	53.969	-0.031	-0.06%
YB6	53.836	-0.164	-0.30%
ZB1	54.484	0.484	0.90%
ZB2	54.786	0.786	1.46%
ZB3	54.698	0.698	1.29%
ZB4	54.403	0.403	0.75%
ZB5	54.419	0.419	0.78%
ZB6	54.859	0.859	1.59%

**Category C (18mm)**

Measurement ID	Measured Value	Error	% Error
XC1	17.864	-0.136	-0.76%
XC2	17.817	-0.183	-1.02%
XC3	17.953	-0.047	-0.26%
XC4	17.864	-0.136	-0.76%
XC5	17.817	-0.183	-1.02%
XC6	17.953	-0.047	-0.26%
XC7	17.666	-0.334	-1.86%
XC8	17.93	-0.070	-0.39%
XC9	17.978	-0.022	-0.12%
XC10	17.833	-0.167	-0.93%
XC11	17.746	-0.254	-1.41%
XC12	17.947	-0.053	-0.29%
XC13	17.949	-0.051	-0.28%
XC14	17.799	-0.201	-1.12%
XC15	18.052	0.052	0.29%
XC16	17.801	-0.199	-1.11%
XC17	17.931	-0.069	-0.38%
XC18	17.782	-0.218	-1.21%
XC19	17.765	-0.235	-1.31%
XC20	17.886	-0.114	-0.63%
XC21	17.703	-0.297	-1.65%
XC22	17.997	-0.003	-0.02%
XC23	17.839	-0.161	-0.89%
XC24	17.74	-0.260	-1.44%
XC25	17.76	-0.240	-1.33%
XC26	17.778	-0.222	-1.23%
XC27	17.927	-0.073	-0.41%
XC28	17.895	-0.105	-0.58%
YC1	17.548	-0.452	-2.51%
YC2	17.709	-0.291	-1.62%
YC3	17.489	-0.511	-2.84%
YC4	17.778	-0.222	-1.23%
YC5	17.463	-0.537	-2.98%
YC6	17.747	-0.253	-1.41%
YC7	17.767	-0.233	-1.29%



YC8	17.782	-0.218	-1.21%
YC9	17.642	-0.358	-1.99%
YC10	17.69	-0.310	-1.72%
YC11	17.72	-0.280	-1.56%
YC12	17.433	-0.567	-3.15%
YC13	17.776	-0.224	-1.24%
YC14	17.574	-0.426	-2.37%
YC15	17.534	-0.466	-2.59%
YC16	17.743	-0.257	-1.43%
YC17	17.668	-0.332	-1.84%
YC18	17.717	-0.283	-1.57%
YC19	17.706	-0.294	-1.63%
YC20	17.496	-0.504	-2.80%
YC21	17.768	-0.232	-1.29%
YC22	17.888	-0.112	-0.62%
YC23	17.735	-0.265	-1.47%
YC24	17.686	-0.314	-1.74%
YC25	17.637	-0.363	-2.02%
YC26	17.661	-0.339	-1.88%
YC27	17.841	-0.159	-0.88%
YC28	17.356	-0.644	-3.58%
ZC1	18.169	0.169	0.94%
ZC2	18.099	0.099	0.55%
ZC3	18.189	0.189	1.05%
ZC4	18.204	0.204	1.13%
ZC5	18.276	0.276	1.53%
ZC6	18.484	0.484	2.69%
ZC7	18.162	0.162	0.90%
ZC8	18.202	0.202	1.12%
ZC9	17.87	-0.130	-0.72%
ZC10	18.167	0.167	0.93%
ZC11	17.978	-0.022	-0.12%
ZC12	18.223	0.223	1.24%
ZC13	18.44	0.440	2.44%
ZC14	18.11	0.110	0.61%
ZC15	18.125	0.125	0.69%
ZC16	18.037	0.037	0.21%
ZC17	18.114	0.114	0.63%



ZC18	18.191	0.191	1.06%
ZC19	18.249	0.249	1.38%
ZC20	18.314	0.314	1.74%
ZC21	18.148	0.148	0.82%
ZC22	18.095	0.095	0.53%
ZC23	17.979	-0.021	-0.12%
ZC24	18.128	0.128	0.71%
ZC25	18.1	0.100	0.56%
ZC26	18.214	0.214	1.19%
ZC27	18.317	0.317	1.76%
ZC28	18.111	0.111	0.62%

Category D (6mm)

Measurement ID	Measured Value	Error	% Error
XD1	5.879	-0.121	-2.02%
XD2	5.773	-0.227	-3.78%
XD3	5.933	-0.067	-1.12%
XD4	5.77	-0.230	-3.83%
XD5	5.816	-0.184	-3.07%
XD6	5.82	-0.180	-3.00%
XD7	5.743	-0.257	-4.28%
XD8	5.883	-0.117	-1.95%
XD9	5.701	-0.299	-4.98%
XD10	5.86	-0.140	-2.33%
XD11	5.785	-0.215	-3.58%
XD12	5.801	-0.199	-3.32%
XD13	5.975	-0.025	-0.42%
XD14	5.782	-0.218	-3.63%
XD15	5.906	-0.094	-1.57%
XD16	5.851	-0.149	-2.48%
XD17	5.847	-0.153	-2.55%
XD18	5.696	-0.304	-5.07%
XD19	5.858	-0.142	-2.37%
XD20	5.738	-0.262	-4.37%
XD21	5.84	-0.160	-2.67%
XD22	5.84	-0.160	-2.67%
XD23	5.871	-0.129	-2.15%



XD24	5.779	-0.221	-3.68%
XD25	5.839	-0.161	-2.68%
XD26	5.726	-0.274	-4.57%
XD27	5.748	-0.252	-4.20%
XD28	5.829	-0.171	-2.85%
XD29	5.877	-0.123	-2.05%
XD30	5.813	-0.187	-3.12%
XD31	5.852	-0.148	-2.47%
XD32	5.891	-0.109	-1.82%
XD33	5.911	-0.089	-1.48%
XD34	5.769	-0.231	-3.85%
XD35	5.969	-0.031	-0.52%
XD36	5.876	-0.124	-2.07%
XD37	5.717	-0.283	-4.72%
XD38	5.852	-0.148	-2.47%
XD39	5.835	-0.165	-2.75%
XD40	5.643	-0.357	-5.95%
XD41	5.624	-0.376	-6.27%
XD42	5.728	-0.272	-4.53%
XD43	5.879	-0.121	-2.02%
XD44	5.815	-0.185	-3.08%
XD45	5.738	-0.262	-4.37%
XD46	5.659	-0.341	-5.68%
XD47	5.807	-0.193	-3.22%
XD48	5.78	-0.220	-3.67%
XD49	5.595	-0.405	-6.75%
XD50	5.866	-0.134	-2.23%
XD51	5.733	-0.267	-4.45%
XD52	5.858	-0.142	-2.37%
XD53	5.71	-0.290	-4.83%
XD54	5.813	-0.187	-3.12%
XD55	5.87	-0.130	-2.17%
XD56	5.87	-0.130	-2.17%
XD57	5.782	-0.218	-3.63%
XD58	5.496	-0.504	-8.40%
XD59	5.589	-0.411	-6.85%
XD60	5.674	-0.326	-5.43%
YD1	5.479	-0.521	-8.68%



YD2	5.591	-0.409	-6.82%
YD3	5.56	-0.440	-7.33%
YD4	5.522	-0.478	-7.97%
YD5	5.605	-0.395	-6.58%
YD6	5.504	-0.496	-8.27%
YD7	5.398	-0.602	-10.03%
YD8	5.64	-0.360	-6.00%
YD9	5.551	-0.449	-7.48%
YD10	5.392	-0.608	-10.13%
YD11	5.541	-0.459	-7.65%
YD12	5.619	-0.381	-6.35%
YD13	5.423	-0.577	-9.62%
YD14	5.549	-0.451	-7.52%
YD15	5.598	-0.402	-6.70%
YD16	5.526	-0.474	-7.90%
YD17	5.438	-0.562	-9.37%
YD18	5.578	-0.422	-7.03%
YD19	5.55	-0.450	-7.50%
YD20	5.478	-0.522	-8.70%
YD21	5.554	-0.446	-7.43%
YD22	5.616	-0.384	-6.40%
YD23	5.549	-0.451	-7.52%
YD24	5.529	-0.471	-7.85%
YD25	5.759	-0.241	-4.02%
YD26	5.596	-0.404	-6.73%
YD27	5.51	-0.490	-8.17%
YD28	5.61	-0.390	-6.50%
YD29	5.568	-0.432	-7.20%
YD30	5.539	-0.461	-7.68%
YD31	5.538	-0.462	-7.70%
YD32	5.645	-0.355	-5.92%
YD33	5.554	-0.446	-7.43%
YD34	5.509	-0.491	-8.18%
YD35	5.623	-0.377	-6.28%
YD36	5.505	-0.495	-8.25%
YD37	5.427	-0.573	-9.55%
YD38	5.575	-0.425	-7.08%
YD39	5.625	-0.375	-6.25%



YD40	5.58	-0.420	-7.00%
YD41	5.556	-0.444	-7.40%
YD42	5.651	-0.349	-5.82%
YD43	5.635	-0.365	-6.08%
YD44	5.583	-0.417	-6.95%
YD45	5.735	-0.265	-4.42%
YD46	5.55	-0.450	-7.50%
YD47	5.498	-0.502	-8.37%
YD48	5.653	-0.347	-5.78%
YD49	5.712	-0.288	-4.80%
YD50	5.591	-0.409	-6.82%
YD51	5.52	-0.480	-8.00%
YD52	5.647	-0.353	-5.88%
YD53	5.653	-0.347	-5.78%
YD54	5.549	-0.451	-7.52%
YD55	5.528	-0.472	-7.87%
YD56	5.515	-0.485	-8.08%
YD57	5.529	-0.471	-7.85%
YD58	5.555	-0.445	-7.42%
YD59	5.727	-0.273	-4.55%
YD60	5.69	-0.310	-5.17%
ZD1	5.845	-0.155	-2.58%
ZD2	5.8	-0.200	-3.33%
ZD3	5.896	-0.104	-1.73%
ZD4	6.158	0.158	2.63%
ZD5	5.881	-0.119	-1.98%
ZD6	5.852	-0.148	-2.47%
ZD7	5.941	-0.059	-0.98%
ZD8	6.154	0.154	2.57%
ZD9	6.124	0.124	2.07%
ZD10	6.078	0.078	1.30%
ZD11	6.129	0.129	2.15%
ZD12	6.109	0.109	1.82%
ZD13	6.09	0.090	1.50%
ZD14	6.238	0.238	3.97%
ZD15	6.104	0.104	1.73%
ZD16	6.144	0.144	2.40%
ZD17	6.127	0.127	2.12%



ZD18	6.152	0.152	2.53%
ZD19	6.125	0.125	2.08%
ZD20	6.092	0.092	1.53%
ZD21	5.916	-0.084	-1.40%
ZD22	5.925	-0.075	-1.25%
ZD23	5.963	-0.037	-0.62%
ZD24	6.136	0.136	2.27%
ZD25	5.833	-0.167	-2.78%
ZD26	5.731	-0.269	-4.48%
ZD27	5.839	-0.161	-2.68%
ZD28	5.843	-0.157	-2.62%
ZD29	6.194	0.194	3.23%
ZD30	6.041	0.041	0.68%
ZD31	6.104	0.104	1.73%
ZD32	6.065	0.065	1.08%
ZD33	6.021	0.021	0.35%
ZD34	6.237	0.237	3.95%
ZD35	5.955	-0.045	-0.75%
ZD36	6.057	0.057	0.95%
ZD37	5.997	-0.003	-0.05%
ZD38	6.061	0.061	1.02%
ZD39	6.118	0.118	1.97%
ZD40	6.111	0.111	1.85%
ZD41	5.779	-0.221	-3.68%
ZD42	5.885	-0.115	-1.92%
ZD43	5.908	-0.092	-1.53%
ZD44	6.025	0.025	0.42%
ZD45	5.811	-0.189	-3.15%
ZD46	5.997	-0.003	-0.05%
ZD47	6.006	0.006	0.10%
ZD48	6.064	0.064	1.07%
ZD49	6.278	0.278	4.63%
ZD50	6.148	0.148	2.47%
ZD51	6.119	0.119	1.98%
ZD52	6.126	0.126	2.10%
ZD53	6.039	0.039	0.65%
ZD54	6.244	0.244	4.07%
ZD55	6.15	0.150	2.50%



ZD56	5.985	-0.015	-0.25%
ZD57	6.038	0.038	0.63%
ZD58	6.031	0.031	0.52%
ZD59	6.05	0.050	0.83%
ZD60	5.958	-0.042	-0.70%

Category E (2mm)

Measurement ID	Measured Value	Error	% Error
XE1	2.190	0.190	9.50%
XE2	2.164	0.164	8.20%
XE3	2.212	0.212	10.60%
XE4	2.112	0.112	5.60%
XE5	2.278	0.278	13.90%
XE6	2.251	0.251	12.55%
XE7	2.192	0.192	9.60%
XE8	2.259	0.259	12.95%
XE9	2.375	0.375	18.75%
XE10	2.171	0.171	8.55%
XE11	2.177	0.177	8.85%
XE12	2.355	0.355	17.75%
XE13	2.293	0.293	14.65%
XE14	2.102	0.102	5.10%
XE15	2.187	0.187	9.35%
XE16	2.170	0.170	8.50%
XE17	2.288	0.288	14.40%
XE18	2.264	0.264	13.20%
XE19	2.126	0.126	6.30%
XE20	2.322	0.322	16.10%
XE21	2.125	0.125	6.25%
XE22	2.242	0.242	12.10%
XE23	2.164	0.164	8.20%
XE24	2.121	0.121	6.05%
XE25	2.194	0.194	9.70%
XE26	2.258	0.258	12.90%
XE27	2.259	0.259	12.95%
XE28	2.234	0.234	11.70%
XE29	2.368	0.368	18.40%



XE30	2.105	0.105	5.25%
XE31	2.159	0.159	7.95%
XE32	2.241	0.241	12.05%
XE33	2.171	0.171	8.55%
XE34	2.241	0.241	12.05%
XE35	2.178	0.178	8.90%
XE36	2.174	0.174	8.70%
XE37	2.180	0.180	9.00%
XE38	2.266	0.266	13.30%
XE39	2.164	0.164	8.20%
XE40	2.190	0.190	9.50%
XE41	2.413	0.413	20.65%
XE42	2.308	0.308	15.40%
XE43	2.291	0.291	14.55%
XE44	2.309	0.309	15.45%
XE45	2.252	0.252	12.60%
XE46	2.142	0.142	7.10%
XE47	2.280	0.280	14.00%
XE48	2.250	0.250	12.50%
XE49	2.366	0.366	18.30%
XE50	2.248	0.248	12.40%
XE51	2.259	0.259	12.95%
XE52	2.392	0.392	19.60%
XE53	2.243	0.243	12.15%
XE54	2.211	0.211	10.55%
XE55	2.331	0.331	16.55%
XE56	2.289	0.289	14.45%
XE57	2.158	0.158	7.90%
XE58	2.191	0.191	9.55%
XE59	2.298	0.298	14.90%
XE60	2.339	0.339	16.95%
XE61	2.291	0.291	14.55%
XE62	2.589	0.589	29.45%
XE63	2.118	0.118	5.90%
YE1	2.279	0.279	13.95%
YE2	2.531	0.531	26.55%
YE3	2.448	0.448	22.40%
YE4	2.471	0.471	23.55%



YE5	2.477	0.477	23.85%
YE6	2.502	0.502	25.10%
YE7	2.533	0.533	26.65%
YE8	2.439	0.439	21.95%
YE9	2.456	0.456	22.80%
YE10	2.568	0.568	28.40%
YE11	2.556	0.556	27.80%
YE12	2.413	0.413	20.65%
YE13	2.57	0.570	28.50%
YE14	2.527	0.527	26.35%
YE15	2.412	0.412	20.60%
YE16	2.55	0.550	27.50%
YE17	2.38	0.380	19.00%
YE18	2.469	0.469	23.45%
YE19	2.449	0.449	22.45%
YE20	2.586	0.586	29.30%
YE21	2.519	0.519	25.95%
YE22	2.177	0.177	8.85%
YE23	2.5	0.500	25.00%
YE24	2.334	0.334	16.70%
YE25	2.506	0.506	25.30%
YE26	2.416	0.416	20.80%
YE27	2.393	0.393	19.65%
YE28	2.39	0.390	19.50%
YE29	2.458	0.458	22.90%
YE30	2.414	0.414	20.70%
YE31	2.478	0.478	23.90%
YE32	2.455	0.455	22.75%
YE33	2.372	0.372	18.60%
YE34	2.499	0.499	24.95%
YE35	2.417	0.417	20.85%
YE36	2.386	0.386	19.30%
YE37	2.593	0.593	29.65%
YE38	2.508	0.508	25.40%
YE39	2.406	0.406	20.30%
YE40	2.408	0.408	20.40%
YE41	2.49	0.490	24.50%
YE42	2.363	0.363	18.15%



YE43	2.241	0.241	12.05%
YE44	2.349	0.349	17.45%
YE45	2.423	0.423	21.15%
YE46	2.387	0.387	19.35%
YE47	2.36	0.360	18.00%
YE48	2.446	0.446	22.30%
YE49	2.391	0.391	19.55%
YE50	2.395	0.395	19.75%
YE51	2.378	0.378	18.90%
YE52	2.401	0.401	20.05%
YE53	2.386	0.386	19.30%
YE54	2.424	0.424	21.20%
YE55	2.325	0.325	16.25%
YE56	2.391	0.391	19.55%
YE57	2.513	0.513	25.65%
YE58	2.567	0.567	28.35%
YE59	2.379	0.379	18.95%
YE60	2.452	0.452	22.60%
YE61	2.318	0.318	15.90%
YE62	2.374	0.374	18.70%
YE63	2.335	0.335	16.75%
ZE1	2.300	0.300	15.00%
ZE2	2.184	0.184	9.20%
ZE3	2.217	0.217	10.85%
ZE4	1.987	-0.013	-0.65%
ZE5	1.872	-0.128	-6.40%
ZE6	2.264	0.264	13.20%
ZE7	2.193	0.193	9.65%
ZE8	2.106	0.106	5.30%
ZE9	1.877	-0.123	-6.15%
ZE10	1.974	-0.026	-1.30%
ZE11	1.999	-0.001	-0.05%
ZE12	2.105	0.105	5.25%
ZE13	1.987	-0.013	-0.65%
ZE14	1.933	-0.067	-3.35%
ZE15	1.931	-0.069	-3.45%
ZE16	2.063	0.063	3.15%
ZE17	2.036	0.036	1.80%



ZE18	2.025	0.025	1.25%
ZE19	1.814	-0.186	-9.30%
ZE20	2.118	0.118	5.90%
ZE21	2.247	0.247	12.35%
ZE22	2.204	0.204	10.20%
ZE23	2.075	0.075	3.75%
ZE24	2.133	0.133	6.65%
ZE25	1.907	-0.093	-4.65%
ZE26	2.004	0.004	0.20%
ZE27	2.225	0.225	11.25%
ZE28	2.309	0.309	15.45%
ZE29	2.327	0.327	16.35%
ZE30	1.982	-0.018	-0.90%
ZE31	1.956	-0.044	-2.20%
ZE32	2.074	0.074	3.70%
ZE33	2.094	0.094	4.70%
ZE34	2.042	0.042	2.10%
ZE35	1.890	-0.110	-5.50%
ZE36	2.124	0.124	6.20%
ZE37	2.085	0.085	4.25%
ZE38	2.137	0.137	6.85%
ZE39	2.058	0.058	2.90%
ZE40	2.057	0.057	2.85%
ZE41	2.007	0.007	0.35%
ZE42	2.150	0.150	7.50%
ZE43	2.141	0.141	7.05%
ZE44	2.198	0.198	9.90%
ZE45	2.161	0.161	8.05%
ZE46	1.925	-0.075	-3.75%
ZE47	2.174	0.174	8.70%
ZE48	2.109	0.109	5.45%
ZE49	2.137	0.137	6.85%
ZE50	2.070	0.070	3.50%
ZE51	1.861	-0.139	-6.95%
ZE52	1.845	-0.155	-7.75%
ZE53	1.958	-0.042	-2.10%
ZE54	2.013	0.013	0.65%
ZE55	2.070	0.070	3.50%



ZE56	1.893	-0.107	-5.35%
ZE57	1.917	-0.083	-4.15%
ZE58	2.010	0.010	0.50%
ZE59	2.193	0.193	9.65%
ZE60	2.093	0.093	4.65%
ZE61	2.017	0.017	0.85%
ZE62	2.152	0.152	7.60%
ZE63	2.244	0.244	12.20%



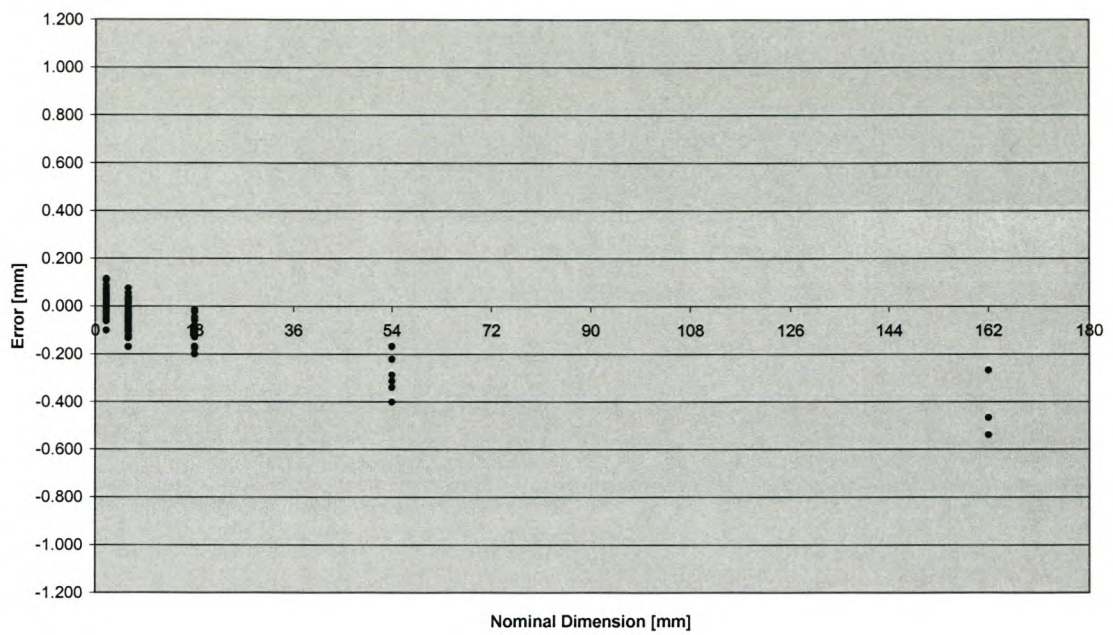
Appendix C

*Dimensional Accuracy Data
Sheets and Graphs for SLS
Process*

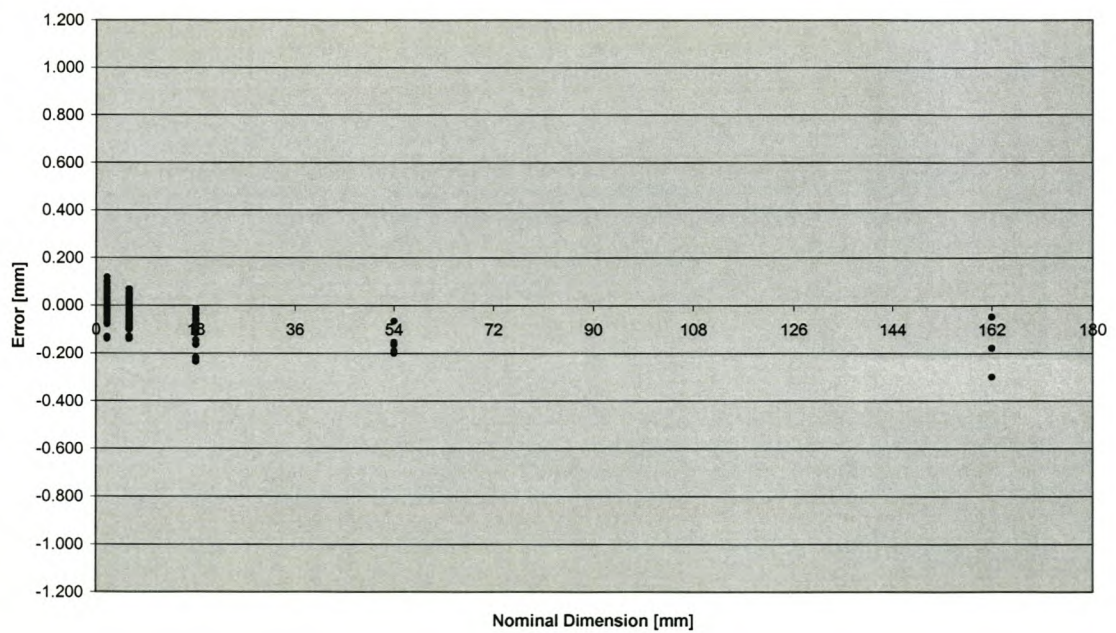


Category	A		B		C		D		E	
Nominal Value	162	mm	54	mm	18	mm	6	mm	2	mm
Sample Count	3	mm	6	mm	28	mm	60	mm	63	mm
Average Error	-0.425	mm	-0.289	mm	-0.105	mm	-0.041	mm	0.015	mm
Std Dev	0.140	mm	0.084	mm	0.043	mm	0.050	mm	0.045	mm
Average Error	-0.176	mm	-0.156	mm	-0.102	mm	-0.029	mm	0.003	mm
Std Dev	0.126	mm	0.048	mm	0.059	mm	0.053	mm	0.061	mm
Average Error	0.324	mm	-0.036	mm	-0.067	mm	-0.120	mm	0.152	mm
Std Dev	0.079	mm	0.045	mm	0.060	mm	0.057	mm	0.085	mm

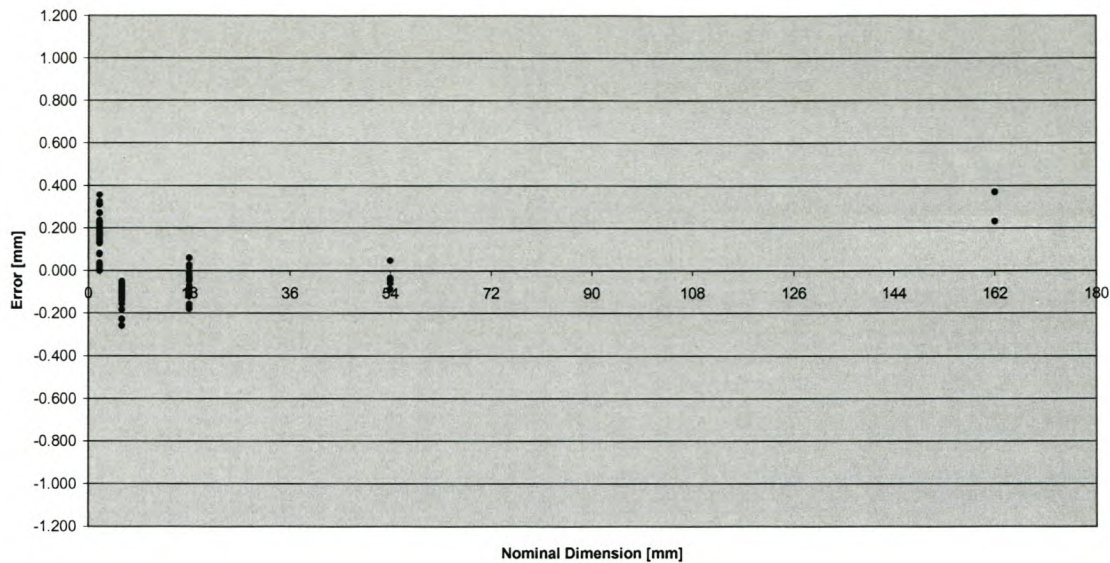
Scatterplot of Measured Errors
to SLS Process
X-Direction



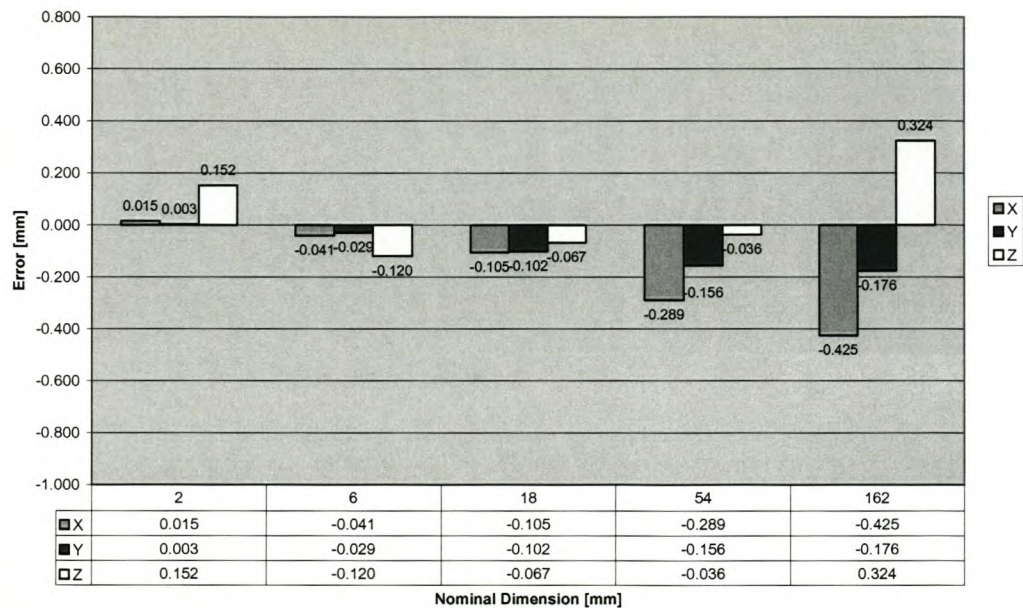
Scatterplot of Measured Errors
to SLS Process
Y-Direction



Scatterplot of Measured Errors
to SLS Process
Z-Direction



Measured Errors per Nominal Dimension for SLS Process



**Category A (162mm)**

Measurement ID	Measured Value	Error	% Error
XA1	161.732	-0.268	-0.17%
XA2	161.533	-0.467	-0.29%
XA3	161.461	-0.539	-0.33%
YA1	161.952	-0.048	-0.03%
YA2	161.821	-0.179	-0.11%
YA3	161.700	-0.300	-0.19%
ZA1	162.232	0.232	0.14%
ZA2	162.370	0.370	0.23%
ZA3	162.369	0.369	0.23%

Category B (54mm)

Measurement ID	Measured Value	Error	% Error
XB1	53.686	-0.314	-0.58%
XB2	53.598	-0.402	-0.74%
XB3	53.660	-0.34	-0.63%
XB4	53.832	-0.168	-0.31%
XB5	53.713	-0.287	-0.53%
XB6	53.779	-0.221	-0.41%
YB1	53.934	-0.066	-0.12%
YB2	53.843	-0.157	-0.29%
YB3	53.809	-0.191	-0.35%
YB4	53.799	-0.201	-0.37%
YB5	53.834	-0.166	-0.31%
YB6	53.846	-0.154	-0.29%
ZB1	53.912	-0.088	-0.16%
ZB2	53.939	-0.061	-0.11%
ZB3	53.965	-0.035	-0.06%
ZB4	53.956	-0.044	-0.08%
ZB5	53.962	-0.038	-0.07%
ZB6	54.047	0.047	0.09%

**Category C (18mm)**

Measurement ID	Measured Value	Error	% Error
XC1	17.906	-0.094	-0.52%
XC2	17.872	-0.128	-0.71%
XC3	17.898	-0.102	-0.57%
XC4	17.876	-0.124	-0.69%
XC5	17.976	-0.024	-0.13%
XC6	17.918	-0.082	-0.46%
XC7	17.913	-0.087	-0.48%
XC8	17.892	-0.108	-0.60%
XC9	17.823	-0.177	-0.98%
XC10	17.939	-0.061	-0.34%
XC11	17.954	-0.046	-0.26%
XC12	17.912	-0.088	-0.49%
XC13	17.951	-0.049	-0.27%
XC14	17.986	-0.014	-0.08%
XC15	17.870	-0.130	-0.72%
XC16	17.906	-0.094	-0.52%
XC17	17.902	-0.098	-0.54%
XC18	17.901	-0.099	-0.55%
XC19	17.886	-0.114	-0.63%
XC20	17.800	-0.200	-1.11%
XC21	17.829	-0.171	-0.95%
XC22	17.890	-0.110	-0.61%
XC23	17.831	-0.169	-0.94%
XC24	17.878	-0.122	-0.68%
XC25	17.916	-0.084	-0.47%
XC26	17.883	-0.117	-0.65%
XC27	17.878	-0.122	-0.68%
XC28	17.872	-0.128	-0.71%
YC1	17.781	-0.219	-1.22%
YC2	17.893	-0.107	-0.59%
YC3	17.883	-0.117	-0.65%
YC4	17.927	-0.073	-0.41%
YC5	17.936	-0.064	-0.36%
YC6	17.942	-0.058	-0.32%
YC7	17.853	-0.147	-0.82%



YC8	17.774	-0.226	-1.26%
YC9	17.893	-0.107	-0.59%
YC10	17.961	-0.039	-0.22%
YC11	17.895	-0.105	-0.58%
YC12	17.910	-0.090	-0.50%
YC13	17.978	-0.022	-0.12%
YC14	17.835	-0.165	-0.92%
YC15	17.765	-0.235	-1.31%
YC16	17.882	-0.118	-0.66%
YC17	17.959	-0.041	-0.23%
YC18	17.923	-0.077	-0.43%
YC19	17.966	-0.034	-0.19%
YC20	17.985	-0.015	-0.08%
YC21	17.944	-0.056	-0.31%
YC22	17.835	-0.165	-0.92%
YC23	17.921	-0.079	-0.44%
YC24	17.885	-0.115	-0.64%
YC25	17.890	-0.110	-0.61%
YC26	17.930	-0.070	-0.39%
YC27	17.914	-0.086	-0.48%
YC28	17.898	-0.102	-0.57%
ZC1	17.919	-0.081	-0.45%
ZC2	17.963	-0.037	-0.21%
ZC3	17.919	-0.081	-0.45%
ZC4	17.841	-0.159	-0.88%
ZC5	17.901	-0.099	-0.55%
ZC6	17.886	-0.114	-0.63%
ZC7	17.833	-0.167	-0.93%
ZC8	17.958	-0.042	-0.23%
ZC9	18.027	0.027	0.15%
ZC10	17.987	-0.013	-0.07%
ZC11	17.972	-0.028	-0.16%
ZC12	18.015	0.015	0.08%
ZC13	18.059	0.059	0.33%
ZC14	18.013	0.013	0.07%
ZC15	17.915	-0.085	-0.47%
ZC16	17.952	-0.048	-0.27%
ZC17	17.952	-0.048	-0.27%



ZC18	17.952	-0.048	-0.27%
ZC19	17.878	-0.122	-0.68%
ZC20	17.925	-0.075	-0.42%
ZC21	17.833	-0.167	-0.93%
ZC22	17.820	-0.180	-1.00%
ZC23	17.911	-0.089	-0.49%
ZC24	17.930	-0.070	-0.39%
ZC25	17.911	-0.089	-0.49%
ZC26	17.953	-0.047	-0.26%
ZC27	17.978	-0.022	-0.12%
ZC28	17.918	-0.082	-0.46%

Category D (6mm)

Measurement ID	Measured Value	Error	% Error
XD1	6.075	0.075	1.25%
XD2	5.972	-0.028	-0.47%
XD3	5.970	-0.030	-0.50%
XD4	5.953	-0.047	-0.78%
XD5	6.027	0.027	0.45%
XD6	5.976	-0.024	-0.40%
XD7	5.964	-0.036	-0.60%
XD8	5.970	-0.030	-0.50%
XD9	5.943	-0.057	-0.95%
XD10	5.899	-0.101	-1.68%
XD11	5.979	-0.021	-0.35%
XD12	5.957	-0.043	-0.72%
XD13	5.899	-0.101	-1.68%
XD14	5.967	-0.033	-0.55%
XD15	5.914	-0.086	-1.43%
XD16	5.968	-0.032	-0.53%
XD17	5.902	-0.098	-1.63%
XD18	5.952	-0.048	-0.80%
XD19	5.977	-0.023	-0.38%
XD20	6.016	0.016	0.27%
XD21	6.038	0.038	0.63%
XD22	6.053	0.053	0.88%
XD23	5.995	-0.005	-0.08%



XD24	5.934	-0.066	-1.10%
XD25	5.990	-0.010	-0.17%
XD26	5.979	-0.021	-0.35%
XD27	5.943	-0.057	-0.95%
XD28	5.969	-0.031	-0.52%
XD29	5.876	-0.124	-2.07%
XD30	5.913	-0.087	-1.45%
XD31	5.897	-0.103	-1.72%
XD32	5.964	-0.036	-0.60%
XD33	5.927	-0.073	-1.22%
XD34	5.893	-0.107	-1.78%
XD35	5.953	-0.047	-0.78%
XD36	5.987	-0.013	-0.22%
XD37	5.916	-0.084	-1.40%
XD38	5.957	-0.043	-0.72%
XD39	5.998	-0.002	-0.03%
XD40	6.036	0.036	0.60%
XD41	6.030	0.030	0.50%
XD42	6.053	0.053	0.88%
XD43	6.019	0.019	0.32%
XD44	5.904	-0.096	-1.60%
XD45	6.011	0.011	0.18%
XD46	5.953	-0.047	-0.78%
XD47	5.939	-0.061	-1.02%
XD48	5.967	-0.033	-0.55%
XD49	5.949	-0.051	-0.85%
XD50	5.992	-0.008	-0.13%
XD51	5.866	-0.134	-2.23%
XD52	5.955	-0.045	-0.75%
XD53	5.897	-0.103	-1.72%
XD54	5.829	-0.171	-2.85%
XD55	5.910	-0.090	-1.50%
XD56	5.962	-0.038	-0.63%
XD57	5.892	-0.108	-1.80%
XD58	5.950	-0.050	-0.83%
XD59	5.988	-0.012	-0.20%
XD60	5.987	-0.013	-0.22%
YD1	5.956	-0.044	-0.73%



YD2	5.945	-0.055	-0.92%
YD3	5.926	-0.074	-1.23%
YD4	5.868	-0.132	-2.20%
YD5	5.922	-0.078	-1.30%
YD6	5.899	-0.101	-1.68%
YD7	5.943	-0.057	-0.95%
YD8	5.967	-0.033	-0.55%
YD9	5.988	-0.012	-0.20%
YD10	5.995	-0.005	-0.08%
YD11	5.960	-0.040	-0.67%
YD12	5.952	-0.048	-0.80%
YD13	6.005	0.005	0.08%
YD14	6.002	0.002	0.03%
YD15	6.017	0.017	0.28%
YD16	6.036	0.036	0.60%
YD17	6.030	0.030	0.50%
YD18	6.046	0.046	0.77%
YD19	6.018	0.018	0.30%
YD20	6.055	0.055	0.92%
YD21	5.928	-0.072	-1.20%
YD22	5.908	-0.092	-1.53%
YD23	5.951	-0.049	-0.82%
YD24	5.929	-0.071	-1.18%
YD25	5.860	-0.140	-2.33%
YD26	5.908	-0.092	-1.53%
YD27	5.914	-0.086	-1.43%
YD28	5.930	-0.070	-1.17%
YD29	5.984	-0.016	-0.27%
YD30	6.018	0.018	0.30%
YD31	5.999	-0.001	-0.02%
YD32	5.967	-0.033	-0.55%
YD33	6.008	0.008	0.13%
YD34	5.998	-0.002	-0.03%
YD35	5.962	-0.038	-0.63%
YD36	6.013	0.013	0.22%
YD37	6.068	0.068	1.13%
YD38	6.049	0.049	0.82%
YD39	5.997	-0.003	-0.05%



YD40	6.040	0.040	0.67%
YD41	5.868	-0.132	-2.20%
YD42	5.904	-0.096	-1.60%
YD43	5.869	-0.131	-2.18%
YD44	5.868	-0.132	-2.20%
YD45	5.934	-0.066	-1.10%
YD46	5.933	-0.067	-1.12%
YD47	5.950	-0.050	-0.83%
YD48	5.991	-0.009	-0.15%
YD49	5.971	-0.029	-0.48%
YD50	5.948	-0.052	-0.87%
YD51	6.022	0.022	0.37%
YD52	5.975	-0.025	-0.42%
YD53	5.985	-0.015	-0.25%
YD54	6.011	0.011	0.18%
YD55	6.019	0.019	0.32%
YD56	6.013	0.013	0.22%
YD57	6.031	0.031	0.52%
YD58	5.962	-0.038	-0.63%
YD59	6.012	0.012	0.20%
YD60	6.045	0.045	0.75%
ZD1	5.917	-0.083	-1.38%
ZD2	5.941	-0.059	-0.98%
ZD3	5.916	-0.084	-1.40%
ZD4	5.914	-0.086	-1.43%
ZD5	5.923	-0.077	-1.28%
ZD6	5.865	-0.135	-2.25%
ZD7	5.934	-0.066	-1.10%
ZD8	5.773	-0.227	-3.78%
ZD9	5.924	-0.076	-1.27%
ZD10	5.949	-0.051	-0.85%
ZD11	5.917	-0.083	-1.38%
ZD12	5.881	-0.119	-1.98%
ZD13	5.893	-0.107	-1.78%
ZD14	5.936	-0.064	-1.07%
ZD15	5.879	-0.121	-2.02%
ZD16	5.877	-0.123	-2.05%
ZD17	5.915	-0.085	-1.42%



ZD18	5.867	-0.133	-2.22%
ZD19	5.769	-0.231	-3.85%
ZD20	5.864	-0.136	-2.27%
ZD21	5.875	-0.125	-2.08%
ZD22	5.842	-0.158	-2.63%
ZD23	5.893	-0.107	-1.78%
ZD24	5.934	-0.066	-1.10%
ZD25	5.876	-0.124	-2.07%
ZD26	5.911	-0.089	-1.48%
ZD27	5.922	-0.078	-1.30%
ZD28	5.771	-0.229	-3.82%
ZD29	5.860	-0.140	-2.33%
ZD30	5.920	-0.080	-1.33%
ZD31	5.927	-0.073	-1.22%
ZD32	5.896	-0.104	-1.73%
ZD33	5.876	-0.124	-2.07%
ZD34	5.910	-0.090	-1.50%
ZD35	5.864	-0.136	-2.27%
ZD36	5.865	-0.135	-2.25%
ZD37	5.948	-0.052	-0.87%
ZD38	5.867	-0.133	-2.22%
ZD39	5.740	-0.260	-4.33%
ZD40	5.888	-0.112	-1.87%
ZD41	5.742	-0.258	-4.30%
ZD42	5.815	-0.185	-3.08%
ZD43	5.816	-0.184	-3.07%
ZD44	5.882	-0.118	-1.97%
ZD45	5.868	-0.132	-2.20%
ZD46	5.927	-0.073	-1.22%
ZD47	5.923	-0.077	-1.28%
ZD48	5.773	-0.227	-3.78%
ZD49	5.903	-0.097	-1.62%
ZD50	5.905	-0.095	-1.58%
ZD51	5.918	-0.082	-1.37%
ZD52	5.880	-0.120	-2.00%
ZD53	5.906	-0.094	-1.57%
ZD54	5.914	-0.086	-1.43%
ZD55	5.914	-0.086	-1.43%



ZD56	5.868	-0.132	-2.20%
ZD57	5.937	-0.063	-1.05%
ZD58	5.855	-0.145	-2.42%
ZD59	5.741	-0.259	-4.32%
ZD60	5.899	-0.101	-1.68%

Category E (2mm)

Measurement ID	Measured Value	Error	% Error
XE1	1.898	-0.102	-5.10%
XE2	1.986	-0.014	-0.70%
XE3	2.004	0.004	0.20%
XE4	2.026	0.026	1.30%
XE5	1.986	-0.014	-0.70%
XE6	1.966	-0.034	-1.70%
XE7	2.015	0.015	0.75%
XE8	2.004	0.004	0.20%
XE9	2.039	0.039	1.95%
XE10	2.032	0.032	1.60%
XE11	2.064	0.064	3.20%
XE12	1.990	-0.010	-0.50%
XE13	2.058	0.058	2.90%
XE14	2.029	0.029	1.45%
XE15	2.028	0.028	1.40%
XE16	2.004	0.004	0.20%
XE17	2.086	0.086	4.30%
XE18	2.051	0.051	2.55%
XE19	1.998	-0.002	-0.10%
XE20	2.012	0.012	0.60%
XE21	1.937	-0.063	-3.15%
XE22	1.965	-0.035	-1.75%
XE23	1.947	-0.053	-2.65%
XE24	1.977	-0.023	-1.15%
XE25	2.010	0.010	0.50%
XE26	2.036	0.036	1.80%
XE27	1.942	-0.058	-2.90%
XE28	2.033	0.033	1.65%



XE29	2.007	0.007	0.35%
XE30	2.108	0.108	5.40%
XE31	2.058	0.058	2.90%
XE32	2.040	0.040	2.00%
XE33	2.064	0.064	3.20%
XE34	2.030	0.030	1.50%
XE35	2.076	0.076	3.80%
XE36	2.046	0.046	2.30%
XE37	2.007	0.007	0.35%
XE38	2.014	0.014	0.70%
XE39	2.020	0.020	1.00%
XE40	1.997	-0.003	-0.15%
XE41	1.974	-0.026	-1.30%
XE42	1.958	-0.042	-2.10%
XE43	1.951	-0.049	-2.45%
XE44	1.957	-0.043	-2.15%
XE45	1.940	-0.060	-3.00%
XE46	1.978	-0.022	-1.10%
XE47	2.050	0.050	2.50%
XE48	1.966	-0.034	-1.70%
XE49	2.076	0.076	3.80%
XE50	2.006	0.006	0.30%
XE51	2.024	0.024	1.20%
XE52	2.011	0.011	0.55%
XE53	2.004	0.004	0.20%
XE54	2.050	0.050	2.50%
XE55	2.039	0.039	1.95%
XE56	2.107	0.107	5.35%
XE57	2.115	0.115	5.75%
XE58	2.031	0.031	1.55%
XE59	2.076	0.076	3.80%
XE60	2.031	0.031	1.55%
XE61	2.012	0.012	0.60%
XE62	1.958	-0.042	-2.10%
XE63	2.067	0.067	3.35%
YE1	2.092	0.092	4.60%
YE2	2.046	0.046	2.30%
YE3	2.023	0.023	1.15%



YE4	2.093	0.093	4.65%
YE5	2.067	0.067	3.35%
YE6	2.051	0.051	2.55%
YE7	2.056	0.056	2.80%
YE8	2.062	0.062	3.10%
YE9	1.993	-0.007	-0.35%
YE10	1.975	-0.025	-1.25%
YE11	2.000	0.000	0.00%
YE12	2.033	0.033	1.65%
YE13	2.006	0.006	0.30%
YE14	1.994	-0.006	-0.30%
YE15	1.959	-0.041	-2.05%
YE16	1.945	-0.055	-2.75%
YE17	1.922	-0.078	-3.90%
YE18	1.951	-0.049	-2.45%
YE19	1.961	-0.039	-1.95%
YE20	1.936	-0.064	-3.20%
YE21	1.862	-0.138	-6.90%
YE22	1.997	-0.003	-0.15%
YE23	2.092	0.092	4.60%
YE24	2.030	0.030	1.50%
YE25	2.060	0.060	3.00%
YE26	2.049	0.049	2.45%
YE27	2.093	0.093	4.65%
YE28	2.073	0.073	3.65%
YE29	2.099	0.099	4.95%
YE30	2.005	0.005	0.25%
YE31	1.963	-0.037	-1.85%
YE32	1.974	-0.026	-1.30%
YE33	1.994	-0.006	-0.30%
YE34	1.981	-0.019	-0.95%
YE35	2.006	0.006	0.30%
YE36	1.954	-0.046	-2.30%
YE37	1.996	-0.004	-0.20%
YE38	1.929	-0.071	-3.55%
YE39	1.967	-0.033	-1.65%
YE40	1.988	-0.012	-0.60%
YE41	1.925	-0.075	-3.75%



YE42	1.868	-0.132	-6.60%
YE43	2.052	0.052	2.60%
YE44	2.117	0.117	5.85%
YE45	2.079	0.079	3.95%
YE46	2.117	0.117	5.85%
YE47	2.101	0.101	5.05%
YE48	2.031	0.031	1.55%
YE49	2.035	0.035	1.75%
YE50	2.003	0.003	0.15%
YE51	1.977	-0.023	-1.15%
YE52	2.026	0.026	1.30%
YE53	1.977	-0.023	-1.15%
YE54	1.987	-0.013	-0.65%
YE55	1.969	-0.031	-1.55%
YE56	2.000	0.000	0.00%
YE57	1.961	-0.039	-1.95%
YE58	1.927	-0.073	-3.65%
YE59	1.945	-0.055	-2.75%
YE60	2.017	0.017	0.85%
YE61	1.991	-0.009	-0.45%
YE62	1.965	-0.035	-1.75%
YE63	1.862	-0.138	-6.90%
ZE1	2.181	0.181	9.05%
ZE2	2.166	0.166	8.30%
ZE3	2.015	0.015	0.75%
ZE4	2.171	0.171	8.55%
ZE5	2.183	0.183	9.15%
ZE6	2.036	0.036	1.80%
ZE7	2.177	0.177	8.85%
ZE8	2.145	0.145	7.25%
ZE9	2.151	0.151	7.55%
ZE10	2.128	0.128	6.40%
ZE11	2.001	0.001	0.05%
ZE12	2.189	0.189	9.45%
ZE13	2.168	0.168	8.40%
ZE14	2.031	0.031	1.55%
ZE15	2.159	0.159	7.95%
ZE16	2.181	0.181	9.05%



ZE17	2.028	0.028	1.40%
ZE18	2.198	0.198	9.90%
ZE19	2.157	0.157	7.85%
ZE20	2.182	0.182	9.10%
ZE21	2.356	0.356	17.80%
ZE22	2.204	0.204	10.20%
ZE23	2.234	0.234	11.70%
ZE24	2.081	0.081	4.05%
ZE25	2.171	0.171	8.55%
ZE26	2.180	0.180	9.00%
ZE27	2.025	0.025	1.25%
ZE28	2.181	0.181	9.05%
ZE29	2.143	0.143	7.15%
ZE30	2.203	0.203	10.15%
ZE31	2.189	0.189	9.45%
ZE32	1.999	-0.001	-0.05%
ZE33	2.158	0.158	7.90%
ZE34	2.209	0.209	10.45%
ZE35	2.036	0.036	1.80%
ZE36	2.139	0.139	6.95%
ZE37	2.229	0.229	11.45%
ZE38	1.998	-0.002	-0.10%
ZE39	2.167	0.167	8.35%
ZE40	2.206	0.206	10.30%
ZE41	2.164	0.164	8.20%
ZE42	2.311	0.311	15.55%
ZE43	2.323	0.323	16.15%
ZE44	2.271	0.271	13.55%
ZE45	2.077	0.077	3.85%
ZE46	2.268	0.268	13.40%
ZE47	2.225	0.225	11.25%
ZE48	2.026	0.026	1.30%
ZE49	2.138	0.138	6.90%
ZE50	2.135	0.135	6.75%
ZE51	2.202	0.202	10.10%
ZE52	2.150	0.150	7.50%
ZE53	2.003	0.003	0.15%
ZE54	2.166	0.166	8.30%



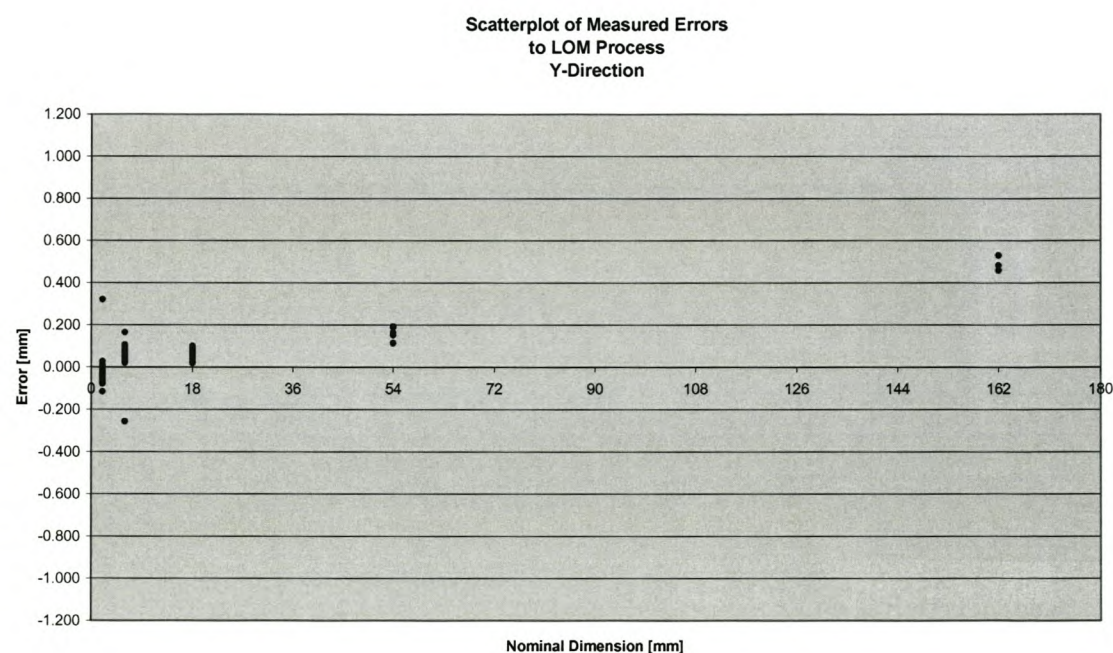
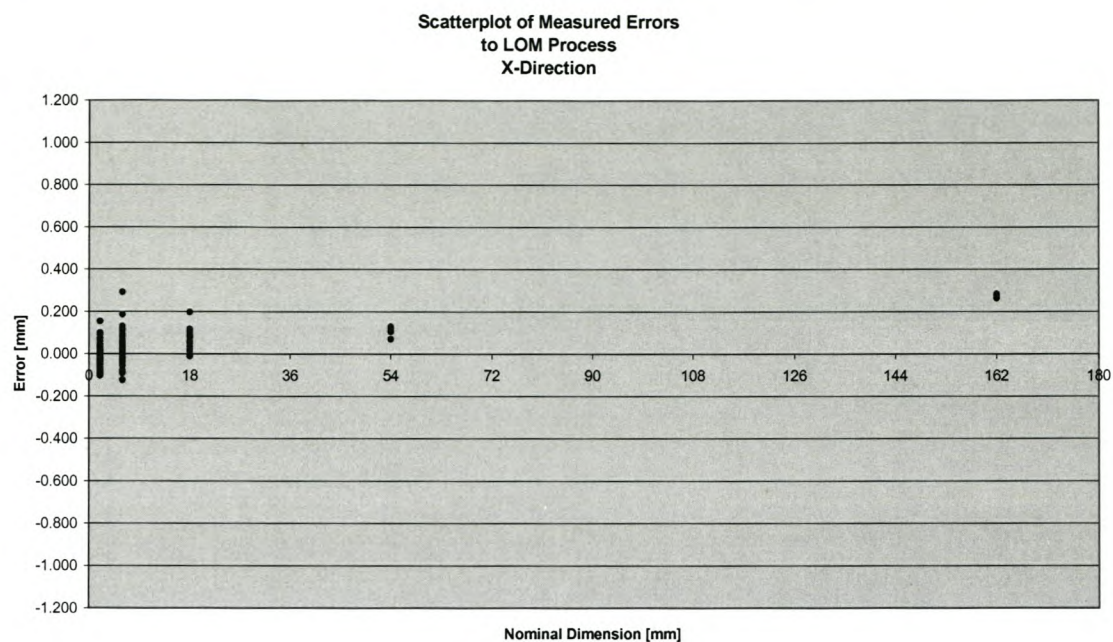
ZE55	2.162	0.162	8.10%
ZE56	2.025	0.025	1.25%
ZE57	2.143	0.143	7.15%
ZE58	2.172	0.172	8.60%
ZE59	2.013	0.013	0.65%
ZE60	2.153	0.153	7.65%
ZE61	2.217	0.217	10.85%
ZE62	2.196	0.196	9.80%
ZE63	2.309	0.309	15.45%

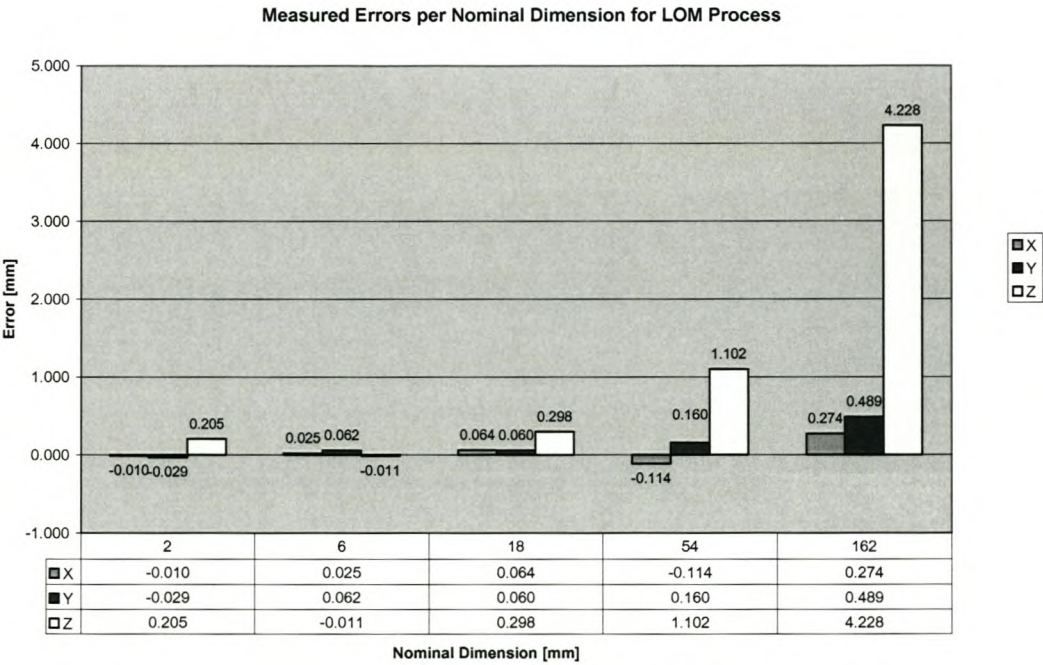
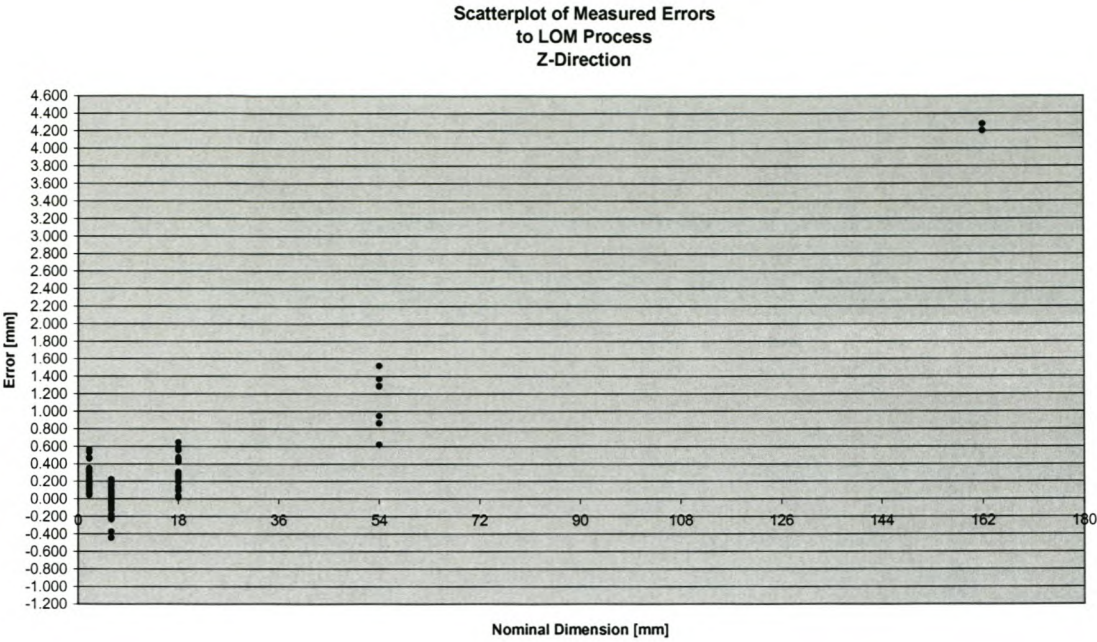


Appendix D *Dimensional Accuracy Data
Sheets and Graphs for LOM
Process*



Category	A		B		C		D		E	
Nominal Value	162	mm	54	mm	18	mm	6	mm	2	mm
Sample Count	3	mm	6	mm	28	mm	60	mm	63	mm
Average Error	0.274	mm	-0.114	mm	0.064	mm	0.025	mm	-0.010	mm
Std Dev	0.010	mm	0.541	mm	0.043	mm	0.072	mm	0.052	mm
Average Error	0.489	mm	0.160	mm	0.060	mm	0.062	mm	-0.029	mm
Std Dev	0.036	mm	0.029	mm	0.024	mm	0.049	mm	0.052	mm
Average Error	4.228	mm	1.102	mm	0.298	mm	-0.011	mm	0.205	mm
Std Dev	0.045	mm	0.345	mm	0.179	mm	0.135	mm	0.113	mm







Category A (162mm)

Measurement ID	Measured Value	Error	% Error
XA1	162.283	0.283	0.17%
XA2	162.275	0.275	0.17%
XA3	162.263	0.263	0.16%
YA1	162.529	0.529	0.33%
YA2	162.481	0.481	0.30%
YA3	162.458	0.458	0.28%
ZA1	166.280	4.280	2.64%
ZA2	166.204	4.204	2.60%
ZA3	166.201	4.201	2.59%

Category B (54mm)

Measurement ID	Measured Value	Error	% Error
XB1	52.783	-1.217	-2.25%
XB2	54.105	0.105	0.19%
XB3	54.129	0.129	0.24%
XB4	54.108	0.108	0.20%
XB5	54.121	0.121	0.22%
XB6	54.070	0.07	0.13%
YB1	54.153	0.153	0.28%
YB2	54.193	0.193	0.36%
YB3	54.188	0.188	0.35%
YB4	54.163	0.163	0.30%
YB5	54.114	0.114	0.21%
YB6	54.151	0.151	0.28%
ZB1	55.289	1.289	2.39%
ZB2	54.947	0.947	1.75%
ZB3	54.620	0.62	1.15%
ZB4	55.371	1.371	2.54%
ZB5	55.519	1.519	2.81%
ZB6	54.863	0.863	1.60%

**Category C (18mm)**

Measurement ID	Measured Value	Error	% Error
XC1	18.101	0.101	0.56%
XC2	18.011	0.011	0.06%
XC3	18.080	0.080	0.44%
XC4	18.083	0.083	0.46%
XC5	18.058	0.058	0.32%
XC6	18.075	0.075	0.42%
XC7	18.196	0.196	1.09%
XC8	18.086	0.086	0.48%
XC9	17.991	-0.009	-0.05%
XC10	17.987	-0.013	-0.07%
XC11	18.090	0.090	0.50%
XC12	18.035	0.035	0.19%
XC13	18.009	0.009	0.05%
XC14	18.074	0.074	0.41%
XC15	18.060	0.060	0.33%
XC16	18.022	0.022	0.12%
XC17	18.076	0.076	0.42%
XC18	18.108	0.108	0.60%
XC19	18.034	0.034	0.19%
XC20	18.061	0.061	0.34%
XC21	18.085	0.085	0.47%
XC22	18.117	0.117	0.65%
XC23	18.050	0.050	0.28%
XC24	18.049	0.049	0.27%
XC25	18.085	0.085	0.47%
XC26	18.088	0.088	0.49%
XC27	18.054	0.054	0.30%
XC28	18.035	0.035	0.19%
YC1	18.025	0.025	0.14%
YC2	18.039	0.039	0.22%
YC3	18.058	0.058	0.32%
YC4	18.084	0.084	0.47%
YC5	18.049	0.049	0.27%
YC6	18.096	0.096	0.53%
YC7	18.100	0.100	0.56%



YC8	18.026	0.026	0.14%
YC9	18.056	0.056	0.31%
YC10	18.071	0.071	0.39%
YC11	18.080	0.080	0.44%
YC12	18.041	0.041	0.23%
YC13	18.065	0.065	0.36%
YC14	18.096	0.096	0.53%
YC15	18.036	0.036	0.20%
YC16	18.091	0.091	0.51%
YC17	18.056	0.056	0.31%
YC18	18.038	0.038	0.21%
YC19	18.070	0.070	0.39%
YC20	18.071	0.071	0.39%
YC21	18.075	0.075	0.42%
YC22	18.027	0.027	0.15%
YC23	18.083	0.083	0.46%
YC24	18.050	0.050	0.28%
YC25	18.041	0.041	0.23%
YC26	18.019	0.019	0.11%
YC27	18.061	0.061	0.34%
YC28	18.087	0.087	0.48%
ZC1	18.592	0.592	3.29%
ZC2	18.185	0.185	1.03%
ZC3	18.554	0.554	3.08%
ZC4	18.240	0.240	1.33%
ZC5	18.094	0.094	0.52%
ZC6	18.246	0.246	1.37%
ZC7	18.423	0.423	2.35%
ZC8	18.564	0.564	3.13%
ZC9	18.225	0.225	1.25%
ZC10	18.098	0.098	0.54%
ZC11	18.196	0.196	1.09%
ZC12	18.645	0.645	3.58%
ZC13	18.030	0.030	0.17%
ZC14	18.458	0.458	2.54%
ZC15	18.192	0.192	1.07%
ZC16	18.014	0.014	0.08%
ZC17	18.446	0.446	2.48%



ZC18	18.304	0.304	1.69%
ZC19	18.247	0.247	1.37%
ZC20	18.280	0.280	1.56%
ZC21	18.471	0.471	2.62%
ZC22	18.575	0.575	3.19%
ZC23	18.134	0.134	0.74%
ZC24	18.122	0.122	0.68%
ZC25	18.298	0.298	1.66%
ZC26	18.254	0.254	1.41%
ZC27	18.196	0.196	1.09%
ZC28	18.270	0.270	1.50%

Category D (6mm)

Measurement ID	Measured Value	Error	% Error
XD1	6.045	0.045	0.75%
XD2	5.961	-0.039	-0.65%
XD3	6.065	0.065	1.08%
XD4	5.923	-0.077	-1.28%
XD5	6.087	0.087	1.45%
XD6	6.004	0.004	0.07%
XD7	6.064	0.064	1.07%
XD8	5.944	-0.056	-0.93%
XD9	6.053	0.053	0.88%
XD10	6.065	0.065	1.08%
XD11	5.877	-0.123	-2.05%
XD12	6.067	0.067	1.12%
XD13	5.983	-0.017	-0.28%
XD14	5.979	-0.021	-0.35%
XD15	6.055	0.055	0.92%
XD16	6.056	0.056	0.93%
XD17	6.053	0.053	0.88%
XD18	5.913	-0.087	-1.45%
XD19	6.292	0.292	4.87%
XD20	5.921	-0.079	-1.32%
XD21	6.186	0.186	3.10%
XD22	5.975	-0.025	-0.42%
XD23	6.015	0.015	0.25%



XD24	6.093	0.093	1.55%
XD25	6.009	0.009	0.15%
XD26	6.044	0.044	0.73%
XD27	6.040	0.040	0.67%
XD28	6.063	0.063	1.05%
XD29	6.052	0.052	0.87%
XD30	6.064	0.064	1.07%
XD31	5.875	-0.125	-2.08%
XD32	6.048	0.048	0.80%
XD33	5.943	-0.057	-0.95%
XD34	5.992	-0.008	-0.13%
XD35	6.115	0.115	1.92%
XD36	5.968	-0.032	-0.53%
XD37	5.994	-0.006	-0.10%
XD38	6.036	0.036	0.60%
XD39	6.079	0.079	1.32%
XD40	6.029	0.029	0.48%
XD41	6.107	0.107	1.78%
XD42	5.990	-0.010	-0.17%
XD43	6.058	0.058	0.97%
XD44	5.955	-0.045	-0.75%
XD45	5.956	-0.044	-0.73%
XD46	5.989	-0.011	-0.18%
XD47	6.031	0.031	0.52%
XD48	6.015	0.015	0.25%
XD49	6.053	0.053	0.88%
XD50	6.121	0.121	2.02%
XD51	5.907	-0.093	-1.55%
XD52	6.061	0.061	1.02%
XD53	6.017	0.017	0.28%
XD54	6.036	0.036	0.60%
XD55	6.059	0.059	0.98%
XD56	6.017	0.017	0.28%
XD57	5.942	-0.058	-0.97%
XD58	5.990	-0.010	-0.17%
XD59	6.131	0.131	2.18%
XD60	6.027	0.027	0.45%
YD1	6.030	0.030	0.50%



YD2	6.087	0.087	1.45%
YD3	6.053	0.053	0.88%
YD4	6.065	0.065	1.08%
YD5	6.073	0.073	1.22%
YD6	6.056	0.056	0.93%
YD7	6.024	0.024	0.40%
YD8	6.106	0.106	1.77%
YD9	6.069	0.069	1.15%
YD10	6.020	0.020	0.33%
YD11	6.078	0.078	1.30%
YD12	6.087	0.087	1.45%
YD13	6.029	0.029	0.48%
YD14	6.092	0.092	1.53%
YD15	6.104	0.104	1.73%
YD16	6.056	0.056	0.93%
YD17	6.083	0.083	1.38%
YD18	6.053	0.053	0.88%
YD19	6.088	0.088	1.47%
YD20	6.103	0.103	1.72%
YD21	6.048	0.048	0.80%
YD22	6.074	0.074	1.23%
YD23	6.024	0.024	0.40%
YD24	6.041	0.041	0.68%
YD25	6.056	0.056	0.93%
YD26	6.063	0.063	1.05%
YD27	6.057	0.057	0.95%
YD28	6.070	0.070	1.17%
YD29	6.022	0.022	0.37%
YD30	6.072	0.072	1.20%
YD31	6.068	0.068	1.13%
YD32	6.067	0.067	1.12%
YD33	6.043	0.043	0.72%
YD34	6.075	0.075	1.25%
YD35	6.100	0.100	1.67%
YD36	6.100	0.100	1.67%
YD37	6.089	0.089	1.48%
YD38	6.046	0.046	0.77%
YD39	6.068	0.068	1.13%



YD40	6.100	0.100	1.67%
YD41	6.054	0.054	0.90%
YD42	6.080	0.080	1.33%
YD43	6.032	0.032	0.53%
YD44	6.021	0.021	0.35%
YD45	6.062	0.062	1.03%
YD46	6.066	0.066	1.10%
YD47	6.056	0.056	0.93%
YD48	6.066	0.066	1.10%
YD49	6.054	0.054	0.90%
YD50	6.066	0.066	1.10%
YD51	6.165	0.165	2.75%
YD52	6.059	0.059	0.98%
YD53	6.056	0.056	0.93%
YD54	6.091	0.091	1.52%
YD55	6.076	0.076	1.27%
YD56	6.089	0.089	1.48%
YD57	6.084	0.084	1.40%
YD58	6.062	0.062	1.03%
YD59	6.082	0.082	1.37%
YD60	5.743	-0.257	-4.28%
ZD1	5.966	-0.034	-0.57%
ZD2	6.020	0.020	0.33%
ZD3	5.870	-0.130	-2.17%
ZD4	5.768	-0.232	-3.87%
ZD5	5.902	-0.098	-1.63%
ZD6	5.952	-0.048	-0.80%
ZD7	6.178	0.178	2.97%
ZD8	6.045	0.045	0.75%
ZD9	6.098	0.098	1.63%
ZD10	5.930	-0.070	-1.17%
ZD11	6.147	0.147	2.45%
ZD12	5.987	-0.013	-0.22%
ZD13	6.036	0.036	0.60%
ZD14	5.770	-0.230	-3.83%
ZD15	5.993	-0.007	-0.12%
ZD16	6.156	0.156	2.60%
ZD17	6.026	0.026	0.43%



ZD18	6.036	0.036	0.60%
ZD19	6.086	0.086	1.43%
ZD20	6.194	0.194	3.23%
ZD21	6.106	0.106	1.77%
ZD22	6.035	0.035	0.58%
ZD23	6.024	0.024	0.40%
ZD24	5.975	-0.025	-0.42%
ZD25	5.784	-0.216	-3.60%
ZD26	5.958	-0.042	-0.70%
ZD27	6.223	0.223	3.72%
ZD28	6.092	0.092	1.53%
ZD29	6.094	0.094	1.57%
ZD30	5.938	-0.062	-1.03%
ZD31	6.139	0.139	2.32%
ZD32	6.025	0.025	0.42%
ZD33	6.029	0.029	0.48%
ZD34	5.909	-0.091	-1.52%
ZD35	5.786	-0.214	-3.57%
ZD36	6.001	0.001	0.02%
ZD37	5.938	-0.062	-1.03%
ZD38	5.878	-0.122	-2.03%
ZD39	6.062	0.062	1.03%
ZD40	6.148	0.148	2.47%
ZD41	6.185	0.185	3.08%
ZD42	6.160	0.160	2.67%
ZD43	6.012	0.012	0.20%
ZD44	6.068	0.068	1.13%
ZD45	5.624	-0.376	-6.27%
ZD46	5.880	-0.120	-2.00%
ZD47	5.787	-0.213	-3.55%
ZD48	6.080	0.080	1.33%
ZD49	5.932	-0.068	-1.13%
ZD50	5.958	-0.042	-0.70%
ZD51	5.997	-0.003	-0.05%
ZD52	5.984	-0.016	-0.27%
ZD53	6.051	0.051	0.85%
ZD54	5.951	-0.049	-0.82%
ZD55	6.016	0.016	0.27%



ZD56	5.557	-0.443	-7.38%
ZD57	5.985	-0.015	-0.25%
ZD58	5.954	-0.046	-0.77%
ZD59	5.819	-0.181	-3.02%
ZD60	6.034	0.034	0.57%

Category E (2mm)

Measurement ID	Measured Value	Error	% Error
XE1	2.154	0.154	7.70%
XE2	1.906	-0.094	-4.70%
XE3	1.960	-0.040	-2.00%
XE4	2.090	0.090	4.50%
XE5	1.917	-0.083	-4.15%
XE6	1.926	-0.074	-3.70%
XE7	1.980	-0.020	-1.00%
XE8	2.009	0.009	0.45%
XE9	2.019	0.019	0.95%
XE10	1.976	-0.024	-1.20%
XE11	2.073	0.073	3.65%
XE12	1.992	-0.008	-0.40%
XE13	2.015	0.015	0.75%
XE14	1.998	-0.002	-0.10%
XE15	1.997	-0.003	-0.15%
XE16	1.988	-0.012	-0.60%
XE17	1.896	-0.104	-5.20%
XE18	1.947	-0.053	-2.65%
XE19	2.016	0.016	0.80%
XE20	1.951	-0.049	-2.45%
XE21	2.072	0.072	3.60%
XE22	1.982	-0.018	-0.90%
XE23	1.905	-0.095	-4.75%
XE24	2.013	0.013	0.65%
XE25	1.964	-0.036	-1.80%
XE26	1.924	-0.076	-3.80%
XE27	1.930	-0.070	-3.50%
XE28	1.986	-0.014	-0.70%



XE29	1.931	-0.069	-3.45%
XE30	2.000	0.000	0.00%
XE31	1.991	-0.009	-0.45%
XE32	2.028	0.028	1.40%
XE33	2.042	0.042	2.10%
XE34	2.090	0.090	4.50%
XE35	1.976	-0.024	-1.20%
XE36	1.910	-0.090	-4.50%
XE37	2.037	0.037	1.85%
XE38	1.986	-0.014	-0.70%
XE39	1.967	-0.033	-1.65%
XE40	1.976	-0.024	-1.20%
XE41	1.972	-0.028	-1.40%
XE42	1.972	-0.028	-1.40%
XE43	2.020	0.020	1.00%
XE44	1.934	-0.066	-3.30%
XE45	1.975	-0.025	-1.25%
XE46	2.072	0.072	3.60%
XE47	1.969	-0.031	-1.55%
XE48	2.006	0.006	0.30%
XE49	2.030	0.030	1.50%
XE50	1.984	-0.016	-0.80%
XE51	1.958	-0.042	-2.10%
XE52	1.969	-0.031	-1.55%
XE53	2.057	0.057	2.85%
XE54	1.958	-0.042	-2.10%
XE55	1.979	-0.021	-1.05%
XE56	1.947	-0.053	-2.65%
XE57	1.981	-0.019	-0.95%
XE58	1.950	-0.050	-2.50%
XE59	2.045	0.045	2.25%
XE60	2.011	0.011	0.55%
XE61	2.008	0.008	0.40%
XE62	1.948	-0.052	-2.60%
XE63	2.098	0.098	4.90%
YE1	2.028	0.028	1.40%
YE2	1.971	-0.029	-1.45%
YE3	1.946	-0.054	-2.70%



YE4	1.980	-0.020	-1.00%
YE5	1.963	-0.037	-1.85%
YE6	1.954	-0.046	-2.30%
YE7	2.006	0.006	0.30%
YE8	1.962	-0.038	-1.90%
YE9	1.920	-0.080	-4.00%
YE10	2.005	0.005	0.25%
YE11	1.977	-0.023	-1.15%
YE12	1.938	-0.062	-3.10%
YE13	1.976	-0.024	-1.20%
YE14	1.944	-0.056	-2.80%
YE15	1.927	-0.073	-3.65%
YE16	1.993	-0.007	-0.35%
YE17	1.970	-0.030	-1.50%
YE18	1.943	-0.057	-2.85%
YE19	1.952	-0.048	-2.40%
YE20	1.927	-0.073	-3.65%
YE21	1.970	-0.030	-1.50%
YE22	2.013	0.013	0.65%
YE23	1.973	-0.027	-1.35%
YE24	1.965	-0.035	-1.75%
YE25	1.985	-0.015	-0.75%
YE26	2.005	0.005	0.25%
YE27	1.952	-0.048	-2.40%
YE28	1.992	-0.008	-0.40%
YE29	1.969	-0.031	-1.55%
YE30	1.979	-0.021	-1.05%
YE31	1.970	-0.030	-1.50%
YE32	1.995	-0.005	-0.25%
YE33	1.932	-0.068	-3.40%
YE34	1.964	-0.036	-1.80%
YE35	1.949	-0.051	-2.55%
YE36	1.960	-0.040	-2.00%
YE37	1.961	-0.039	-1.95%
YE38	1.952	-0.048	-2.40%
YE39	1.932	-0.068	-3.40%
YE40	1.989	-0.011	-0.55%
YE41	1.939	-0.061	-3.05%



YE42	1.978	-0.022	-1.10%
YE43	2.001	0.001	0.05%
YE44	1.953	-0.047	-2.35%
YE45	1.968	-0.032	-1.60%
YE46	2.007	0.007	0.35%
YE47	1.994	-0.006	-0.30%
YE48	1.970	-0.030	-1.50%
YE49	1.973	-0.027	-1.35%
YE50	1.978	-0.022	-1.10%
YE51	1.964	-0.036	-1.80%
YE52	1.970	-0.030	-1.50%
YE53	1.885	-0.115	-5.75%
YE54	1.938	-0.062	-3.10%
YE55	1.968	-0.032	-1.60%
YE56	1.946	-0.054	-2.70%
YE57	1.948	-0.052	-2.60%
YE58	1.988	-0.012	-0.60%
YE59	1.951	-0.049	-2.45%
YE60	1.945	-0.055	-2.75%
YE61	1.929	-0.071	-3.55%
YE62	2.320	0.320	16.00%
YE63	1.950	-0.050	-2.50%
ZE1	2.342	0.342	17.10%
ZE2	2.145	0.145	7.25%
ZE3	2.126	0.126	6.30%
ZE4	2.333	0.333	16.65%
ZE5	2.458	0.458	22.90%
ZE6	2.155	0.155	7.75%
ZE7	2.235	0.235	11.75%
ZE8	2.210	0.210	10.50%
ZE9	2.155	0.155	7.75%
ZE10	2.171	0.171	8.55%
ZE11	2.098	0.098	4.90%
ZE12	2.207	0.207	10.35%
ZE13	2.147	0.147	7.35%
ZE14	2.184	0.184	9.20%
ZE15	2.302	0.302	15.10%
ZE16	2.092	0.092	4.60%



ZE17	2.057	0.057	2.85%
ZE18	2.170	0.170	8.50%
ZE19	2.202	0.202	10.10%
ZE20	2.069	0.069	3.45%
ZE21	2.098	0.098	4.90%
ZE22	2.234	0.234	11.70%
ZE23	2.072	0.072	3.60%
ZE24	2.161	0.161	8.05%
ZE25	2.145	0.145	7.25%
ZE26	2.226	0.226	11.30%
ZE27	2.293	0.293	14.65%
ZE28	2.188	0.188	9.40%
ZE29	2.144	0.144	7.20%
ZE30	2.163	0.163	8.15%
ZE31	2.198	0.198	9.90%
ZE32	2.097	0.097	4.85%
ZE33	2.190	0.190	9.50%
ZE34	2.141	0.141	7.05%
ZE35	2.130	0.130	6.50%
ZE36	2.327	0.327	16.35%
ZE37	2.192	0.192	9.60%
ZE38	2.254	0.254	12.70%
ZE39	2.349	0.349	17.45%
ZE40	2.222	0.222	11.10%
ZE41	2.108	0.108	5.40%
ZE42	2.158	0.158	7.90%
ZE43	2.107	0.107	5.35%
ZE44	2.047	0.047	2.35%
ZE45	2.127	0.127	6.35%
ZE46	2.046	0.046	2.30%
ZE47	2.470	0.470	23.50%
ZE48	2.317	0.317	15.85%
ZE49	2.177	0.177	8.85%
ZE50	2.531	0.531	26.55%
ZE51	2.344	0.344	17.20%
ZE52	2.216	0.216	10.80%
ZE53	2.055	0.055	2.75%
ZE54	2.310	0.310	15.50%



ZE55	2.102	0.102	5.10%
ZE56	2.230	0.230	11.50%
ZE57	2.223	0.223	11.15%
ZE58	2.106	0.106	5.30%
ZE59	2.559	0.559	27.95%
ZE60	2.199	0.199	9.95%
ZE61	2.296	0.296	14.80%
ZE62	2.318	0.318	15.90%
ZE63	2.181	0.181	9.05%



Appendix E

*Geometric Accuracy Data
Sheets and Graphs for 3DP
Process – Using Plaster
Powder*



Profile of Surface Data

Date Measured: 22 April 2003

Max Deviation: 1.391 mm (Measure Nr. 2)

Mean Deviation: 0.288 mm

Min Deviation: -1.497 mm (Measure Nr. 78)

Best Fit Changes Required:

	X	Y	Z
Shift:	-0.094 mm	-0.241 mm	0.368 mm
Rotation:	-0.046°	-0.179°	-0.105°

Measure Nr	Deviation X	Deviation Y	Deviation Z	Total Deviation
1	-1.336	0	0	1.336
2	-1.391	0	0	1.391
3	-1.373	0	0	1.373
4	-0.799	0.601	0.01	1
5	-0.891	0.594	0.01	1.071
6	-0.824	0.655	-0.22	1.075
7	-0.685	0.529	-0.062	0.868
8	-0.5	0.274	0.181	0.598
9	-1.068	0	0	1.068
10	-0.315	0.237	0.146	0.42
11	-0.267	0.229	0.134	0.377
12	-0.16	0.099	0.082	0.205
13	-0.821	0	0	0.821
14	-0.414	0	0.138	0.437
15	-0.481	0	0.151	0.504
16	-0.267	-0.174	0.147	0.35
17	-0.748	0	0	0.748
18	-0.243	-0.268	0.172	0.4
19	-0.472	-0.437	0.179	0.668
20	-0.423	-0.219	0.391	0.616
21	-0.715	-0.816	-0.114	1.091



22	-0.9	-1.039	-0.093	1.378
23	-1.056	0	0	1.056
24	-0.961	-0.951	-0.017	1.352
25	-0.97	-0.872	-0.015	1.304
26	0	0.001	-0.454	-0.454
27	0	0.001	-0.479	-0.479
28	0	0.002	-0.813	-0.813
29	0	0.002	-0.939	-0.939
30	0	0.002	-0.945	-0.945
31	-0.032	-0.182	0.304	0.356
32	0.287	0.002	-0.653	-0.713
33	0.317	0.001	-0.619	-0.695
34	0.163	0.009	-0.2	-0.258
35	0.153	0.265	-0.305	-0.432
36	0	0.12	-0.104	-0.159
37	0	-0.018	0.012	0.022
38	0	-0.053	0.032	0.062
39	0	0.103	-0.061	-0.119
40	0	-0.175	0.041	0.18
41	0	-0.427	0.101	0.439
42	0	-0.024	0.035	0.043
43	0	-0.631	-0.081	0.636
44	0	-0.411	-1.183	1.252
45	0	-0.81	-0.014	0.811
46	0	-0.703	-0.012	0.703
47	-0.089	-0.093	0.059	0.142
48	-0.133	-0.114	0.075	0.19
49	-0.184	-0.338	0.071	0.391
50	0	-0.543	0	0.543
51	0	-0.626	0	0.626
52	0	-0.301	-0.198	-0.36
53	0	-0.169	-0.102	-0.197
54	0	-0.154	-0.079	-0.173
55	0	-0.364	-0.193	-0.413
56	0	0.001	-0.003	-0.003
57	0	-0.013	-0.143	-0.144
58	0	0.113	0.01	0.113
59	0	0.708	-0.176	0.729



60	0	0.496	0.009	0.496
61	0	0.474	0.008	0.474
62	0.871	0	0	0.871
63	0.853	0	0	0.853
64	0.913	0	0	0.913
65	0.623	-0.423	0	0.753
66	0.503	-0.382	0	0.632
67	0.725	0	0	0.725
68	0.04	-0.01	0.008	0.042
69	0.674	0	0	0.674
70	-0.008	0	-0.002	-0.008
71	0.687	0	0	0.687
72	0.602	0	0	0.602
73	0.696	0	0	0.696
74	0.684	0.286	0	0.741
75	0.389	0.341	0	0.517
76	0.027	0.167	0.202	0.263
77	0	-0.423	-1.066	-1.147
78	0	0.123	-1.492	-1.497
79	0	0.692	-0.643	-0.944
80	-0.22	0.27	-0.336	-0.483
81	-0.398	0.117	-0.691	-0.806
82	0.608	-0.203	0.02	0.641
83	0.621	0	0	0.621
84	0.712	0	0	0.712
85	-0.006	0.66	0.212	0.693
86	0.02	-0.027	0.011	0.036
87	0.057	-0.041	0.014	0.072
88	0	0	0.424	0.424
89	0.002	-0.295	0.336	0.447
90	0.003	-0.359	0.019	0.359
91	0.005	-0.356	0.019	0.357
92	0	-0.153	0.094	0.18
93	0	-0.055	0.034	0.065
94	0	0.028	-0.017	-0.033
95	0	0.071	-0.044	-0.084
96	0	0.086	-0.053	-0.101
97	0	0.052	-0.032	-0.061



98	-0.095	-0.004	0.003	0.095
99	-0.001	0	0	0.001
100	0.056	0.002	-0.002	-0.056
101	0.389	-0.017	0.011	0.39
102	0.312	-0.014	0.009	0.313
103	0.402	-0.018	0.011	0.402
104	0	0	0.443	0.443
105	0.293	-0.349	0.295	0.543
106	0.284	-0.347	0.023	0.449
107	0.3	-0.358	0.024	0.468
108	0.256	-0.302	-0.071	0.403
109	0.295	-0.354	-0.158	0.487
110	0.296	-0.359	0.025	0.466
111	0.061	-0.081	0.049	0.113
112	0.251	-0.33	0.022	0.415
113	-0.089	0.111	-0.191	-0.238
114	0.42	-0.153	0.023	0.448
115	0.444	-0.162	0.152	0.496
116	0.519	-0.189	0.178	0.581
117	0.482	-0.176	0.166	0.54
118	0.395	-0.144	0.135	0.441
119	0.036	0.1	0	-0.107
120	0.023	0.064	0	-0.068
121	0.174	0.478	0	0.508
122	0.185	0.509	0	0.542
123	0	0	0.459	0.459
124	0.238	0.015	0.23	0.331
125	0.33	0.02	0.017	0.331
126	0.344	0.023	0.018	0.345
127	0.381	0.021	-0.065	0.387
128	0.539	0.033	-0.102	0.55
129	0.598	0.037	0.032	0.6
130	0.273	0.018	0.132	0.304
131	0.673	0.058	0.035	0.676
132	-0.119	-0.01	-0.207	-0.239
133	0	0	0.432	0.432
134	0.115	0.128	0.172	0.243
135	0.037	0.042	0.003	0.056



136	0.132	0.148	0.01	0.199
137	0.129	0.145	-0.011	0.194
138	0.292	0.311	-0.034	0.428
139	0.296	0.319	0.023	0.436
140	0.159	0.158	0.108	0.249
141	0.439	0.427	0.032	0.613
142	-0.095	-0.094	-0.194	-0.236
143	0	0	-1.165	-1.165
144	0	0	-1.296	-1.296
145	0	0	-1.298	-1.298
146	0	0	-1.051	-1.051
147	0	0	0.489	0.489
148	-0.005	0.215	0.221	0.308
149	-0.007	0.288	0.015	0.288
150	0	0.334	0.047	0.337
151	0	0.436	0.061	0.44
152	0	0.404	0.057	0.408
153	0	0.442	0.062	0.447
154	0	0.409	0.058	0.413
155	0	0	0.345	0.345
156	0	0	0.176	0.176
157	-0.683	0	0.53	0.864
158	-1.001	0	0.177	1.016
159	-0.887	0	0.157	0.901
160	-0.902	0	0.16	0.916
161	-0.758	0	0.134	0.77
162	-0.427	0	0.076	0.434
163	0	0.295	0	0.295
164	0	0.306	0	0.306
165	0	0.256	0	0.256
166	0	0.364	0	0.364
167	0	0.36	0	0.36
168	0	0.412	0	0.412
169	0	0.45	0	0.45
170	0	0.463	0	0.463
171	0	0.54	0	0.54
172	0	0.501	0	0.501
173	0	0.527	0	0.527



174	0	0.488	0	0.488
175	0	0.295	0	0.295
176	0	0.04	0	-0.04
177	0	0.288	0	-0.288
178	0	0.342	0	-0.342
179	0	0.439	0	-0.439
180	0	0	0.339	0.339
181	-0.571	-0.008	0.57	0.807
182	-0.926	-0.012	0.049	0.927
183	-0.664	0	0.197	0.693
184	-0.643	0	0.191	0.671
185	-0.622	0	0.185	0.649
186	-0.519	0	0.12	0.533
187	-0.43	0	0.099	0.441
188	-0.36	0	0.083	0.369
189	0	-0.054	0	0.054
190	0	0.087	0	-0.087
191	0	0.198	0	-0.198
192	0	0	0.346	0.346
193	-0.267	-0.289	0.301	0.495
194	-0.301	-0.32	0.023	0.44
195	-0.299	-0.322	0.023	0.44
196	-0.165	-0.185	-0.024	0.249
197	-0.155	-0.172	-0.082	0.246
198	-0.011	-0.013	0.001	0.017
199	0.129	0.163	-0.1	-0.231
200	-0.038	-0.046	0.003	0.06
201	-0.019	0.076	-0.077	-0.11
202	0.015	-0.083	0.049	0.097
203	0.045	-0.331	0.105	0.35
204	0.075	-0.55	0.02	0.556
205	-0.162	0.128	-0.447	-0.492
206	-0.111	0.131	-0.23	-0.287
207	-0.038	0.053	-0.06	-0.089
208	0.079	-0.129	0.076	0.169
209	0.172	-0.307	0.1	0.366
210	0.314	-0.587	0.019	0.666
211	-0.056	0.102	-0.061	-0.132



212	-0.165	0.077	-0.196	-0.268
213	-0.075	0.048	-0.066	-0.111
214	-0.041	0.031	-0.021	-0.056
215	0.175	-0.131	0.036	0.222
216	-0.051	0	-0.018	-0.054
217	-0.287	-0.172	-0.18	-0.38
218	-0.139	-0.256	-0.168	-0.337
219	0.001	0.02	0.006	0.021
220	0.542	-0.008	0.028	0.543
221	0.432	0.012	0.023	0.433
222	0.493	0.03	0.026	0.494
223	0.458	0.233	0.027	0.515
224	0.373	0.22	0.023	0.434
225	0.349	0.219	0.022	0.412
226	0.252	0.408	0.025	0.48
227	0.2	0.334	0.02	0.39
228	0.173	0.3	0.018	0.347
229	-0.016	0.353	0.019	0.354
230	-0.016	0.329	0.017	0.33
231	0.13	0	-0.184	-0.225
232	0.128	0	-0.134	-0.185
233	-0.192	0	0.064	0.202
234	0.144	0	-0.441	-0.464
235	0.141	-0.112	-0.259	-0.316
236	0.236	0.019	-0.302	-0.384
237	0.183	0.016	-0.099	-0.208
238	0.084	0.044	-0.563	-0.571
239	0.147	0.134	-0.485	-0.524
240	0.163	0.175	-0.333	-0.41
241	0.127	0.144	-0.164	-0.252
242	0.03	0.037	-0.024	-0.054
243	-0.199	-0.251	0.063	0.326
244	-0.427	-0.538	0	0.687
245	0.041	0.196	-0.544	-0.579
246	0.06	0.215	-0.333	-0.401
247	0.058	0.177	-0.168	-0.251
248	-0.019	-0.053	0.031	0.064
249	-0.171	-0.468	0.105	0.51



250	-0.28	-0.552	0	0.619
251	0	-0.503	0	0.503
252	0	-0.831	-0.438	0.939
253	0	-0.656	0	0.656
254	0	0.075	0.053	0.091
255	0	-0.17	0	0.17
256	0	-0.368	0	0.368
257	0	-0.915	-0.563	1.075
258	0	-0.593	0	0.593
259	0	-0.459	-0.491	0.672
260	0	-0.247	0	0.247
261	0	-0.352	0	0.352
262	0	-0.741	-0.45	0.867
263	0	-0.53	0	0.53
264	0	-0.386	-0.341	0.515
265	0	-0.163	0	0.163
266	0	-0.362	0	0.362
267	0.033	-0.432	0	0.433
268	0.381	-0.615	0	0.724
269	0	-0.212	0	0.212
270	0.183	-0.004	0.086	0.202
271	-0.016	0.007	-0.983	-0.983
272	0.702	-0.369	0	0.793
274	0.908	0	0	0.908
275	0.551	0.272	0	0.614
276	0.601	0.306	0	0.675
277	0.408	0.362	0	0.546
278	0.435	0.392	0	0.586
279	0.303	0.453	0	0.545
280	0.348	0.529	0	0.633
281	0	0.637	-0.017	0.637
282	0	0.768	-0.004	0.768
283	0	0.379	0	0.379
284	0	0.481	0	0.481
285	0	0.733	0	0.733
286	0	0.538	0	0.538
287	0	0.567	0	0.567



288	0.481	0	-0.397	-0.624
289	-0.346	0.583	0	0.678
290	-0.349	0.595	0	0.689
291	-0.395	0.466	0	0.611
292	-0.421	0.49	0	0.646
293	-0.523	0.422	0	0.672
294	-0.547	0.446	0	0.706



Appendix F

*Geometric Accuracy Data
Sheets and Graphs for 3DP
Process – Using Starch
Powder*



Profile of Surface Data

Date Measured: 26 March 2003

Max Deviation: 3.814 mm (Measure Nr. 59)

Mean Deviation: 1.110 mm

Min Deviation: -1.570 mm (Measure Nr. 27)

Best Fit Changes Required:

	X	Y	Z
Shift:	-0.305 mm	-0.107 mm	-0.013 mm
Rotation:	-0.229°	0.018°	0.407°

Measure Nr.	Deviation X	Deviation Y	Deviation Z	Total Deviation
1	-2.191	0	0	2.191
2	-2.129	0	0	2.129
3	-1.943	0	0	1.943
4	-1.666	1.749	0.031	2.415
5	-1.577	2.039	0.036	2.578
6	-2.157	2.419	-1.309	3.495
7	-1.808	1.767	-0.583	2.594
8	-0.671	0.438	0.504	0.946
9	-1.948	0	0	1.948
10	-1.355	0.759	0.315	1.585
11	-1.106	0.527	0.35	1.274
12	-0.887	0.322	0.178	0.96
13	-1.965	0	0	1.965
14	-0.603	0	0.054	0.605
15	-1.157	0	0	1.157
16	-0.48	-0.102	0.058	0.494
17	-2.12	0	0	2.12
18	-0.99	-0.12	0.099	1.002
19	-0.635	-0.3	0.107	0.71
20	0.192	0.068	-0.078	-0.218
21	-1.233	-0.904	-0.344	1.567



22	-1.058	-1.366	-0.024	1.728
23	-2.179	0	0	2.179
24	-1.275	-0.615	-0.011	1.416
25	-1.136	-0.63	-0.011	1.299
26	0	0.004	-1.402	-1.402
27	0	0.004	-1.57	-1.57
28	0	0.004	-1.344	-1.344
29	0	0.004	-1.387	-1.387
30	0	0.004	-1.502	-1.502
31	-0.029	0.068	0.07	0.102
32	0.088	0.001	-0.288	-0.302
33	0.115	0.001	-0.367	-0.385
34	0.123	0.012	-0.401	-0.42
35	-0.295	-0.5	0.316	0.661
36	0	0.773	-0.341	-0.845
37	0	0.468	-0.333	-0.574
38	0	0.365	-0.197	-0.415
39	0	0.131	-0.071	-0.149
40	0	-0.563	0.113	0.574
41	0	-0.165	0.034	0.169
42	0	0.508	-0.698	-0.863
43	0	-0.805	-0.168	0.822
44	0	-2.641	-0.046	2.642
45	0	-0.656	-0.011	0.656
46	0	-0.672	-0.012	0.672
47	-0.413	-0.706	0.495	0.956
48	-0.138	-0.525	0.288	0.614
49	-0.614	-1.28	0.259	1.443
50	0	-1.744	0	1.744
51	0	-1.589	0	1.589
52	0	0.059	0.034	0.068
53	0	0.687	0.532	0.869
54	0	0.911	0.457	1.02
55	0	0.954	0.467	1.062
56	0	0.668	0.607	0.903
57	0	0.64	0.604	0.88
58	0	2.64	-0.423	2.674



59	0	3.575	-1.329	3.814
60	0	2.808	0.049	2.808
61	0	2.638	0.046	2.639
62	1.703	0	0	1.703
63	1.601	0	0	1.601
64	1.419	0	0	1.419
65	1.283	-0.867	0	1.549
66	1.353	-0.996	0	1.68
67	1.492	0	0	1.492
68	0.571	-0.116	0.106	0.592
69	1.527	0	0	1.527
70	1.031	0	0	1.031
71	1.57	0	0	1.57
72	1.75	0	0	1.75
73	1.808	0	0	1.808
74	1.365	1.231	0	1.839
75	1.344	1.223	0	1.817
76	-0.084	-0.029	-0.036	-0.096
77	0	-0.357	-1.122	-1.178
78	0	0.072	-1.279	-1.281
79	0	0.229	-0.226	-0.321
80	0.011	-0.01	0.014	0.021
81	-0.154	0.04	-0.24	-0.288
82	1.585	-0.755	0.074	1.757
83	1.616	0	0	1.616
84	1.451	0	0	1.451
85	-0.147	0	-0.192	-0.242
86	0.426	-0.45	0.267	0.674
87	0.675	-0.449	0.133	0.821
88	0	0	0.156	0.156
89	0.001	-0.159	0.235	0.284
90	0.006	-1.396	0.073	1.398
91	0.004	-1.559	0.082	1.562
92	0	-0.69	0.422	0.809
93	0	-0.608	0.372	0.713
94	0	-0.531	0.324	0.622
95	0	-0.552	0.337	0.647
96	0	-0.458	0.28	0.537



97	0	-0.344	0.21	0.403
98	-1.862	-0.083	0.051	1.865
99	-1.871	-0.084	0.051	1.873
100	-1.868	-0.084	0.051	1.871
101	1.151	-0.051	0.031	1.153
102	1.144	-0.051	0.031	1.146
103	1.154	-0.052	0.032	1.156
104	0	0	0.127	0.127
105	0.094	-0.135	0.174	0.24
106	0.721	-1.065	0.067	1.288
107	0.773	-1.129	0.072	1.37
108	0.998	-1.456	-0.577	1.857
109	1.151	-1.643	-0.326	2.032
110	0.755	-1.088	0.071	1.326
111	0.332	-0.51	0.292	0.675
112	0.813	-1.295	0.08	1.532
113	0.056	-0.088	0.134	0.17
114	1.158	-0.429	0.065	1.236
115	0.782	-0.284	0.268	0.874
116	0.717	-0.261	0.246	0.802
117	0.701	-0.255	0.241	0.784
118	0.698	-0.254	0.24	0.781
119	-0.594	-1.632	0	1.737
120	-0.547	-1.503	0	1.599
121	0.464	1.274	0	1.355
122	0.504	1.386	0	1.475
123	0	0	-0.007	-0.007
124	0.108	0.003	0.074	0.13
125	1.036	0.045	0.054	1.038
126	1.127	0.054	0.059	1.13
127	1.604	0.104	-0.603	1.717
128	1.911	0.164	-0.49	1.979
129	1.229	0.108	0.066	1.236
130	0.435	0.037	0.21	0.484
131	1.314	0.127	0.069	1.322
132	-0.053	-0.005	-0.07	-0.087
133	0	0	-0.081	-0.081
134	0.179	0.147	0.11	0.256



135	0.967	0.731	0.064	1.214
136	0.954	0.73	0.063	1.203
137	1.335	1.002	-0.602	1.774
138	1.704	1.265	-0.718	2.241
139	1.032	0.812	0.07	1.315
140	0.394	0.32	0.244	0.564
141	1.131	0.88	0.075	1.435
142	0.067	0.051	0.099	0.13
143	0	0	-0.817	-0.817
144	0	0	-0.872	-0.872
145	0	0	-0.843	-0.843
146	0	0	-0.777	-0.777
147	0	0	-0.02	-0.02
148	-0.007	0.431	0.263	0.505
149	-0.024	1.394	0.073	1.396
150	0	1.513	0.213	1.528
151	0	1.447	0.203	1.461
152	0	1.427	0.201	1.441
153	0	1.526	0.215	1.541
154	0	1.462	0.205	1.476
155	0	0	-0.048	-0.048
156	0	0	-0.294	-0.294
157	-0.211	0	0.22	0.305
158	-1.575	0	0.278	1.599
159	-1.459	0	0.258	1.482
160	-1.312	0	0.232	1.332
161	-1.234	0	0.218	1.253
162	-1.238	0	0.219	1.257
163	0	1.847	0	1.847
164	0	1.852	0	1.852
165	0	1.813	0	1.813
166	0	2.073	0	2.073
167	0	2.097	0	2.097
168	0	2.048	0	2.048
169	0	2.034	0	2.034
170	0	2.085	0	2.085
171	0	2.109	0	2.109
172	0	2.212	0	2.212



173	0	2.315	0	2.315
174	0	2.102	0	2.102
175	0	2.336	0	2.336
176	0	-1.058	0	1.058
177	0	-0.967	0	0.967
178	0	-0.654	0	0.654
179	0	-0.733	0	0.733
180	0	0	-0.005	-0.005
181	-0.635	-0.079	0.409	0.76
182	-1.782	-0.208	0.094	1.797
183	-1.416	0	0.421	1.477
184	-1.428	0	0.424	1.49
185	-1.344	0	0.353	1.39
186	-1.454	0	0.336	1.493
187	-1.41	0	0.325	1.447
188	-1.355	0	0.313	1.39
189	0	-1.282	0	1.282
190	0	-1.244	0	1.244
191	0	-1.323	0	1.323
192	0	0	0.133	0.133
193	-0.401	-0.481	0.351	0.718
194	-1.05	-1.224	0.084	1.615
195	-1.048	-1.326	0.089	1.692
196	-1.273	-1.61	-0.907	2.244
197	-1.348	-1.729	-0.185	2.2
198	-0.98	-1.265	0.086	1.602
199	-0.432	-0.575	0.346	0.798
200	-0.969	-1.256	0.083	1.588
201	-0.015	0.063	-0.075	-0.099
202	0.03	-0.151	0.121	0.195
203	0.122	-0.735	0.324	0.812
204	0.225	-1.645	0.25	1.679
205	-0.156	0.136	-0.46	-0.505
206	-0.032	0.038	-0.065	-0.082
207	0.16	-0.234	0.238	0.37
208	0.291	-0.477	0.327	0.647
209	0.547	-0.993	0.398	1.201
210	0.767	-1.447	0.148	1.645



211	0.358	-0.3	0.348	0.582
212	0.057	-0.026	0.06	0.087
213	0.198	-0.124	0.146	0.276
214	0.575	-0.444	0.242	0.766
215	0.94	-0.823	0.142	1.258
216	0.129	-0.041	0.035	0.139
217	0.488	0.12	0.03	0.503
218	0.169	0.157	0.048	0.236
219	0.012	0.141	0.062	0.154
220	1.492	-0.305	0.08	1.525
221	1.509	-0.241	0.08	1.531
222	1.49	-0.018	0.078	1.493
223	1.375	0.415	0.075	1.438
224	1.426	0.492	0.079	1.511
225	1.382	0.484	0.077	1.467
226	1.086	1.038	0.079	1.505
227	1.113	1.029	0.079	1.518
228	1.198	1.182	0.088	1.685
229	0.195	1.735	0.091	1.748
230	0.23	1.724	0.091	1.741
231	0.091	0	-0.133	-0.161
232	-0.052	0	0.054	0.075
233	-0.765	0	0.302	0.823
234	0.102	0	-0.323	-0.339
235	0.048	0.001	-0.089	-0.101
236	-0.091	-0.014	0.119	0.151
237	-0.444	-0.101	0.309	0.55
238	0.07	0.047	-0.457	-0.464
239	0.067	0.054	-0.189	-0.208
240	-0.081	-0.072	0.13	0.169
241	-0.381	-0.359	0.38	0.646
242	-0.63	-0.618	0.384	0.963
243	-1.065	-1.093	0.285	1.553
244	-1.344	-1.4	0	1.941
245	0.025	0.163	-0.388	-0.421
246	0.014	0.059	-0.08	-0.1
247	-0.06	-0.199	0.165	0.266
248	-0.269	-0.828	0.39	0.954



249	-0.518	-1.479	0.267	1.59
250	-0.897	-1.728	0	1.947
251	-0.164	-1.657	0	1.665
252	0	-2.159	-1.626	2.702
253	0	-1.997	0	1.997
254	0	0.301	-0.016	-0.301
255	0	-1.052	0	1.052
256	0	-1.93	0	1.93
257	0	-2.32	-1.688	2.869
258	0	-2.232	0	2.232
259	0	0.09	-0.039	-0.098
260	0	-1.796	0	1.796
261	0	-2.092	0	2.092
262	0	-2.224	-1.536	2.703
263	0	-2.144	0	2.144
264	0	0.214	-0.028	-0.216
265	0	-1.886	0	1.886
266	0	-2.05	0	2.05
267	0.169	-1.962	0	1.969
268	0.856	-1.433	0	1.669
269	0	-1.962	0	1.962
270	2.688	-0.049	-0.804	2.806
271	0.544	-0.011	0.261	0.603
272	-0.404	0.021	-1.105	-1.177
273	1.352	-0.599	0	1.479
274	1.41	0	0	1.41
275	1.624	0.895	0	1.854
276	0.571	0.308	1.652	1.775
277	1.475	1.355	0	2.003
278	0.458	0.422	1.316	1.456
279	1.194	1.858	0	2.208
280	0.397	0.618	1.207	1.412
281	0	2.356	-0.985	2.554
282	0	2.352	-0.583	2.424
283	0	2.427	0	2.427
284	0	2.576	0	2.576
285	0	2.694	0	2.694
286	0	2.699	0	2.699



287	0	2.645	0	2.645
288	0.46	0	-0.59	-0.748
289	-1.297	2.118	0	2.484
290	-0.222	0.358	1.986	2.031
291	-1.63	1.824	0	2.446
292	-1.607	1.79	0	2.405
293	-1.916	1.536	0	2.455
294	-1.801	1.52	0	2.357



Appendix G

*Geometric Accuracy Data
Sheets and Graphs for SLS
Process*



Profile of Surface Data

Date Measured: 25 November 2003

Max Deviation: 0.302 mm (Measure Nr. 137)

Mean Deviation: -0.044 mm

Min Deviation: -0.454 mm (Measure Nr. 281)

Best Fit Changes Required:

	X	Y	Z
Shift:	-0.017 mm	-0.014 mm	0.021 mm
Rotation:	0.006°	0.004°	0.005°

Measure Nr.	Deviation X	Deviation Y	Deviation Z	Total Deviation
1	0.002	0	0	-0.002
2	0.029	0	0	-0.029
3	0.037	0	0	-0.037
4	0.083	-0.052	-0.001	-0.098
5	0.1	-0.066	-0.001	-0.12
6	-0.03	0.029	-0.014	0.044
7	0.118	-0.117	0.004	-0.166
8	0.115	-0.144	-0.099	-0.209
9	0.195	0	0	-0.195
10	0.109	-0.14	-0.076	-0.193
11	0.134	-0.121	-0.068	-0.193
12	0.16	-0.093	-0.081	-0.202
13	0.216	0	0	-0.216
14	0.136	0	-0.15	-0.202
15	0.108	0	-0.139	-0.176
16	0.17	0.1	-0.114	-0.228
17	0.185	0	0	-0.185
18	0.064	0.134	-0.049	-0.156
19	0.089	0.117	-0.055	-0.157
20	-0.006	-0.016	0.001	0.017



21	0.024	0.031	0.005	-0.04
22	0	0	0	0
23	0.073	0	0	-0.073
24	0.034	0.037	0.001	-0.05
25	0.039	0.035	0.001	-0.052
26	0	0.055	-0.055	-0.077
27	0	-0.004	0.001	0.005
28	0	0.062	-0.049	-0.079
29	0	0.017	-0.005	-0.018
30	0	-0.036	0.014	0.038
31	0	-0.006	0	0.006
32	0	-0.065	-0.216	0.225
33	0	-0.041	-0.001	0.041
34	0	0.061	0.001	-0.061
35	0	0.029	-0.021	-0.036
36	0	0.063	-0.018	-0.065
37	-0.103	-0.004	0	0.103
38	-0.245	-0.01	0	0.245
39	-0.02	-0.022	0.005	0.03
40	0.081	0.051	-0.031	-0.1
41	0.056	0.054	-0.026	-0.082
42	0.063	0.04	-0.062	-0.097
43	0.064	0.005	-0.057	-0.086
44	0.059	0	-0.027	-0.065
45	0.056	0	-0.036	-0.067
46	0.127	-0.028	-0.055	-0.141
47	0	0.001	-0.202	-0.202
48	0	0.001	-0.268	-0.268
49	0	0	-0.116	-0.116
50	0	0	-0.067	-0.067
51	0	0	-0.18	-0.18
52	0	-0.073	-0.055	-0.092
53	0	-0.099	-0.044	-0.108
54	0	-0.03	-0.018	-0.035
55	0	-0.001	-0.001	-0.001
56	0	-0.049	-0.027	-0.056
57	0	-0.052	-0.039	-0.065



58	0	-0.014	0	-0.014
59	0	0.228	-0.126	0.261
60	0	-0.027	0	-0.027
61	0	-0.093	-0.002	-0.093
62	0	0	0.185	0.185
63	0	0	0.066	0.066
64	0	0	0.062	0.062
65	0.123	0	-0.022	-0.124
66	0.124	0	-0.022	-0.126
67	0.184	0	-0.033	-0.187
68	0.169	0	-0.03	-0.172
69	0.198	0	-0.035	-0.201
70	0	0.059	0	-0.059
71	0	0.07	0	-0.07
72	0	0.068	0	-0.068
73	0	0.057	0	-0.057
74	0	0	0.266	0.266
75	0.008	0	-0.009	-0.012
76	0.112	-0.006	-0.006	-0.112
77	0.039	0	-0.012	-0.041
78	-0.069	0	0.021	0.072
79	-0.035	0	0.01	0.036
80	0.109	0	-0.025	-0.112
81	-0.02	0	0.005	0.021
82	0.085	0	-0.02	-0.087
83	0.081	0	-0.11	-0.136
84	0.144	0	-0.147	-0.205
85	0.187	0	-0.086	-0.206
86	0	0.044	0	-0.044
87	0	0.173	0	-0.173
88	0	0.013	0	-0.013
89	0.008	0	-0.023	-0.025
90	0.002	0	-0.004	-0.004
91	-0.001	0	0.001	0.002
92	0.049	0.016	-0.047	-0.07
93	0.091	0.099	-0.033	-0.138
94	0.071	0.072	-0.056	-0.116



95	0.002	0.002	-0.003	-0.005
96	-0.005	-0.004	0.011	0.013
97	-0.02	-0.012	0.075	0.078
98	-0.006	-0.001	0.043	0.044
99	0.036	0.042	-0.027	-0.061
100	0.044	0.048	-0.003	-0.065
101	0.092	0.095	0.052	-0.142
102	0.107	0.105	0.042	-0.156
103	0.093	0.087	-0.007	-0.128
104	0.02	0.019	0.013	-0.03
105	-0.039	-0.035	0.105	0.118
106	0	0	0.298	0.298
107	0.021	0.025	0	-0.033
108	-0.002	-0.025	0.078	0.082
109	-0.002	-0.008	0.013	0.015
110	0.004	0.016	-0.016	-0.023
111	0.025	0.101	-0.059	-0.119
112	0.03	0.122	-0.026	-0.128
113	0.013	0.07	-0.005	-0.071
114	0	-0.045	-0.026	0.052
115	0	0.126	-0.011	-0.126
116	0.027	0.053	0	-0.06
117	-0.011	0.034	0	-0.036
118	0	-0.001	0	0.001
119	0	0.074	0	-0.074
120	0	0.036	0	-0.036
121	-0.013	0.146	0	-0.147
122	-0.063	0.095	0	-0.114
123	0	-0.03	-0.009	0.032
124	0	-0.083	-0.027	0.087
125	0	-0.009	-0.032	-0.033
126	0	-0.015	0.017	0.023
127	0	0.126	-0.047	-0.134
128	0	-0.074	0.156	0.173
129	0	0.112	0	-0.112
130	0	0.165	0	-0.165
131	0	0.142	0	-0.142



132	0	-0.051	0	0.051
133	0.13	-0.003	-0.137	0.189
134	-0.053	0.001	-0.008	-0.054
135	-0.086	0.004	-0.184	-0.203
136	-0.075	0.036	0	-0.083
137	0	0	0.302	0.302
138	0.001	-0.065	0.081	0.104
139	-0.004	0.108	-0.006	-0.108
140	-0.004	0.097	-0.005	-0.097
141	0	0.001	-0.001	-0.001
142	0	0.018	-0.011	-0.021
143	0	0.013	-0.008	-0.016
144	0	0.017	-0.01	-0.02
145	0	0.023	-0.014	-0.027
146	0	0.02	-0.012	-0.023
147	-0.001	0.004	-0.005	-0.006
148	-0.003	0.014	-0.013	-0.019
149	-0.01	0.052	-0.03	-0.061
150	-0.018	0.105	-0.034	-0.112
151	-0.019	0.119	-0.017	-0.122
152	0.075	-0.003	0.002	0.075
153	0.082	-0.004	0.002	0.082
154	0.149	-0.007	0.004	0.149
155	0.029	-0.026	0.073	0.082
156	0.016	-0.02	0.032	0.041
157	-0.025	0.037	-0.037	-0.058
158	-0.03	0.053	-0.034	-0.07
159	-0.036	0.067	-0.025	-0.08
160	-0.066	0.129	-0.018	-0.146
161	0	0	0.274	0.274
162	0.065	-0.068	0.147	0.174
163	-0.061	0.064	-0.005	-0.089
164	-0.052	0.055	-0.004	-0.076
165	0.086	-0.02	-0.018	0.09
166	-0.024	0.03	0.016	-0.042
167	-0.015	0.021	-0.001	-0.026
168	0.012	-0.016	0.01	0.022



169	-0.015	0.022	-0.001	-0.027
170	-0.026	0.033	-0.024	-0.049
171	-0.032	0.015	-0.038	-0.052
172	-0.064	0.041	-0.055	-0.094
173	-0.092	0.073	-0.055	-0.13
174	-0.109	0.1	-0.025	-0.15
175	0.009	-0.003	0.001	0.01
176	0.049	-0.018	0.017	0.055
177	0.021	-0.007	0.007	0.023
178	-0.005	0.002	-0.002	-0.005
179	0.031	-0.011	0.011	0.035
180	-0.023	-0.062	0	0.066
181	0.002	0.004	0	-0.004
182	-0.004	0.006	-0.008	-0.011
183	0	0	0.265	0.265
184	0.046	0.001	0.046	0.065
185	0.011	0	0.001	0.011
186	0.019	0.001	0.001	0.02
187	-0.034	-0.002	0.013	-0.037
188	0.061	0.003	-0.017	0.063
189	0.043	0.003	0.002	0.043
190	0.019	0.002	0.009	0.021
191	0.103	0.008	0.005	0.104
192	-0.004	0	-0.005	-0.007
193	0	0	-0.283	-0.283
194	-0.084	0.026	-0.075	-0.116
195	-0.014	0.003	-0.001	-0.015
196	0.021	-0.003	0.001	0.021
197	-0.037	0	-0.002	-0.037
198	0	0	0.2	0.2
199	0.049	0.049	0.064	0.094
200	-0.002	-0.002	0	-0.003
201	0.019	0.016	0.001	0.025
202	-0.03	-0.024	0.005	-0.038
203	-0.006	-0.006	0.005	-0.01
204	-0.028	-0.025	-0.002	-0.038
205	-0.037	-0.032	-0.024	-0.054



206	0.011	0.009	0.001	0.014
207	-0.119	-0.026	-0.18	-0.217
208	-0.002	-0.001	0	-0.002
209	0.023	0.006	0.001	0.023
210	-0.073	-0.026	-0.004	-0.078
211	-0.071	-0.077	-0.178	-0.207
212	-0.034	-0.032	-0.002	-0.047
213	-0.04	-0.036	-0.003	-0.054
214	-0.079	-0.076	-0.006	-0.11
215	0	0	-0.318	-0.318
216	0	0	-0.335	-0.335
217	0	0	-0.36	-0.36
218	-0.019	-0.114	-0.108	-0.158
219	-0.021	-0.115	-0.006	-0.117
220	-0.017	-0.082	-0.004	-0.083
221	0.011	0.006	0	0.013
222	-0.032	-0.029	0	-0.043
223	-0.029	-0.039	0	-0.048
224	-0.068	-0.091	0	-0.113
225	-0.028	-0.024	0	-0.037
226	-0.053	-0.029	0	-0.06
227	0.063	0	0	0.063
228	0.01	0	0	0.01
229	0.003	0	0	0.003
230	-0.018	0	0	-0.018
231	0.004	-0.002	0	0.005
232	-0.046	0.027	-0.003	-0.053
233	-0.017	0	0	-0.017
234	-0.1	0.078	-0.099	-0.161
235	0	0.12	-0.153	-0.194
236	-0.014	0	0	-0.014
237	-0.151	0.011	-0.118	-0.192
238	0	0.033	-0.288	-0.29
239	0	-0.066	-0.209	-0.219
240	-0.031	0	0	-0.031
241	-0.128	-0.065	-0.089	-0.169
242	0.027	0	0	0.027



243	0.06	0.028	0.047	0.082
244	-0.011	-0.009	0	-0.015
245	-0.082	0.012	-0.082	-0.117
246	-0.024	0.01	-0.015	-0.03
247	-0.051	0	-0.025	-0.057
248	0.07	-0.043	0.004	0.082
249	0.082	0	0	0.082
250	-0.013	0.001	-0.001	-0.013
251	-0.038	0.02	-0.012	-0.044
252	-0.114	0.13	-0.123	-0.213
253	0	0	0.191	0.191
254	0.001	0.028	0.03	0.041
255	0	-0.009	0	-0.009
256	0	0.048	0.007	0.048
257	0	-0.085	-0.012	-0.086
258	0	-0.104	-0.015	-0.105
259	0	-0.021	-0.003	-0.021
260	0	-0.089	-0.012	-0.089
261	0	0.05	0	0.05
262	0	0.043	0	0.043
263	0	0.01	0	0.01
264	0	-0.013	0	-0.013
265	0	-0.02	0	-0.02
266	0	0.018	0	0.018
267	0	0.002	0	0.002
268	0	0.039	0	0.039
269	0	0.004	0	0.004
270	0	0.045	0	0.045
271	0	-0.033	0	-0.033
272	0	-0.036	0	-0.036
273	0	-0.017	0	-0.017
274	0	-0.164	0	-0.164
275	0	-0.123	0	-0.123
276	0	-0.116	0	-0.116
277	0	-0.084	0	-0.084
278	0	-0.053	0	-0.053
279	0	-0.133	0	-0.133



280	0	-0.189	0	-0.189
281	0.311	0	-0.331	-0.454
282	0.077	-0.118	0	-0.141
283	0.103	-0.159	0	-0.189
284	0.096	-0.106	0	-0.143
285	0.079	-0.087	0	-0.118
286	0.069	-0.058	0	-0.09
287	0.094	-0.078	0	-0.122
288	0.023	0.064	0	0.068
289	0.031	0.086	0	0.092
290	0.036	0	0	0.036



<i>Appendix H</i>	<i>Geometric Accuracy Data Sheets and Graphs for LOM Process</i>
-------------------	--



Profile of Surface Data

Date Measured: 28 November 2003

Max Deviation: 3.167 mm (Measure Nr. 156)

Mean Deviation: 0.082 mm

Min Deviation: -2.421 mm (Measure Nr. 152)

Best Fit Changes Required:

	X	Y	Z
Shift:	-0.259 mm	0.020 mm	0.237 mm
Rotation:	0.223°	-0.196°	-0.111°

Measure Nr.	Deviation X	Deviation Y	Deviation Z	Total Deviation
1	-0.902	0	0	0.902
2	-0.863	0	0	0.863
3	-0.816	0	0	0.816
4	-0.556	0.128	0.002	0.571
5	-0.406	0.148	0.003	0.432
6	-0.576	0.28	-0.018	0.641
7	-0.377	0.299	-0.109	0.493
8	0.225	-0.085	-0.057	-0.247
9	-0.608	0	0	0.608
10	0.024	-0.007	-0.004	-0.025
11	0.095	-0.043	-0.023	-0.107
12	0.18	-0.048	-0.061	-0.196
13	-0.42	0	0	0.42
14	0.334	0.001	-0.204	-0.392
15	0.252	0	-0.15	-0.293
16	0.001	0	0	-0.001
17	-0.461	0	0	0.461
18	-0.276	-0.177	0.098	0.343
19	-0.348	-0.293	0.103	0.467
20	0.058	0.019	-0.026	-0.066



21	-0.888	-0.794	-0.198	1.208
22	-0.979	-0.931	-0.016	1.351
23	-0.709	0	0	0.709
24	-0.865	-0.854	-0.015	1.216
25	-0.957	-0.901	-0.016	1.315
26	0	0.003	-1.092	-1.092
27	0	0.003	-1.28	-1.28
28	0	0.003	-1.096	-1.096
29	0	0.003	-1	-1
30	0	0.003	-1.231	-1.231
31	0	0.447	-0.545	-0.705
32	0	0.172	-0.095	-0.197
33	0	0.381	-0.236	-0.449
34	0	-0.122	0.024	0.125
35	0	0.827	-0.867	-1.198
36	0	-0.842	-0.19	0.863
37	0	0.418	-0.249	-0.487
38	0	-0.079	0.015	0.08
39	0	-0.771	-0.466	-0.901
40	0	-0.691	-0.409	-0.803
41	0	-0.923	-0.638	-1.122
42	0	-0.926	-0.381	-1.002
43	0	-0.455	0.04	-0.456
44	0	-0.96	-0.653	-1.161
45	0	-0.951	-0.38	-1.024
46	0.5	0.087	0.079	0.514
47	0.439	0.001	-0.559	-0.711
48	0.005	-0.026	-0.007	-0.028
49	0.409	0.03	-0.708	-0.818
50	-0.073	0.023	-0.018	-0.079
51	0.015	-0.014	0.009	0.022
52	0.106	0.182	-0.099	-0.233
53	-0.146	-0.144	0.044	0.209
54	-0.506	-0.036	0	0.508
55	-0.572	-0.037	0	0.573
56	0	-0.89	-0.016	0.89
57	0	-0.779	-0.014	0.779



58	0	-0.786	-0.014	0.786
59	0	0.283	-0.047	0.287
60	0	-0.528	-0.009	-0.528
61	0	-0.637	-0.011	-0.637
62	0	0	1.554	1.554
63	0	0	1.314	1.314
64	-0.305	0	1.161	1.2
65	0.049	0	-0.009	-0.049
66	0.108	0	-0.019	-0.11
67	0.122	0	-0.021	-0.123
68	0.147	0	-0.026	-0.15
69	0.118	0	-0.021	-0.12
70	0	0.36	0	-0.36
71	0	0.258	0	-0.258
72	0	0.218	0	-0.218
73	0	0.181	0	-0.181
74	0	0	1.576	1.576
75	-0.516	0.014	1.137	1.248
76	-0.002	0	0.002	0.003
77	-0.142	0	0.042	0.148
78	-0.051	0	0.015	0.053
79	-0.02	0	0.006	0.021
80	0.041	0	-0.009	-0.042
81	0.085	0	-0.02	-0.087
82	0.192	0	-0.044	-0.197
83	0	0.144	0	-0.144
84	0	0.056	0	-0.056
85	0	0.09	0	-0.09
86	0.4	0	-0.595	-0.717
87	0.426	0	-0.459	-0.626
88	0.352	0	-0.164	-0.388
89	0.187	0	-0.567	-0.597
90	0.308	0.016	-0.555	-0.635
91	0.356	0.082	-0.443	-0.574
92	0.345	0.116	-0.29	-0.466
93	0	0	1.704	1.704
94	-0.377	-0.359	1.105	1.222



95	-0.036	-0.035	0.052	0.073
96	0.136	0.14	-0.01	-0.195
97	0.256	0.27	0.06	-0.377
98	0.271	0.274	0.165	-0.419
99	0.073	0.075	-0.006	-0.105
100	0.053	0.056	-0.037	-0.085
101	0.046	0.052	-0.004	-0.07
102	0.117	0.049	-0.551	-0.566
103	0.186	0.14	-0.511	-0.561
104	0.236	0.205	-0.436	-0.536
105	0.252	0.244	-0.305	-0.465
106	0.167	0.177	-0.119	-0.271
107	-0.163	-0.176	0.043	0.244
108	-0.594	-0.651	0	0.881
109	0.036	0.178	-0.449	-0.485
110	0.062	0.259	-0.355	-0.444
111	0.072	0.28	-0.245	-0.379
112	0.036	0.132	-0.07	-0.154
113	-0.085	-0.316	0.058	0.332
114	0.122	0.005	-0.003	-0.122
115	0.079	0.004	-0.002	-0.079
116	0.001	0	0	-0.001
117	0	0	1.82	1.82
118	0.011	-0.62	0.941	1.127
119	0.001	-0.074	0.018	0.076
120	0	-0.019	0.001	0.019
121	0	-0.512	0.313	0.6
122	0	-0.471	0.288	0.552
123	0	-0.347	0.212	0.407
124	0	-0.215	0.131	0.252
125	0	-0.122	0.075	0.143
126	0	0.092	-0.056	-0.108
127	-0.072	0.277	-0.328	-0.435
128	-0.067	0.311	-0.234	-0.395
129	-0.034	0.199	-0.1	-0.225
130	0.039	-0.256	0.044	0.262
131	0	-1.186	-0.911	1.495



132	0	-1.222	-0.967	1.558
133	0	-1.012	-0.706	1.234
134	0	-0.735	0	0.735
135	0	-0.734	0	0.734
136	0	-0.673	0	0.673
137	-0.439	-0.772	0	0.888
138	-0.183	-0.919	0	0.937
139	0	-0.873	-1.112	1.413
140	0	1.635	0	-1.635
141	0	1.702	0	-1.702
142	0	-0.374	0	0.374
143	0	-0.654	0	0.654
144	0	-0.552	0	0.552
145	0	-0.8	0	0.8
146	0	-0.798	0	0.798
147	0	-0.664	0	0.664
148	0.044	-0.655	0	0.656
149	0.241	-0.388	0	0.457
150	0	-0.666	0	0.666
151	-0.574	0.011	-0.226	-0.617
152	-1.697	1.727	0	-2.421
153	1.242	-0.023	-0.419	1.311
154	0.256	-0.146	0	0.295
155	-0.16	0.18	-0.469	-0.527
156	1.172	-1.655	2.434	3.167
157	-0.191	0.304	-0.279	-0.455
158	-0.181	0.296	-0.194	-0.398
159	-0.09	0.15	-0.059	-0.184
160	0.057	-0.096	0.016	0.113
161	0	0	1.534	1.534
162	0.49	-0.616	1.061	1.321
163	0.307	-0.366	0.058	0.481
164	0.269	-0.325	0.022	0.423
165	0.185	-0.232	0.001	0.297
166	0.055	-0.067	-0.051	0.101
167	0.272	-0.333	0.023	0.431
168	0.192	-0.239	0.147	0.341



169	0.239	-0.303	0.02	0.387
170	-0.112	0.14	-0.224	-0.287
171	0.366	-0.016	0.01	0.366
172	0.221	-0.01	0.006	0.221
173	0.048	-0.002	0.001	0.048
174	-0.135	0.121	-0.111	-0.212
175	-0.478	0.191	-0.454	-0.686
176	0.003	0.139	-0.161	-0.213
177	-0.049	0.002	-0.001	-0.049
178	0.103	-0.088	0.016	0.136
179	0.672	-0.239	0.037	0.714
180	0.733	-0.267	0.252	0.82
181	0.639	-0.233	0.219	0.714
182	0.48	-0.175	0.165	0.537
183	0.42	-0.153	0.144	0.47
184	-0.025	-0.069	0	0.073
185	-0.044	-0.121	0	0.128
186	0.23	-0.122	0	0.26
187	-0.168	0	0	-0.168
188	-0.127	0	0	-0.127
189	-0.173	0	-0.062	-0.184
190	-0.215	0	-0.086	-0.232
191	0.119	-0.068	0	0.136
192	0.154	-0.079	0.008	0.173
193	0.058	0	0	0.058
194	0.104	0	0	0.104
195	-0.253	0.086	-0.097	-0.284
196	0.197	0	0	0.197
197	-0.388	-0.013	0.202	-0.438
198	0.214	0	0	0.214
199	0.121	-0.084	-0.107	0.182
200	0.053	0	0	0.053
201	0.044	0.034	0	0.055
202	-0.089	-0.067	0	-0.111
203	0	-0.549	-2.265	-2.33
204	0	0.372	-2.113	-2.145
205	0	0.911	-1.345	-1.625



206	0.221	-0.089	0.009	0.238
207	-0.699	0.065	-0.589	-0.916
208	-0.652	0.247	-0.549	-0.887
209	0.144	0.349	0.286	0.473
210	0.157	0	0	0.157
211	0.111	0	0	0.111
212	-0.799	0	-0.663	-1.038
213	-0.371	0.311	-0.183	-0.518
214	-0.359	0.307	-0.147	-0.495
215	-0.023	-0.064	0	-0.068
216	-0.064	-0.177	0	-0.188
217	0	0	1.392	1.392
218	0.826	0.005	1.057	1.341
219	0.636	0.004	0.045	0.638
220	0.515	0.002	0.027	0.516
221	0.304	0.004	-0.067	0.312
222	0.262	0.006	-0.127	0.292
223	0.424	0.009	0.023	0.425
224	0.236	0.005	0.113	0.262
225	0.367	0.01	0.019	0.367
226	-0.289	-0.01	-0.443	-0.529
227	0	0	-1.023	-1.023
228	-0.037	0.013	-0.015	-0.043
229	0.499	-0.14	0.027	0.519
230	0.45	-0.117	0.024	0.466
231	0.074	-0.001	0.004	0.074
232	0	0	-0.986	-0.986
233	-0.29	-0.092	-0.139	-0.334
234	0.203	0.065	0.011	0.213
235	0.091	0.03	0.005	0.096
236	-0.091	-0.03	-0.005	-0.096
237	0	0	1.423	1.423
238	0.637	0.525	0.965	1.27
239	0.421	0.368	0.051	0.562
240	0.35	0.316	0.025	0.472
241	0.131	0.116	-0.028	0.178
242	0.076	0.073	-0.056	0.119



243	0.25	0.224	0.018	0.336
244	0.08	0.073	0.052	0.12
245	0.075	0.074	0.006	0.105
246	-0.244	-0.231	-0.35	-0.485
247	0	0	-1.02	-1.02
248	-0.335	-0.406	-0.425	-0.677
249	-0.007	-0.008	-0.001	-0.011
250	-0.085	-0.104	-0.007	-0.135
251	-0.202	-0.239	-0.016	-0.313
252	0	0	-0.858	-0.858
253	-0.042	-0.474	-0.446	-0.653
254	-0.018	-0.134	-0.007	-0.136
255	-0.03	-0.203	-0.011	-0.206
256	-0.26	-0.137	0	-0.293
257	-0.267	-0.229	0	-0.352
258	-0.195	-0.275	0	-0.337
259	0.008	0.011	0.019	0.023
260	-0.017	-0.014	-0.032	-0.039
261	-0.004	-0.002	-0.005	-0.007
262	0	0	1.54	1.54
263	0.026	0.76	0.969	1.232
264	0.006	0.482	0.031	0.483
265	0.007	0.435	0.023	0.436
266	0	0.454	0.064	0.458
267	0	0.329	0.046	0.333
268	0	0.297	0.042	0.3
269	0	0.216	0.03	0.218
270	0	0.072	-0.034	0.079
271	0	0.168	-0.068	0.181
272	0	-0.125	0	-0.125
273	0	-0.13	0	-0.13
274	0	-0.123	0	-0.123
275	0	-0.208	0	-0.208
276	0	-0.11	0	-0.11
277	1.087	0	-0.619	-1.251
278	-0.002	0.003	0	0.004
279	0.003	-0.005	0	-0.006



280	-0.03	0.036	0	0.047
281	-0.135	0.115	0	0.177
282	-0.126	0.107	0	0.165
283	-0.03	0.036	0	0.047
284	0	0.353	0	0.353
285	0	0.359	0	0.359
286	0	0.409	0	0.409
287	0	0.28	0	0.28
288	0	0.276	0	0.276
289	0	0.258	0	0.258
290	0	0.276	0	0.276
291	0	0.248	0	0.248
292	0	0.234	0	0.234
293	0	0.228	0	0.228
294	0	0.188	0	0.188
295	0	0.191	0	0.191
296	0	0.083	0	0.083



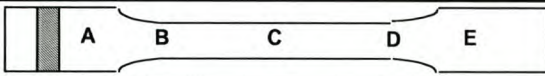
Appendix I

*Strength and Elongation Data
Sheets and Graphs for 3DP
Process – Using Plaster
Powder*

Summary of Tensile Tests

Material: zp100

Number of specimens: 20

	Specimen	Readings to break	Time to break [s]	Max Force [kg]	Break Area [m²]	Max Stress [kPa]	Break occurs at						
	A01	1986	57.565	12.480	104.32E-6	119.629	B	DISQUALIFIED					
	A02	1804	52.287	10.650	98.53E-6	108.094	C						
	A03	1649	47.792	11.790	100.82E-6	116.938	B						
	A04	1485	43.036	13.500	87.95E-6	153.504	C						
	A05	1712	49.619	11.790	98.42E-6	119.796	C						
	A06	1869	54.172	11.940	100.38E-6	118.953	B						
	A07	1880	54.491	11.160	97.13E-6	114.903	C						
	A08	2148	62.263	10.500	96.92E-6	108.334	B						
	A09	2539	73.602	11.400	98.49E-6	115.750	C						
	A10	2032	58.899	10.890	101.20E-6	107.611	B						
	A11	1936	56.115	15.900	108.20E-6	146.945	D						
	A12	1653	47.908	14.100	142.41E-6	99.008	A						
	A13	1931	55.97	14.010	98.38E-6	142.411	C						
	A14	1694	49.097	13.080	99.65E-6	131.265	D						
	A15	2083	60.378	13.620	103.47E-6	131.637	B						
	A16	1972	57.159	13.140	97.38E-6	134.941	C						
	A17	2169	62.872	12.540	99.84E-6	125.598	D						
	A18	1818	52.693	12.120	95.53E-6	126.870	C						
	A19	1676	48.575	12.720	95.67E-6	132.954	D						
A20	1987	57.594	14.520	95.91E-6	151.398	C							
(A01 - A10)	Maximum	2539	73.602	13.500	104.32E-6	153.504	B or C			n	k	Alpha	t _{k,alpha/2}
	Minimum	1485	43.036	10.500	87.95E-6	107.611							
	Std Dev	293	8.508	0.908	4.29E-6	13.255							
	95% UCL	2120	61.459	12.260	101.48E-6	127.833							
	Average	1910	55.373	11.610	98.41E-6	118.351							
(A11 - A20) (excl A12)	95% LCL	1701	49.286	10.960	95.34E-6	108.869	C or D			10	9	5%	2.262
	Maximum	2169	62.872	15.900	108.20E-6	151.398							
	Minimum	1676	48.575	12.120	95.53E-6	125.598							
	Std Dev	165	4.778	1.163	4.19E-6	8.954							
	95% UCL	2045	59.278	14.410	102.56E-6	142.885							
TOTALS (A01 - A20) (excl A12)	Average	1918	55.606	13.517	99.34E-6	136.002	C			9	8	5%	2.306
	95% LCL	1792	51.933	12.623	96.11E-6	129.119							
	Maximum	2539	73.602	15.900	108.20E-6	153.504							
	Minimum	1485	43.036	10.500	87.95E-6	107.611							
	Std Dev	235	6.808	1.403	4.15E-6	14.334							
	95% UCL	2027	58.765	13.190	100.85E-6	133.621				19	18	5%	2.101
	Average	1914	55.483	12.513	98.85E-6	126.712							
	95% LCL	1801	52.202	11.837	96.85E-6	119.803							

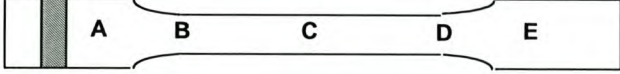


*Appendix J Strength and Elongation Data
Sheets and Graphs for 3DP
Process – Using Starch
Powder*

Summary of Tensile Tests

Material: zp15e

Number of specimens: 20

	Specimen	Readings to break	Time to break [s]	Max Force [kg]	Break Area [m ²]	Max Stress [kPa]	Break occurs at				
	B01	1757	50.924	17.070	141.52E-6	120.617	A	DISQUALIFIED			
	B02	1865	54.056	18.960	140.19E-6	135.243	A				
	B03	1810	52.461	18.630	144.02E-6	129.355	A				
	B04	1770	51.301	16.530	98.54E-6	167.749	B				
	B05	1557	45.124	18.960	96.98E-6	195.498	C				
	B06	1715	49.706	19.980	96.38E-6	207.302	B				
	B07	1609	46.632	19.920	96.38E-6	206.688	D				
	B08	1792	51.939	20.010	97.00E-6	206.280	C				
	B09	1834	53.157	18.750	98.40E-6	190.555	D				
	B10	2001	58.000	20.190	140.37E-6	143.833	E				
	B11	1373	39.788	17.610	98.32E-6	179.113	D				
	B12	1512	43.819	21.360	99.35E-6	214.990	D				
	B13	1749	50.692	21.330	98.53E-6	216.483	D				
	B14	1740	50.431	21.180	99.46E-6	212.946	D				
	B15	1718	49.793	22.140	98.46E-6	224.853	B				
	B16	1650	47.821	22.110	98.81E-6	223.762	D				
	B17	1606	46.545	19.770	97.07E-6	203.668	B				
	B18	1764	51.127	19.380	139.13E-6	139.296	E				
	B19	1562	45.269	18.360	95.00E-6	193.255	B				
	B20	1784	51.707	18.870	94.83E-6	198.996	C				
TOTALS (B04 - B20) (excl B10,B18)	Maximum	1834	53.157	22.140	99.46E-6	224.853	D	Confidence Interval Statistics			
	Minimum	1373	39.788	16.530	94.83E-6	167.749		n	k	Alpha	t _{k,alpha/2}
	Standard Deviation	127	3.682	1.644	1.47E-6	15.837		15	14	5%	2.145
	95% UCL	1735	50.287	20.702	98.38E-6	211.579					
	Average	1665	48.248	19.792	97.57E-6	202.809					
	95% LCL	1594	46.209	18.882	96.76E-6	194.039					